# Investigating the synthesis and regulation of (1,3;1,4)-β-glucan biosynthesis

Submitted by

George Dimitroff, B.Sc. (Hons)

A thesis submitted in fulfilment of the requirements

for the degree of Doctor of Philosophy

School of Agriculture, Food and Wine

University of Adelaide, Waite Campus,

Glen Osmond, SA 5064, Australia

February 2016

# Table of Contents

## Table of Figures

## List of Tables

## Abstract

Cereals such as rice (*Oryza sativa* (*Os*)), barley (*Hordeum vulgare* (*Hv*)) and sorghum (*Sorghum bicolor* (*Sb*)) provide a considerable portion of our daily energy requirements. Their cell wall constituents, such as (1,3;1,4)-β-glucan, survive relatively intact through much of the upper human digestive system to reach the colon, where they are fermented by a range of commensal microorganisms. The products of this fermentation help reduce blood cholesterol levels and ameliorate diseases including coronary heart disease, type II diabetes and colorectal cancer. Efforts have therefore been directed toward understanding the regulation and mechanism of (1,3;1,4)-β-glucan biosynthesis to enhance the human health potential and industrial utility of cereal grain.

Numerous reports suggest that the *CELLULOSE SYNTHASE-LIKE F6* (*CslF6*) gene encodes the synthase responsible for producing the majority of (1,3;1,4)-β-glucan in cereals. These synthase genes contain species-specific polymorphisms that have been shown to influence the amount and structure of (1,3;1,4)-β-glucan produced when they are expressed heterologously in *Nicotiana benthamiana* and barley grain. Here, a chimeric approach exchanged sections of the barley (*Hv)* and sorghum (*Sb)* CSLF6 synthases to identify regions influencing (1,3;1,4)-β-glucan production and structure. Using this approach an 80 amino acid stretch, which contains the conserved TED and QxxRW motifs, was shown to be responsible for much of the difference in (1,3;1,4)-β-glucan production and structure between the barley and sorghum synthases. Of the six amino acid polymorphisms contained within this section, one affected polysaccharide structure whilst another dictated the amount of (1,3;1,4)-β-glucan.

Co-expression in *N. benthamiana* was used to investigate CSLF6 modulation and complex formation. Results from a variety of chimeric, truncated and mutated constructs suggest that a highly variable section of unknown function, termed the class-specific region (CSR), and the $NH_2$-terminal region of CSLF6 are separately able to mediate complex formation and increase (1,3;1,4)-β-glucan production. Expression of a construct missing the CSR indicated that the region was not structurally or functionally required for (1,3;1,4)-β-glucan

synthesis in *N. benthamiana*. A PilZ domain responsible for cofactor binding and cellulose synthase activation in bacteria was also identified at the COOH-terminal end of the $NH_2$-terminal region of CSLF6, and was shown to influence (1,3;1,4)-β-glucan production. Overall, the results presented here have furthered our understanding of the action of the CSLF6 isoform of the (1,3;1,4)-β-glucan synthase enzyme. This brings us closer to having the capacity to precisely control the synthase's function, and allowing the prospect of manipulating cereal tissues to contain the optimal amount of (1,3;1,4)-β-glucan with a defined structure for specific human health and industrial applications.

## Declaration

I, George Dimitroff certify that this work contains no material which has been accepted for the award of any other degree or diploma in my name, in any university or other tertiary institution and, to the best of my knowledge and belief, contains no material previously published or written by another person, except where due reference has been made in the text. In addition, I certify that no part of this work will, in the future, be used in a submission in my name, for any other degree or diploma in any university or other tertiary institution without the prior approval of the University of Adelaide and where applicable, any partner institution responsible for the joint-award of this degree.

I give consent to this copy of my thesis when deposited in the University Library, being made available for loan and photocopying, subject to the provisions of the Copyright Act 1968.

I acknowledge that copyright of published works contained within this thesis resides with the copyright holder(s) of those works. I also give permission for the digital version of my thesis to be made available on the web, via the University's digital research repository, the Library Search and also through web search engines, unless permission has been granted by the University to restrict access for a period of time.

Chapter 2 has been presented as a publication in preparation. **Figure 2-1** and **Figure 2-2** contain work presented in my honours thesis (Dimitroff, 2011) and has been included here because it is a necessary contribution to the first publication in preparation.

George Dimitroff

February 2016

## Acknowledgements

I would like to thank the following organisations and people for their roles in assisting me through my PhD project.

Thanks to the Australian Government, Department of Education and Training for providing an Australian Postgraduate Award, to the Grains Research and Development Corporation for providing a Grains Industry Research Scholarship, and to the ARC Centre of Excellence in Plant Cell Walls, University of Adelaide for providing an ARC COE Plant Cell Walls Scholarship and the facilities required to conduct the research.

To my supervisors Associate Professor Rachel Burton, Dr Alan Little and Professor Geoffrey Fincher, my most sincere gratitude for their guidance, mentorship and support throughout my studies. I would like to thank Professor Vincent Bulone, Professor Alison Roberts, Associate Professor Eric Roberts, Dr Matthew Tucker, Dr Natalie Betts, Dr Marilyn Hendersen, Dr Neil Shirley, Dr Yves Hsieh, Dr Rohan Singh, Mr Jelle Lahnstein, Mr Julian Schwerdt and Ms Shi Fang Khor for their technical knowledge, guidance and friendships. I would also like to thank all current and former members of the Plant Cell Wall group for their friendships and assistance; in particular Kuok Yap, Grace Ang, Ali Saleh Hassan, Christopher Hakachite, Ilaria Marcotuli, and Wai Li Lim for their endless laughter.

Thanks to all of my friends and family for their continued support, particularly my wife Sophia, mother Matoula and father Lio for his 'positive' criticism and weekly fishing trips.

## Abbreviations

| | |
|---|---|
| *As*GLO | *Avena sativa* globulin (oat, grain specific) promoter |
| BCSA | BACTERIAL CELLULOSE SYNTHASE SUBUNIT A |
| *CesA* | CELLULOSE SYNTHASE |
| CR | catalytic region |
| *Csl* | CELLULOSE SYNTHASE-LIKE |
| CSR | class specific region |
| DAP | days after pollination |
| DPI | days post infiltration |
| ExR | The CSLF6 'extra region' |
| F:R | firefly:*Renilla* |
| GFP | green-fluorescent protein from *Aequorea victoria* |
| GUS | beta-glucuronidase gene from *Escherichia coli* |
| HPLC | high performance liquid chromatography |
| *Hv* | *Hordeum vulgare* |
| Kb | kilobase |
| LarII | luciferase assay reagent II |
| LB | luria broth |
| $OD_{600}$ | optical density at 600nm wavelength |
| *Os* | *Oryza sativa* |

| | |
|---|---|
| P-CR | plant-conserved region |
| Q-PCR | quantitative polymerase chain reaction |
| QTL | quantitative trait loci |
| *Sb* | *Sorghum bicolor* |
| S&GR | stop & glo reagent |
| TSS | transcriptional start site |
| 35S | CamV35S constitutive promoter |

# 1. General Introduction.

# 1.0 Introduction

Cell walls account for ~50% of the dry weight of plants and form the structural framework essential for their survival (Doblin et al., 2010). The various wall constituents such as cellulose and (1,3;1,4)-β-glucan also have a significant impact on diverse areas such as human nutrition, the poultry industry, brewing and baking industries and in bioethanol production. Relatively little is known about (1,3;1,4)-β-glucan synthesis, deposition and remodelling. Thus, there is great interest in increasing our understanding of (1,3;1,4)-β-glucan biosynthesis and regulation with the goal of manipulating aspects such as quantity or polysaccharide fine structure.

## 1.1 Plant Cell Walls and (1,3;1,4)-β-Glucan

Plant cell walls are highly diverse and dynamic structures that are modified throughout many processes such as cell growth, division and differentiation (Burton et al., 2008). Unlike animals, which possess a complex skeletal system, much of the structural integrity of individual cells, specific tissue types and whole plants is dependent on the structural composition of their cell walls (Doblin et al., 2010). Cell walls form a semi-rigid structure and are predominantly comprised of polysaccharides, in addition to protein and lignin. Walls provide cells with numerous attributes such as the ability to withstand strong internal and external pressures, both physical and osmotic. They also physically separate the cell from the external environment, providing varying degrees of porosity to allow solutes and signalling molecules to pass to and from the cell, and they can also act as an energy reserve (Heredia et al., 1995; Burton et al., 2010; Scheller and Ulvskov, 2010).

**Figure 1-1** illustrates the generalised architecture of primary plant cell walls; a structural framework of cellulose microfibrils that have high tensile strength, embedded in a gel-like matrix of numerous non-cellulosic polysaccharides (Heredia et al., 1995; Burton et al., 2010). The precise composition of these polysaccharides varies substantially across different species, tissues and cell types depending on the specific role of a particular cell in overall plant form and function. Attempts have been made to define the more common wall compositions, as proposed by Carpita and McCann (2008) with their interpretation of type I and type II plant cell walls. However, as with many highly complex structures that

exist in nature, this model describes two extremes when in fact, a continuum of structures exist (Doblin et al., 2010). Nevertheless, the matrix phase of dicotyledonous plant cell walls predominately consist of xyloglucans and pectic polysaccharides. In monocotyledonous plants, it mostly consists of mannans and heteroxylans with (1,3;1,4)-β-glucans also present in members of the *Poaceae* (Burton et al., 2010; Doblin et al., 2010). In most higher plants, greater strength is required in certain cells, leading to secondary wall development. Lignin, a large polyphenolic molecule, is concomitantly deposited in these walls, which makes them resistant to compressive forces, restricts the passage of small molecules and, in some cases, renders them waterproof (Boerjan et al., 2003).

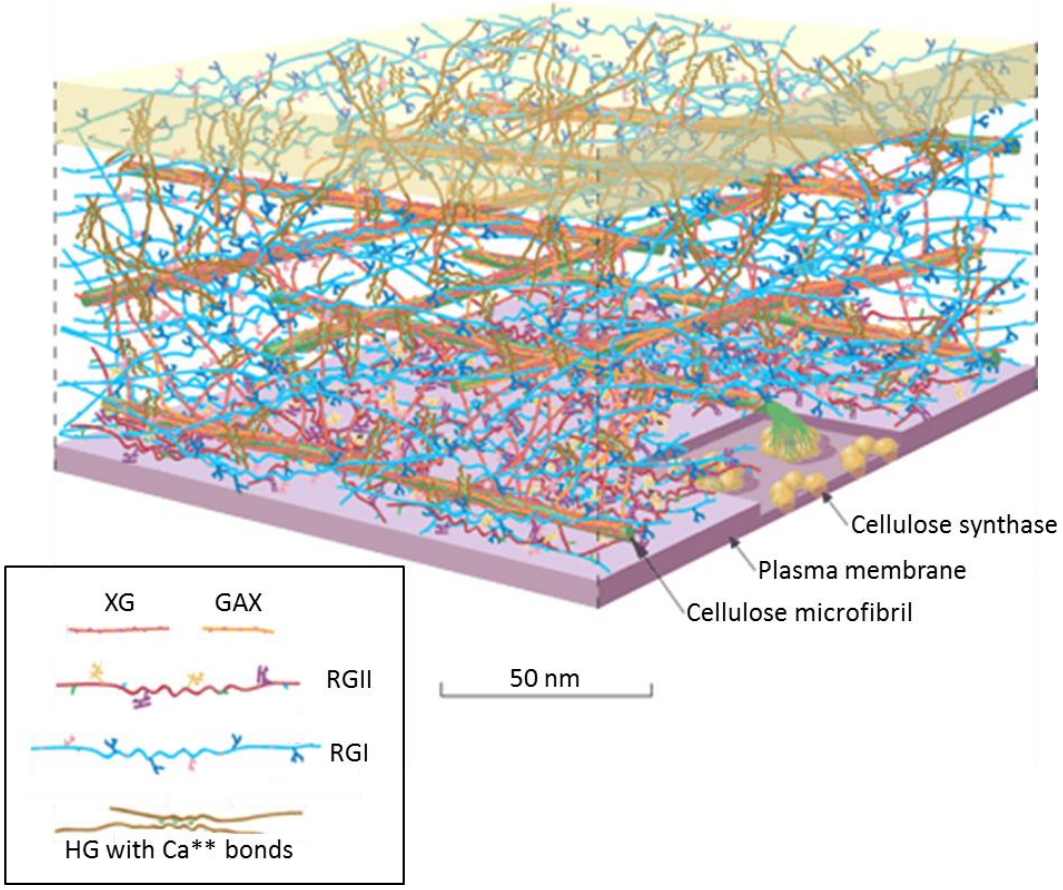


**Figure 1-1. Architecture of plant cell walls.**

An artistic representation of a typical outer layer of a plant cell as described by Somerville et al. (2004). The phospholipid bilayer of the plasma membrane lies on the inner-most surface and forms the first boundary. The middle lamella (brown shaded box) forms the outer-most surface and is rich in pectins, which act to cement cells together. The cell wall (primary wall above) lies in between and forms the semi-rigid structure responsible for the distinctive physical properties of plant cells (Doblin et al., 2010). Cellulose is common to all plant cell walls, whilst the composition of the non-cellulosic polysaccharides, shown as xyloglucan (XG), glucuronoarabinoxylan (GAX), rhamnogalacturonan I and II (RGI and RGII) and homogalacturonan (HG), differs between species and cell types.

## 1.2 The Distribution, Structure and Function of (1,3;1,4)-β-Glucans

(1,3;1,4)-β-Glucan chains are essentially composed of (1,4)-β-linked glucosyl oligosaccharide units joined by single (1,3)-β-linkages (Burton and Fincher, 2009) (**Figure 1-2**). The majority of the oligosaccharide units comprise three (cellotriosyl, DP3) or four (cellotetraosyl, DP4) glucosyl moieties joined by (1,4)-β-linkages, although unit lengths of 5-20 can be found (Woodward et al., 1983). Both the quantity and approximate ratio of cellotriosyl:cellotetraosyl units, termed degree of polymerisation (DP) or DP3:DP4 ratio, varies amongst different species and cell types, conferring varied attributes. In members of the *Poaceae* cellotriosyl and cellotetraosyl units unevenly distributed (Staudte et al., 1983). The intervening (1,3)-β-linkages form a molecular kink and since these are distributed irregularly, they prevent extensive intermolecular alignment of adjoining chains (**Figure 1-2a**). This results in the formation of a soluble gel-like matrix that is predicted to provide some structural support in addition to flexibility and porosity. Amongst the few species outside of the *Poaceae* that contain (1,3;1,4)-β-glucan in their walls, such as bryophytes and algae (Popper and Fry, 2003), DP3:DP4 ratios are typically much higher or much lower with either the cellotriosyl or cellotetraosyl units predominating (**Figure 1-2b**). In these molecules (1,3)-β-linkages are distributed regularly, allowing for extensive intermolecular alignment of adjoining chains to occur. This decreases solubility and allows microfibrils to form. The (1,3;1,4)-β-glucan chains may therefore play a more structural role in the cell walls of these organisms.

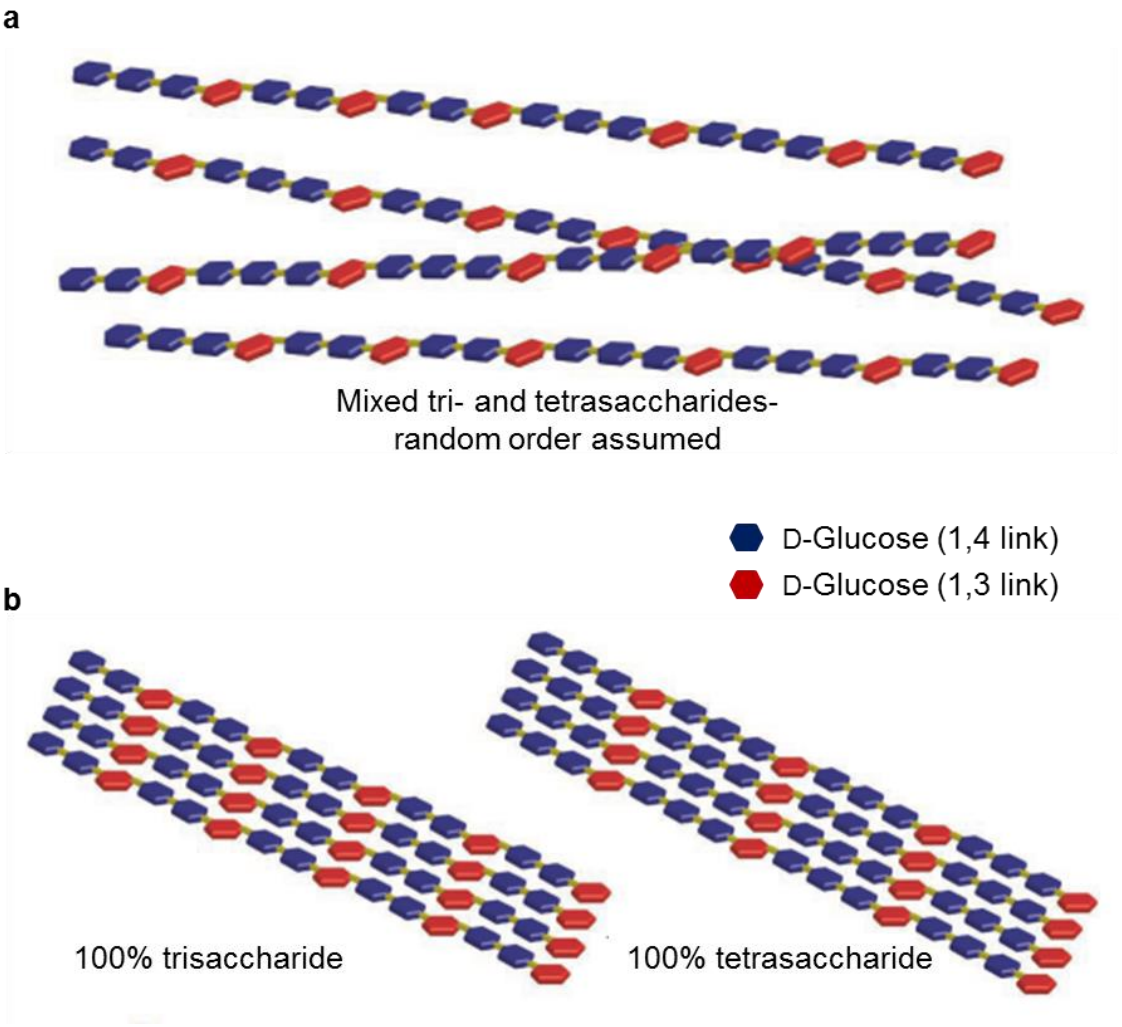


**Figure 1-2. (1,3;1,4)-β-Glucan fine structures.**

(1,3;1,4)-β-Glucan structures with (1,3)- and (1,4)- linked glucose monomers highlighted in red and blue respectively, modified from Burton et al. (2010). (**a**) Shows the chain arrangement when (1,3)-linkages are dispersed irregularly, resulting in the formation of a gel-like matrix. (**b**) Shows the chain arrangement when (1,3)-linkages are dispersed regularly, resulting in intermolecular alignment of chains and microfibril formation.

## 1.3 Human Health and Industrial Applications

Some of the world's most economically important crop and biomass plants include members of the *Poaceae* such as barley, wheat, rice and maize (Burton and Fincher, 2009). Varying quantities of (1,3;1,4)-β-glucan are present within the walls of many of their tissues including grain, leaf and stem. This influences numerous downstream applications for each tissue due to the increased viscosity of aqueous solutions that (1,3;1,4)-β-glucans impart. With respect to human nutrition, (1,3;1,4)-β-glucan is an important component of dietary fibre as it survives moderately intact along its passage through the stomach and small intestine. This occurs because humans do not produce the digestive enzymes necessary for its degradation (Topping, 2007; Collins et al., 2010). The increased solution viscosity in the small intestine is believed to decrease the rate of diffusion of digestive enzymes and degradation products (Dikeman and Fahey, 2006). However recent plant data shows that the presence of (1,3;1,4)-β-glucan in the diet of rats does not increase glucose tolerance or insulin sensitivity, yet is capable of suppressing food intake and increasing cecum fermentation (Belobrajdic et al., 2015). Once in the large intestine, a diverse range of bacteria are able to ferment the soluble dietary fibres, releasing numerous short chain fatty acids that, in turn, impart beneficial effects for human health (Topping and Clifton, 2001). Cumulatively, the presence of dietary fibres in the human diet can help to reduce bowel transit time, prevent constipation, lower blood cholesterol levels (Gallaher et al., 1993), reduce the risk of developing colorectal cancer (Bingham, 1990; Larsson et al., 2005) and help to regulate blood glucose levels for diabetes management (Bornet et al., 1987). There is also the potential to use (1,3;1,4)-β-glucans as functional food ingredients, for example, to improve the mouth-feel of low-fat dairy products (Brennan, 2005).

Conversely, in the poultry industry such non-starchy polysaccharides possess anti-nutritive properties because there is a complete resistance to their breakdown in the short digestive tract, negatively impacting bird health and reducing their growth (Almirall et al., 1995; Jacob and Pescatore, 2012). (1,3;1,4)-β-Glucans also have a negative impact in the brewing industry by interfering with fermentation and slowing the filtration process (Bamforth, 2009).

In the bioethanol industry, cell wall polysaccharides play a significant role with respect to

sugar availability. As much as 50% of dry plant biomass is represented by the wall, yet many of the polysaccharides are difficult and time consuming to ferment, which results in excessive waste (Doblin et al., 2010). Replacing these polysaccharides (e.g. cellulose or heteroxylan) with (1,3;1,4)-β-glucan may alleviate the fermentation issues, increasing bioethanol production and maintaining necessary wall characteristics pivotal to plant survival (Vega-Sάnchez et al., 2012).

## 1.4 (1,3;1,4)-β-Glucan Biosynthesis

### 1.4.1 The Cellulose Synthase Superfamily

As with all plant cell wall polysaccharides, there are large gaps in our understanding of many of the processes involved in (1,3;1,4)-β-glucan biosynthesis. In recent years, steady progress has been made in expanding this understanding. After the discovery of the *CELLULOSE SYNTHASE* (*CESA*) genes by Pear et al. (1996), analysis of various expressed sequence tag (EST) databases revealed a superfamily of genes including the *CesA* and *CELLULOSE-SYNTHASE-LIKE* (*CSL*) genes (Fincher, 2009b) (**Figure 1-3**). Mapping of genes controlling mature barley grain (1,3;1,4)-β-glucan content to specific quantitative trait loci (QTL) (Han et al., 1995) and subsequent identification of *CslF* genes in a syntenic region of the rice genome, was the first step towards isolating the genes involved in (1,3;1,4)-β-glucan biosynthesis. *Arabidopsis thaliana*, which is devoid of (1,3;1,4)-β-glucan, was transformed with rice *OsCslF* genes in proof-of-function experiments. When expressing certain *CslF* genes, (1,3;1,4)-β-glucan was produced and deposited in the cell walls as shown by immunohistochemical and enzymatic methods. This demonstrated that CSLF enzymes are capable of (1,3;1,4)-β-glucan biosynthesis (Burton et al., 2006). More recently the *CslH* gene family also was implicated in (1,3;1,4)-β-glucan biosynthesis when tested using similar experimental approaches (Doblin et al., 2009). In both cases, although expression was driven by the constitutive CamV35S promoter, only a small amount of (1,3;1,4)-β-glucan was synthesised, and in the case of *CslH*, only in certain cell types. It is therefore likely that one or more additional proteins are required to interact with CSLF and CSLH enzymes for efficient synthesis to occur. These proteins may be missing, limiting or poorly equivalent in dicot cells (Burton et al., 2006).

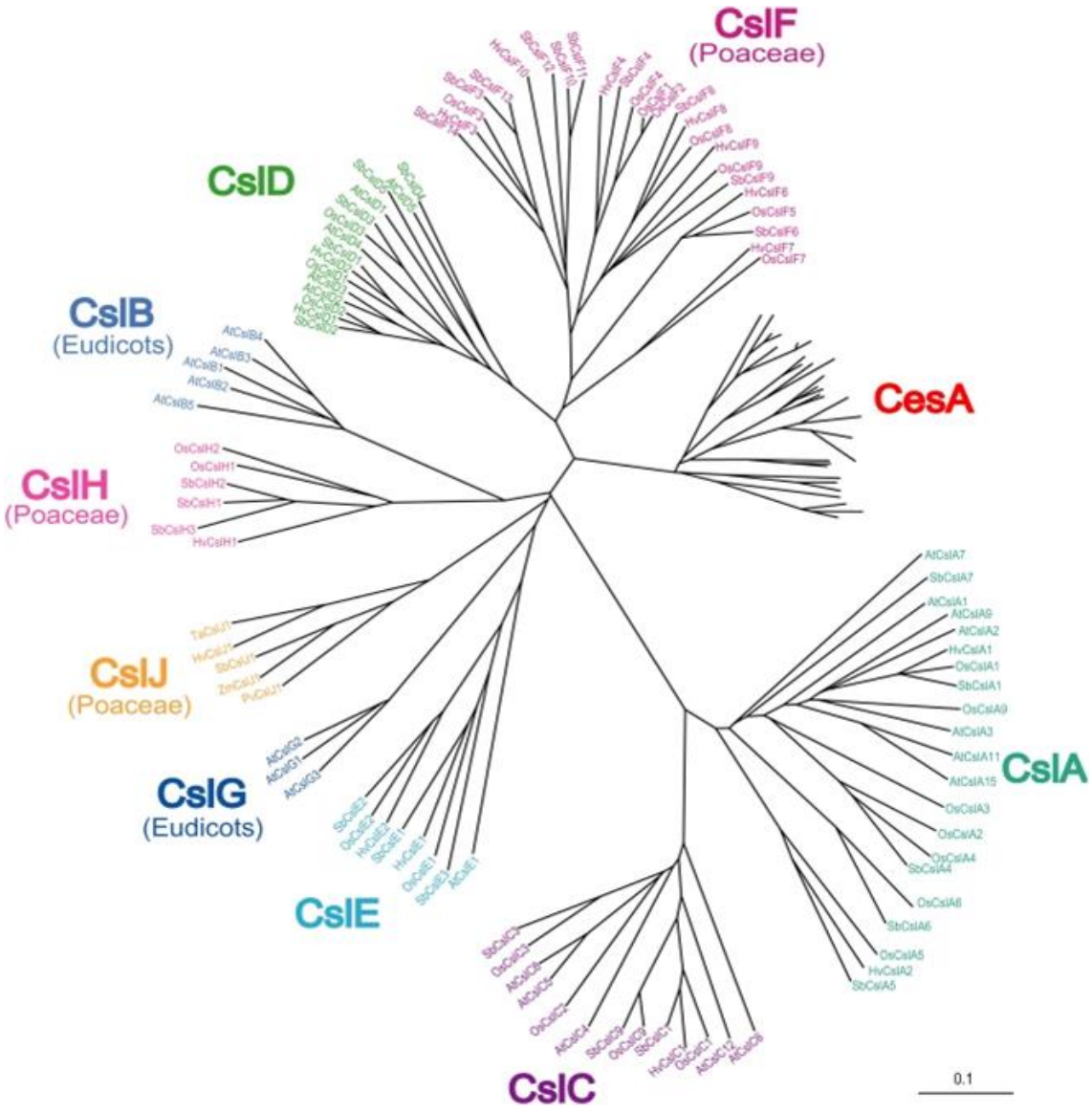


**Figure 1-3. Phylogenetic tree of the *CELLULOSE SYNTHASE* superfamily in higher plants.**

An extended tree of the *CesA* superfamily for *Hv* (barley; *Hordeum vulgare*), *Sb* (sorghum; *Sorghum bicolor*), *Os* (rice, *Oryza sativa*), *At* (mouse-ear cress; *Arabidopsis thaliana*), *Ta* (wheat; *Triticum aestivum*), *Zm* (corn; *Zea mays*) and *Pv* (switchgrass; *Panicum virgatum*) of which the members have been classified into a number of sub-families (Fincher, 2009b). Of these, *CesA*, *CslA*, *CslC* and *CslD* have been identified in all land plants examined; *CslB* and *CslG* have only been identified in dicots and *CslF*, *CslH* and *CslJ* identified only in members of the *Poaceae*.

### 1.4.2 *CslF* Genes in Barley

Since the discovery of the *CslF* gene family, numerous analyses have been performed in an attempt to understand their role and influence in the overall process of (1,3;1,4)-β-glucan biosynthesis. For these studies, barley has proven the most suitable system to investigate, because it possesses ten *CslF* genes (Schreiber et al., 2014) and has (1,3;1,4)-β-glucan levels ranging from ~5% dry weight in walls of stems to ~70% in the walls of starchy endosperm cells (Fincher and Stone, 2004). Transcript analysis by real-time quantitative PCR (Q-PCR) in extracts from sixteen barley tissues has shown that each gene exhibits individual patterns of transcript abundance (Burton et al., 2008). Most display low transcript levels across the tissues examined, with *HvCslF6* the exception since it displays high transcript levels in most tissues. During endosperm development, two *CslF* transcripts stand out. *HvCslF9* transcripts are high in early stages peaking 8 days after pollination (DAP), whilst *HvCslF6* transcript levels are high throughout development, particularly in latter stages around 16-24 DAP. These data therefore suggest that *HvCslF9* and *HvCslF6* primarily influence endosperm (1,3;1,4)-β-glucan production, however, protein levels or activity do not necessarily relate to transcript abundance (Burton et al., 2008; Burton and Fincher, 2009). The influence of specific genes cannot be determined by transcript abundance alone and those *CslF* genes represented to a lesser degree should not be interpreted as being inactive in these tissues.

Experiments have been performed in barley with the intention of increasing (1,3;1,4)-β-glucan levels in grain and vegetative tissues (Burton et al., 2011). *HvCslF4*, *HvCslF6* and *HvCslF8* were tested using the CamV35S constitutive promoter (35S) and *HvCslF3*, *HvCslF4*, *HvCslF6*, *HvCslF8* and *HvCslF9* were tested using the endosperm specific oat globulin (*As*GLO) promoter (Vickers et al., 2006). These genes were selected because their transcripts are found at varying levels in developing grain and at a QTL for grain (1,3;1,4)-β-glucan content (Han et al., 1995). Constitutive expression of *HvCslF6* generated three to four fold higher (1,3;1,4)-β-glucan levels in the leaves, with increases in leaf thickness and cell wall size. Constitutive expression of *HvCslF4* resulted in 50% higher levels of (1,3;1,4)-β-glucan in the grain. When the grain specific promoter was used, only *HvCslF6* resulted in elevated grain (1,3;1,4)-β-glucan levels. All other genes had little or no effect. In summary,

*HvCslF6* and *HvCslF4* exhibited different effects when expressed within different tissues, which showed that increased absolute transcript abundance did not correlate well with final (1,3;1,4)-β-glucan levels. This suggests that other factors are required for increased polysaccharide synthesis. In addition to increased (1,3;1,4)-β-glucan content, the grain DP3:DP4 ratios changed from 2.6:1 in wild-type lines to 2.1:1 and 2.8:1 for *As*GLO:*HvCslF6* and 35S:*HvCslF4* transgenic lines, respectively. This suggests that individual CSLF enzymes are producing (1,3;1,4)-β-glucan with different DP3:DP4 ratios and it is the cumulative action of their activity that gives rise to the final DP3:DP4 ratio in any particular tissue (Burton et al., 2011).

### 1.4.3 CslF Genes and Proteins

Members of the *CslF* gene family are closely related at the nucleotide level and in gene intron:exon structure (Burton et al., 2008) (**Figure 1-4a**). Amongst the barley CSLF enzymes, amino acid identities vary from 40% to 63% with higher values in conserved protein regions. Characteristic of family GT2 glycosyltransferases, the putative catalytic site residues D, D, D, QxxRW (Doblin et al., 2002) are present in each of the CSLF family members. Eight predicted transmembrane helices are evident (Burton et al., 2008), with two located near the $NH_2$-terminus, and six near the COOH-terminus of the protein. CSLF6 differs most noticeably from other CSLF proteins due to the presence of additional amino acids in the 'extra-region' (**Figure 1-4b**). This region is 54 amino acids long in *Hv*CSLF6, compared with 15–20 amino acids in the other CSLF members (Burton et al., 2011) (**Figure 1-4c**).

**a**

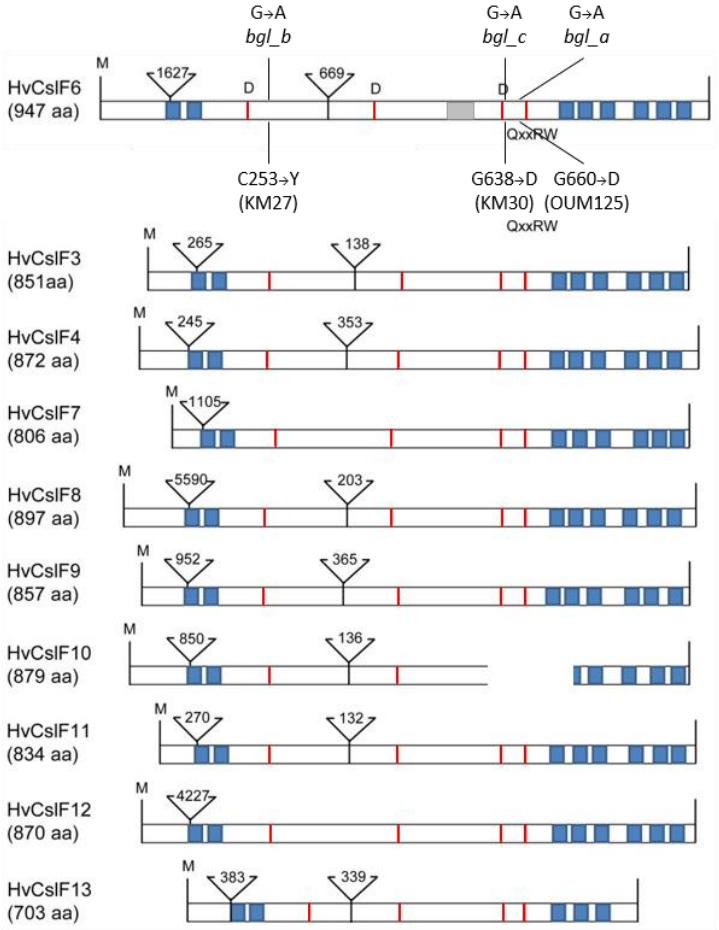
G→A
bgl_b
G→A
bgl_c
G→A
bgl_a
HvCslF6
(947 aa)
M
1627
669
D
D
D
QxxRW
C253→Y
(KM27)
G638→D
(KM30)
G660→D
(OUM125)
QxxRW
HvCslF3
(851aa)
265
138
HvCslF4
(872 aa)
245
353
HvCslF7
(806 aa)
1105
HvCslF8
(897 aa)
5590
203
HvCslF9
(857 aa)
952
365
HvCslF10
(879 aa)
850
136
HvCslF11
(834 aa)
270
132
HvCslF12
(870 aa)
4227
HvCslF13
(703 aa)
383
339

**b**

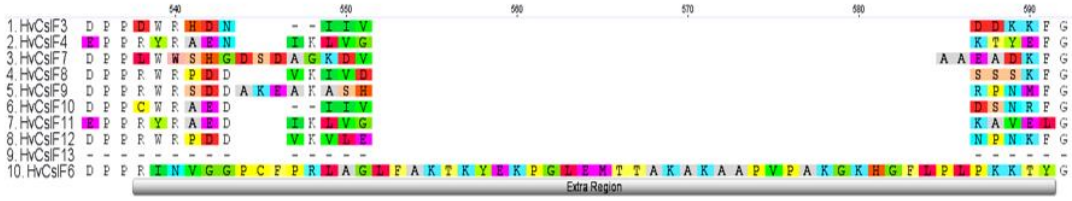
1. HvCslF3
2. HvCslF4
3. HvCslF7
4. HvCslF8
5. HvCslF9
6. HvCslF10
7. HvCslF11
8. HvCslF12
9. HvCslF13
10. HvCslF6
Extra Region

**c**

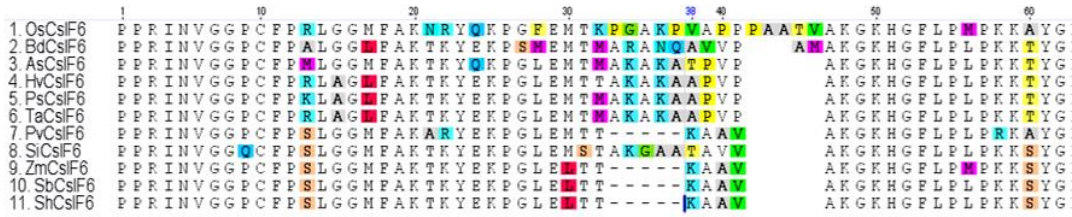
1. OsCslF6
2. BdCslF6
3. AsCslF6
4. HvCslF6
5. PsCslF6
6. TaCslF6
7. PvCslF6
8. SiCslF6
9. ZmCslF6
10. SbCslF6
11. ShCslF6

**Figure 1-4. CSLF gene structure and protein alignment.**

Adapted from Burton et al. (2008), Taketa et al. (2011) and Schreiber et al. (2014), (**a**) shows the structural similarities between each of the barley *CslF* genes. Triangles show intron positions with numbers indicating nucleotide length, red bars show the D, D, D and QxxRW motifs believed to be involved in substrate binding and catalytic activity, blue bars indicate predicted transmembrane helixes, the grey box defines the extra region and in *HvCslF6* the mutations present in *betaglucanless* lines are marked (Taketa et al., 2011). (**b**) The *Hv*CSLF6 extra region aligned against the remaining barley CSLF members. **c** compares the amino acid compositions of the extra regions of *Os* (rice; *Oryza sativa*), *Bd* (purple false brome; *Brachypodium distachyon*), *As* (oat; *Avena sativa*), *Hv* (barley, *Hordeum vulgare*), *Ps* (bluebunch wheatgrass; *Pseudoroegneria spicata*), *Ta* (wheat; *Triticum aestivum*), *Pv* (switchgrass; *Panicum virgatum*), *Si* (foxtail millet; *Setaria italica*), *Zm* (corn; *Zea mays*), *Sb* (sorghum; *Sorghum bicolor*) and *Sh* (sugarcane; *Saccharum hybrida*) CSLF6 synthases.

A study examining three independent *betaglucanless* barley mutants by Taketa et al. (2011) revealed that mutations near the highly conserved regions of *Hv*CSLF6 resulted in lines with no detectable (1,3;1,4)-β-glucan in any of the tissues tested. The detection method used was not the most sensitive method available and confirmation by immunohistochemistry still needs to be performed. The lack of detection was supported by an absence of (1,3;1,4)-β-glucan synthase activity in the microsomal fractions derived from endosperm tissue, compared with that from wild-type lines. When *Hv*CSLF6 was transiently expressed in leaves of *Nicotiana benthamiana*, those from *betaglucanless* lines generated no detectable (1,3;1,4)-β-glucan, as compared to 1-3% dry weight produced by wild-type *Hv*CSLF6. These results therefore imply, that in barley at least, the CSLF6 protein plays a key role in (1,3;1,4)-β-glucan biosynthesis for which other CSLF and CSLH enzymes are unable to compensate. The central role of CSLF6 is supported by data from Nemeth et al. (2010). Here, transformation of wheat with a *TaCslF6* RNA-interference construct generated a fourfold decrease in *TaCslF6* transcript levels in grain at 14 days post anthesis, resulting in a 42.2% reduction of grain (1,3;1,4)-β-glucan. However, there was no notable alteration in the DP3:DP4 ratio of the remaining (1,3;1,4)-β-glucan as a result of CSLF6 suppression. Therefore, if the final DP3:DP4 ratio is a hallmark of each particular synthesising enzyme, then the unaltered ratio suggests that *Ta*CSLF6 is responsible for the majority of the (1,3;1,4)-β-glucan synthesised in wheat grain.

Dimitroff (2011) investigated the function of barley, sorghum and rice CSLF6 enzymes in *Nicotiana benthamiana* leaves and rice callus tissues. In *N. benthamiana* leaves these enzymes generated 1.4%, 2.9% and 0.2% (w/w) (1,3;1,4)-β-glucan, respectively, at DP3:DP4 ratios of 1.68±0.03:1, 0.98±0.01:1 and 1.57±0.01:1, respectively. These values are considerably different from those found in the native starchy endosperm tissues of these species, which are 4–10% at 2.6:1 for barley, 0.06–0.14% at 2.8:1 for sorghum and 0.02% at 1.4:1 for rice (Burton and Fincher, 2012). However, given that the genes were expressed in the *N. benthamiana* background, which does not naturally produce (1,3;1,4)-β-glucan, such an outcome may not be surprising. In rice callus substantially higher (1,3;1,4)-β-glucan amounts were generated with ratios more reflective of those found in the original organisms (Dimitroff, 2011). As in *N. benthamiana*, when comparing *Os*CSLF6 to *Hv*CSLF6, *Os*CSLF6 produced substantially less (1,3;1,4)-β-glucan in rice callus (maximum of 2.5%

versus 16%, respectively) and of a marginally lower DP3:DP4 ratio (2.5-3.1:1 versus 2.7-3.3:1). As for *Sb*CSLF6, only a few lines survived selection. These appeared to contain much lower amounts of (1,3;1,4)-β-glucan and proliferated far more slowly than other lines, suggesting an increased metabolic load. As *Sb*CSLF6 generated twice the amount of (1,3;1,4)-β-glucan as *Hv*CSLF6 in *N. benthamiana*, it is likely that a large amount, possibly exceeding the 16% maximum produced by *Hv*CSLF6, was being synthesised in the rice callus. This may have caused an imbalance in glucose utilization, reducing growth rates and allowing only silenced transformants to proliferate. Such an effect of 'toxic' levels of (1,3;1,4)-β-glucan has previously been reported by Burton et al. (2011). Overall, these results demonstrate how the functions of different CSLF6 enzymes vary according to their source organism and indicate that primary sequence variations are influencing both (1,3;1,4)-β-glucan production and the DP3:DP4 ratio.

Recently Jobling (2015) showed that when expressed in *N. benthamiana* leaves, CSLF6 enzymes from *Bd* (*Brachypodium distachyon*), *Ta* (*Triticum aestivum*), *Hv* (*Hordeum vulgare*), *Zm* (*Zea mays*), *As* (*Avena sativa*), *Os* (*Oryza sativa*) and *Sb* (*Sorghum bicolor*) each produced (1,3;1,4)-β-glucan of a defined DP3:DP4 ratio despite considerable variation in the total levels produced. Although the exact DP3:DP4 ratios differ from Dimitroff (2011), both studies suggest that CSLF6 itself influences the DP3:DP4 ratio and that polymorphisms between species and cultivars influence the final ratio. By generating a series of chimeric constructs between four *CslF6* cDNAs and expressing them *N. benthamiana* leaves, Jobling (2015) was also able to identify a small section of CSLF6 responsible for much of the difference in DP3:DP4 ratio observed between the synthases. Point mutation constructs then defined a Leu to Ile polymorphism in the fourth predicted transmembrane helix to be responsible. CSLF6 enzymes with the Ile typically displayed a DP3:DP4 ratio above 1.4:1 whilst those with the Leu were below 1.4:1. This result demonstrates that CSLF6 pore architecture is one factor that influences DP3:DP4 ratio.

## 1.4.4 Synthesis of (1,3;1,4)-β-Glucan

Many of the enzymes involved in cell wall polysaccharide biosynthesis are integral membrane proteins, making them particularly difficult to purify and characterise. This has substantially hindered our progress in understanding the synthesis, deposition and remodelling of polysaccharides in plant cell walls. Attempts to identify the subcellular location of (1,3;1,4)-β-glucan biosynthesis have been misleading, with some evidence consistently pointing towards (1,3;1,4)-β-glucan synthase activity in the Golgi (Henry and Stone, 1982; Gibeaut and Carpita, 1993) and some evidence pointing towards the plasma membrane as the primary site of synthesis (Wilson et al., 2015). The Golgi synthesis theory has arisen from experiments involving the isolation of cellular membrane fractions and tracking of [$^{14}$C]-glucose incorporation into polysaccharides. *Hv*CSLH has been detected immunocytochemically in the Golgi vesicles and ER of transgenic *Arabidopsis* lines (Doblin et al., 2009), while Carpita and McCann (2010) reported (1,3;1,4)-β-glucan at the periphery of Golgi stacks and in vesicles of cells in developing maize coleoptiles. In contrast, extensive efforts by other groups have consistently been unable to detect (1,3;1,4)-β-glucan associated with the Golgi, even when the wall itself is heavily labelled by the specific antibody (Wilson et al., 2006; Wilson et al., 2012).

One theory has therefore emerged that (1,3;1,4)-β-glucans may be synthesised in a two phase process (Burton and Fincher, 2009). Oligosaccharide units may be synthesised in the Golgi, perhaps by CSLF or CSLH enzymes, attached to a carrier molecule and transported to the wall. In this state, they would not be detected by the (1,3;1,4)-β-glucan-specific monoclonal antibody BG1 (Meikle et al., 1994). Once at the plasma membrane, a single protein or a complex, possibly containing CSLF, CSLH, CSLJ or other biosynthetic enzymes could assemble the units, form the (1,3)-β-linkage and allow the simultaneous deposition of the polysaccharide into the wall (Burton and Fincher, 2009; Fincher, 2009a). Recently Kim et al. (2015) were able to show that in both *N. benthamiana* and *Pichia pastoris*, *Bd*CSLF6 is able to synthesise (1,3;1,4)-β-glucan. Since the protein expressed in *Pichia* was not in contact with any other plant synthase, this suggests that the CSLF6 enzyme is able to catalyse the formation of both the (1,3)- and (1,4)-β-glycosidic linkages present in (1,3;1,4)-β-glucan. However, the authors could not rule out the possibility that *Bd*CSLF6 was

interacting with a yeast enzyme and failed to provide any information regarding the structure of the polysaccharide produced, and if it differed between expression systems (Kim et al., 2015).

Using protease cleavage assays on *Pichia* microsomal fractions, Kim et al. (2015) were also able to show that the $NH_2$-terminus, COOH-terminus and catalytic domain of CSLF6 lie in the cytoplasm (**Figure 1-5**). The synthase therefore appears to be utilizing the cytoplasmic pool of UDP-glucose to synthesise (1,3;1,4)-β-glucan, which is then transported across a membrane. YFP-tagging also placed *Bd*CSLF6 at the Golgi when expressed in *N. benthamiana* leaves. This is contradictory to recent findings by Wilson et al. (2015) who showed that CSLF6 from barley, wheat, ryegrass and maize was found at the endoplasmic reticulum, Golgi, post-Golgi secretory vesicles and the plasma membrane in cryofixed sections from various tissues. The Golgi location of *Bd*CSLF6 reported by Kim et al. (2015) may be due to expression in a non-cereal system. Alternatively, as *Brachypodium* contains four times as much (1,3;1,4)-β-glucan, and with a much higher DP3:DP4 ratio of 5.9:1 compared with less than 3.2:1 in other species (Burton and Fincher, 2012), *Bd*CSLF6 may function differently to other CSLF6 enzymes. In any case, it is clear that our understanding of the location and mechanism of (1,3;1,4)-β-glucan biosynthesis is limited and will be debated for some time.

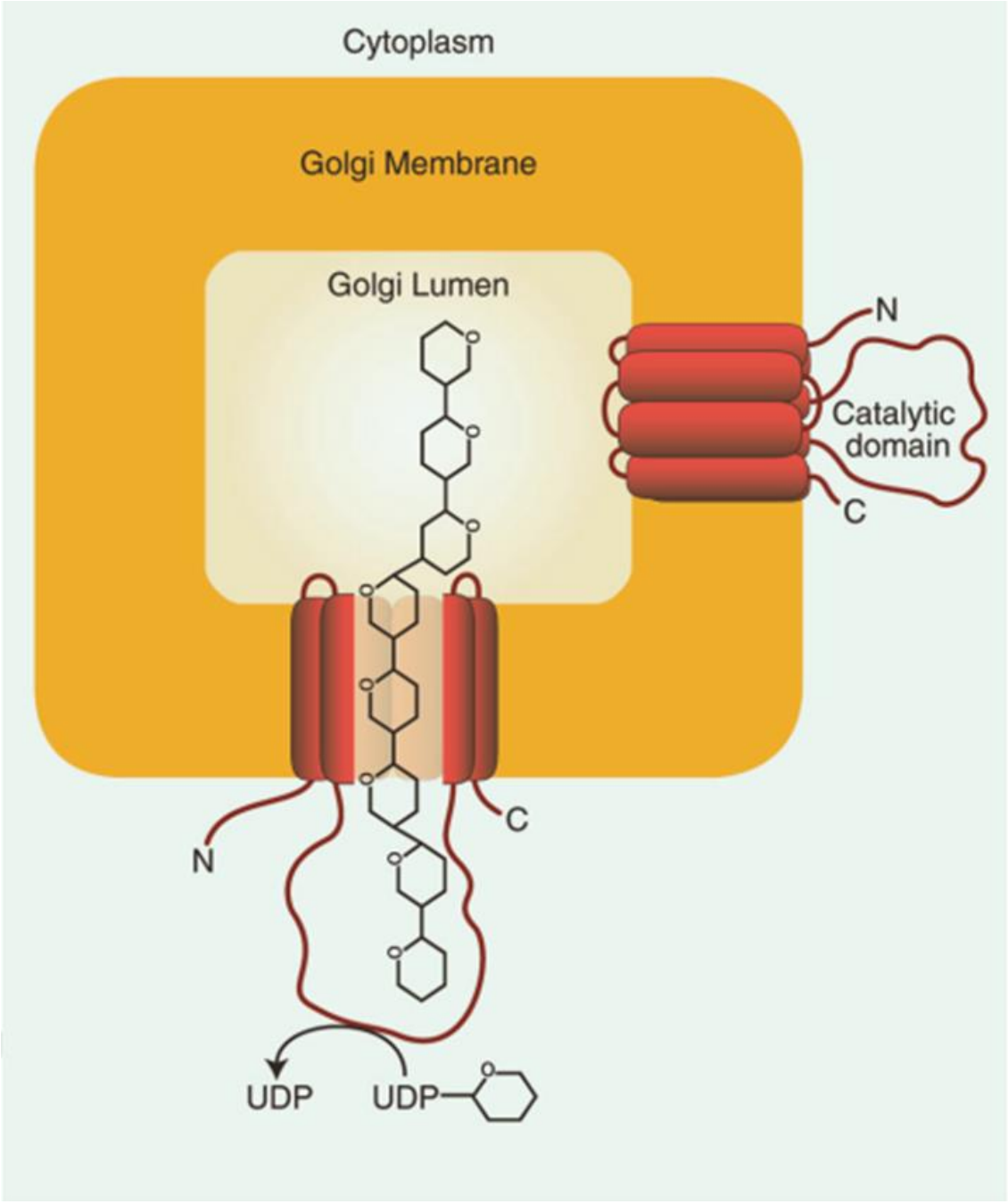


**Figure 1-5. Model of *Bd*CSLF6 membrane topology**

Current model of CSLF6 function in *Brachypodium* showing the synthase (red) embedded in the Golgi membrane with the $NH_2$-terminus, COOH-terminus and catalytic domain in the cytoplasm. UDP-glucose is taken from the cytoplasmic pool, and the elongating (1,3;1,4)-β-glucan chain accumulates in the Golgi lumen prior to wall deposition via an undescribed mechanism. Adapted from Kim et al. (2015).

# 2. (1,3;1,4)-β-Glucan Biosynthesis by the CSLF6 Enzyme in the Poaceae: Determinants of Specific Activity and Product Fine Structure

## 2.0 Abstract

*CELLULOSE SYNTHASE-LIKE F6* (*CslF6*) genes encode polysaccharide synthases responsible for (1,3;1,4)-β-glucan biosynthesis in cereal grains. However, it is not clear how both (1,3)- and (1,4)-linkages are incorporated into a single polysaccharide chain and how the frequency and arrangement of the two linkage types that define the fine structure of the polysaccharide are controlled. Through transient expression in *Nicotiana benthamiana* leaves, three CSLF6 orthologs from different cereal species were shown not only to mediate the synthesis of significantly different amounts of (1,3;1,4)-β-glucan, but also to produce (1,3;1,4)-β-glucans with very different fine structures. Chimeric cDNA constructs with interchanged sections of the barley and sorghum *CslF6* genes were developed to identify regions of the enzyme responsible for these differences. In addition, single amino acids within the catalytic region were shown to influence either (1,3;1,4)-β-glucan production or fine structure. For example, a Y680F mutation in the sorghum protein led to a 72% reduction in the amount of (1,3;1,4)-β-glucan synthesised in the heterologous expression system, while a G638D substitution dramatically changed the fine structure of the polysaccharide. The structural basis of these effects can be rationalized by reference to a homology model of the enzyme and appear to be related to the opening of the UDP-Glc substrate binding site. The regions and amino acid residues identified provide opportunities to manipulate the solubility and amount of (1,3;1,4)-β-glucan in grains and vegetative tissues of the grasses and, in particular, to enhance levels of soluble dietary fibre that are beneficial to human health.

## 2.1 Introduction

Cereal grains of wheat, maize and rice are food staples for the majority of human societies. Their cell walls are composed of a structural framework of cellulosic microfibrils embedded in a matrix phase of non-cellulosic polysaccharides that include predominantly heteroxylans and (1,3;1,4)-β-glucans. The presence of (1,3;1,4)-β-glucan is a distinguishing feature of *Poaceae* cell walls, although the polysaccharide is occasionally found at low levels in other species (Harris and Fincher, 2009). Considerable attention has been given to the beneficial effects of (1,3;1,4)-β-glucan on human health (Brennan, 2005), as a source

of fermentable sugars for bioethanol production (McLaren, 2005) and for its undesirable impact on filtration in the brewery (Bamforth, 2009).

The cereal (1,3;1,4)-β-glucans consist of unbranched and unsubstituted chains in which short stretches of (1,4)-β-linked glucosyl residues are separated by single (1,3)-β-linkages (Woodward et al., 1983). The (1,3)-β-linkages are irregularly spaced and thus form irregularly spaced molecular kinks that limit intermolecular alignment of chains into crystalline fibres (Fincher, 2009b). The overall compositions of cereal grain (1,3;1,4)-β-glucans are typically 25 to 30% (1,3)-β-glucosyl residues and 70 to 75% (1,4)-β-glucosyl residues (Fincher and Stone, 2004). Oligosaccharides of three (cellotriosyl) or four (cellotetraosyl) adjacent (1,4)-β-linked glucosyl residues account for approximately 90% (w/w) of the polysaccharide in barley, with the remainder consisting of longer chains with a degree of polymerisation (DP) of up to 12 to 15 (Woodward et al., 1983). Thus, there are random and non-random elements of linkage arrangement in (1,3;1,4)-β-glucans. The (1,3)-linkages are inserted non-randomly, because two or more adjacent (1,3)-linkages are rarely if ever found, despite the fact that these linkages account for 25 to 30% of linkages in the polymer. In contrast, the cellotriosyl and cellotetraosyl residues are randomly arranged (Staudte et al., 1983).

The ratio of cellotriosyl:cellotetraosyl units is termed the DP3:DP4 ratio, which is a useful indicator of (1,3;1,4)-β-glucan fine structure and hence of its solubility and physicochemical properties (Lazaridou and Biliaderis, 2007). (1,3;1,4)-β-Glucans with very high or very low DP3:DP4 ratios are less soluble than (1,3;1,4)-β-glucans with commonly observed ratios that range from 1.5:1 to 2.5:1, and these differences in fine structure therefore affect the performance of cereal grains in industrial applications (Burton et al., 2010).

Although the structures of (1,3;1,4)-β-glucans are known, progress in understanding the mechanism by which the polysaccharide is synthesised has been relatively slow. Central but currently unanswered questions related to the molecular mechanism of (1,3;1,4)-β-glucan synthesis include: a) How are single (1,3)-β-glucosyl residues inserted in the growing polysaccharide chain? b) How are the cellotriosyl and cellotetraosyl units arranged randomly? c) How is the DP3:DP4 ratio regulated? d) What is the origin of the longer blocks of adjacent (1,4)-β-glucosyl residues?

The genes encoding (1,3;1,4)-β-glucan synthases have been identified (Burton et al., 2006; Doblin et al., 2009). Following the discovery of the *CELLULOSE SYNTHASE* (*CesA*) genes, database analyses revealed a superfamily of genes including both *CesA* and *CELLULOSE SYNTHASE-LIKE* (*Csl*) genes (Richmond and Somerville, 2000; Hazen et al., 2002). There is compelling evidence to suggest that of the genes in the *CslF* clade, *CslF6* is the most influential in (1,3;1,4)-β-glucan biosynthesis. This is based on the high levels of transcription of *CslF* genes in most tissues of barley (Burton et al., 2008), on gene overexpression studies that lead to increased (1,3;1,4)-β-glucan levels in transgenic barley grain (Burton et al., 2011), on beta-glucan-less barley mutants in which the *CslF6* gene is mutated (Taketa et al., 2011) on RNA interference studies that lead to reduced levels of (1,3;1,4)-β-glucans in wheat (Nemeth et al., 2010) and in transposon inserted lines where *CslF6* is knocked out in rice (Vega-Sάnchez et al., 2012).

The amino acid sequence of the CSLF6 enzyme shares many similarities with cellulose synthases of plants (CESA) and bacteria (BCSA). The crystal structure of a BACTERIAL CELLULOSE SYNTHASE A (BSCA) subunit from the bacterium *Rhodobacter sphaeroides* has been defined (Morgan et al., 2013; Morgan et al., 2014). The bacterial BCSA subunit shows many structural similarities to the *in silico* predicted model of a plant CESA (Sethaphong et al., 2013). Two regions that are present in plant CESA enzymes and CSLF6, but not in BCSA, are the plant-conserved region (P-CR) and the highly variable class-specific region (CSR). One feature conserved amongst all cellulose synthases and cellulose synthase-like enzymes is the D, D, TED and QxxRW motifs that comprise the nucleotide sugar-binding and catalytic residues of the active site (Richmond and Somerville, 2000; Morgan et al., 2013). A distinguishing feature of the CSLF6 protein is an insert of approximately 55 amino acid residues that is highly conserved in orthologous CSLF6 proteins in grasses, but which is not found in other members of the CSLF families (Burton et al., 2008).

Here, a chimeric approach has been used to investigate regions and specific amino acids of the CSLF6 protein that influence (1,3;1,4)-β-glucan production and polysaccharide fine structure, as measured by DP3:DP4 ratios, in the heterologous system *Nicotiana benthamiana*. An *in silico* protein-threaded model of CSLF6, based primarily on the BCSA crystal structure, has been used to explain how specific amino acids influence the amount

and fine structure of the (1,3;1,4)-β-glucan synthesised.

## 2.2 Results

### 2.2.1 CSLF6 Orthologs Produce Different Amounts of (1,3;1,4)-β-Glucan with Different Fine Structures

The CSLF6 orthologs from rice, barley and sorghum were transiently expressed in *N. benthamiana* leaves, using *Agrobacterium* infiltration. (1,3;1,4)-β-Glucan was detected in the *N. benthamiana* leaves through immunocytochemical methods in which an antibody specific for the polysaccharide was used to probe tissue sections (**Figure 2-1**). Levels were quantitated following enzymic hydrolysis of the polysaccharide with a specific (1,3;1,4)-β-glucanase, and HPLC analysis of products released was used to determine the DP3:DP4 ratio. In the heterologous *N. benthamiana* system, which is normally devoid of (1,3;1,4)-β-glucan, rice *Os*CSLF6 expression resulted in the smallest amount of (1,3;1,4)-β-glucan, at 0.2% w/w (**Figure 2-2a**). Barley *Hv*CSLF6 expression resulted in 1.4% w/w (1,3;1,4)-β-glucan and sorghum *Sb*CSLF6 expression resulted in 2.9% w/w (1,3;1,4)-β-glucan. The *Os*CSLF6 and *Hv*CSLF6 enzymes produced (1,3;1,4)-β-glucans with DP3:DP4 ratios of 1.57±0.01:1 and 1.68±0.03:1, respectively, whilst the ratio of (1,3;1,4)-β-glucan synthesised by *Sb*CSLF6 was markedly lower at 0.98±0.01:1.

Comparable differences in (1,3;1,4)-β-glucan production and DP3:DP4 ratio were also observed in *Phaseolus vulgaris* leaves using similar experimental techniques, and in stably transformed rice callus tissues (**Figure 2-2 b** and **c**). Amino acid sequences of the CSLF6 enzymes from barley and sorghum have been aligned (**Supplementary Figure 7-1, p128**).

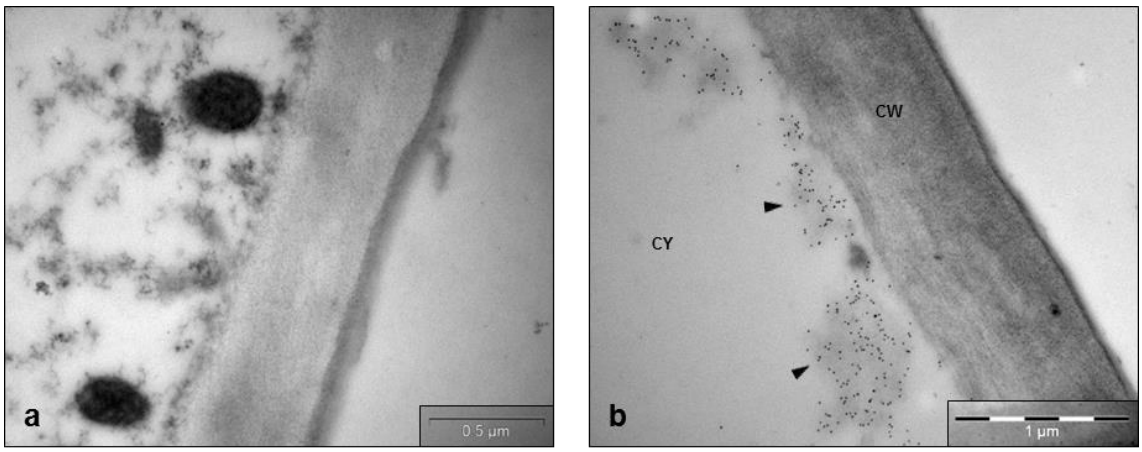


**Figure 2-1: Gold immunolabelling of (1,3;1,4)-β-glucan in *N. benthamiana* leaves.**

Transmission electron micrographs of gold immunolabelled (1,3;1,4)-β-glucan in wild type (**a**) and *Hv*CSLF6 expressing (**b**) *N. benthamiana* leaves. Arrows indicate where labelling is evident on the cytoplasmic (CY) face of the cell wall (CW).

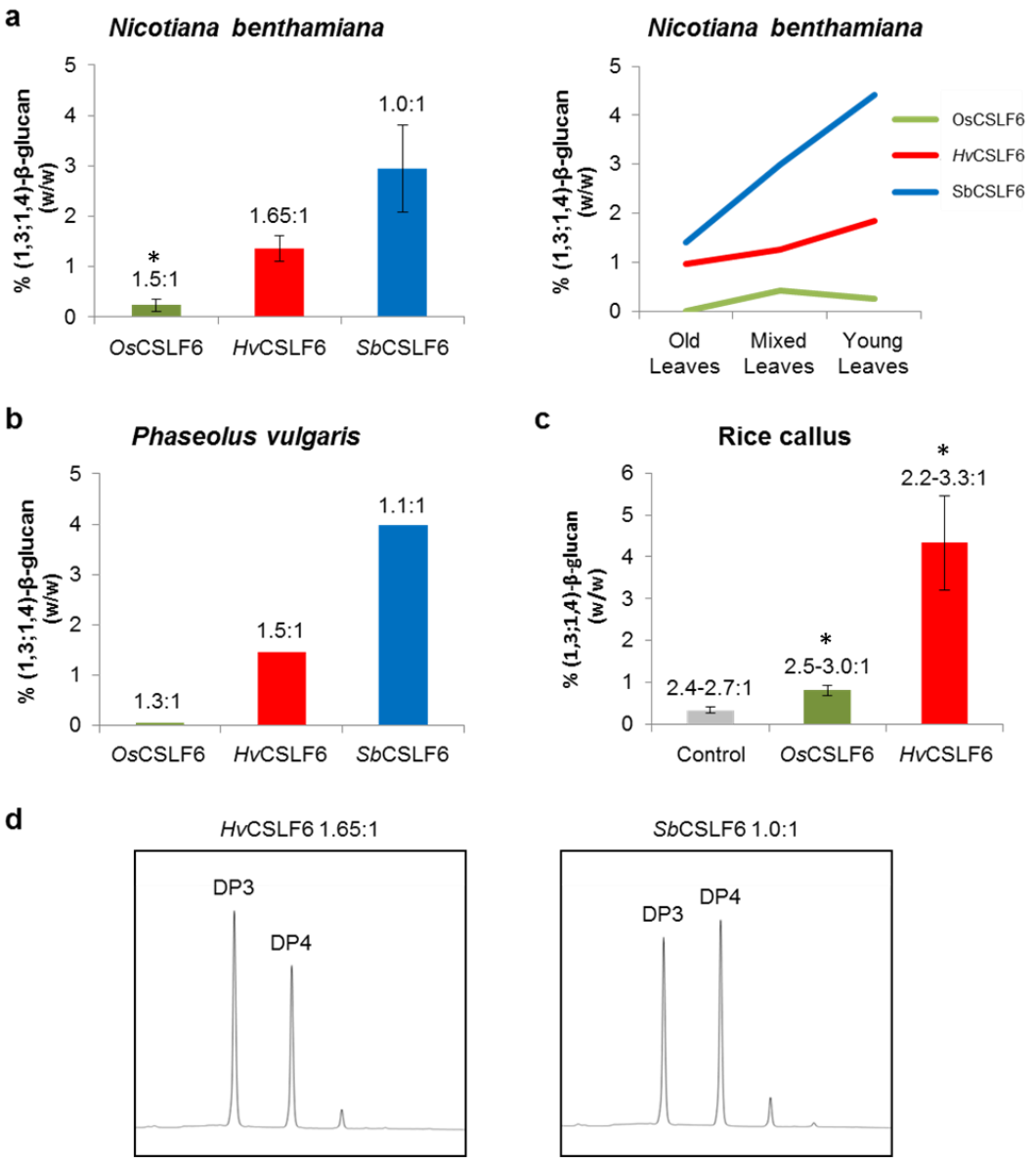


**Figure 2-2. (1,3;1,4)-β-Glucan amounts and fine structure produced by the heterologous expression of CSLF6 orthologs.**

Levels of (1,3;1,4)-β-glucan (% w/w) produced by CSLF6 from *Os*CSLF6, *Hv*CSLF6 and *Sb*CSLF6 when expressed in (**a**) *N. benthamiana* leaves (n = 3), (**b**) *Phaseolus vulgaris* leaves (n = 2) and (**c**) rice callus (n = 15). Asterisk above columns denote statistical significance (P≤0.05). Polysaccharide DP3:DP4 ratios are shown above the columns for the respective synthases and the error bars represent the standard error. (**d**) Dionex traces of DP3 and DP4 peaks post lichenase digestion of (1,3;1,4)-β-glucan samples produced in *N. benthamiana* leaves.

## 2.2.2 Managing Variability in the Heterologous Expression System

We have observed over several years that heterologous expression levels in *N. benthamiana* can vary with the plant tissue and with assay conditions. Here, (1,3;1,4)-β-glucan levels produced by the expression of CSLF6 orthologs varied between replicates and was influenced by factors such as plant age and leaf developmental stage, with the largest amount of (1,3;1,4)-β-glucan observed in younger leaves (**Figure 2-2a**). However, consistent differences in the amount and fine structure of synthesised (1,3;1,4)-β-glucans were observed at all leaf ages, with *Os*CSLF6 always producing the smallest, and *Sb*CSLF6 producing the largest amount of (1,3;1,4)-β-glucan. To reduce variation, all plants were simultaneously infiltrated in triplicate and at the same developmental stage, and leaves in the same relative positions in each plant were used. Under these conditions, clear and consistent differences in (1,3;1,4)-β-glucan levels were observed between experiments when *Hv*CSLF6 and *Sb*CSLF6 were expressed (**Figure 2-3a**). Normalising final (1,3;1,4)-β-glucan levels showed that *Sb*CSLF6 consistently produced about twice as much (1,3;1,4)-β-glucan as *Hv*CSLF6 (**Figure 2-3b**). Irrespective of the total (1,3;1,4)-β-glucan levels produced in each replicate, the DP3:DP4 ratios of the polysaccharides produced by each ortholog remained constant throughout (**Figure 2-3 c** and **d**). These results confirmed the efficacy of the *N. benthamiana* model system for comparative studies on the amounts and fine structures of (1,3;1,4)-β-glucans synthesised during heterologous expression of the CSLF6 enzymes.

Q-PCR was performed across a six day expression time course (**Supplementary Figure 7-2a**, p131). *HvCslF6* transcripts peaked earlier than *SbCslF6* and did not correlate with the relatively consistent increases in (1,3;1,4)-β-glucan levels. These differences between transcript abundance and (1,3;1,4)-β-glucan levels were also evident when measured at six days post infiltration, indicating that differences in (1,3;1,4)-β-glucan levels could not be attributed to differences in transcript abundance. As transcript abundance does not necessarily correlate with protein expression levels or enzyme activity, total protein levels were measured in *N. benthamiana* leaves at six days post infiltration. Total protein levels varied somewhat between experiments but did not correlate with the overall changes in (1,3;1,4)-β-glucan levels produced by *Hv*CSLF6 and *Sb*CSLF6 (**Supplementary Figure 7-3**,

p131). Despite the variation in transcript abundance and total protein levels, the consistent differences in the amount and fine structure of (1,3;1,4)-β-glucan synthesised in the system were therefore attributable to differences in the amino acid sequences of the enzymes. Such sequence differences may directly influence synthesis during catalysis, or the proteins may be differentially targeted or post-translationally modified, resulting in different activities.

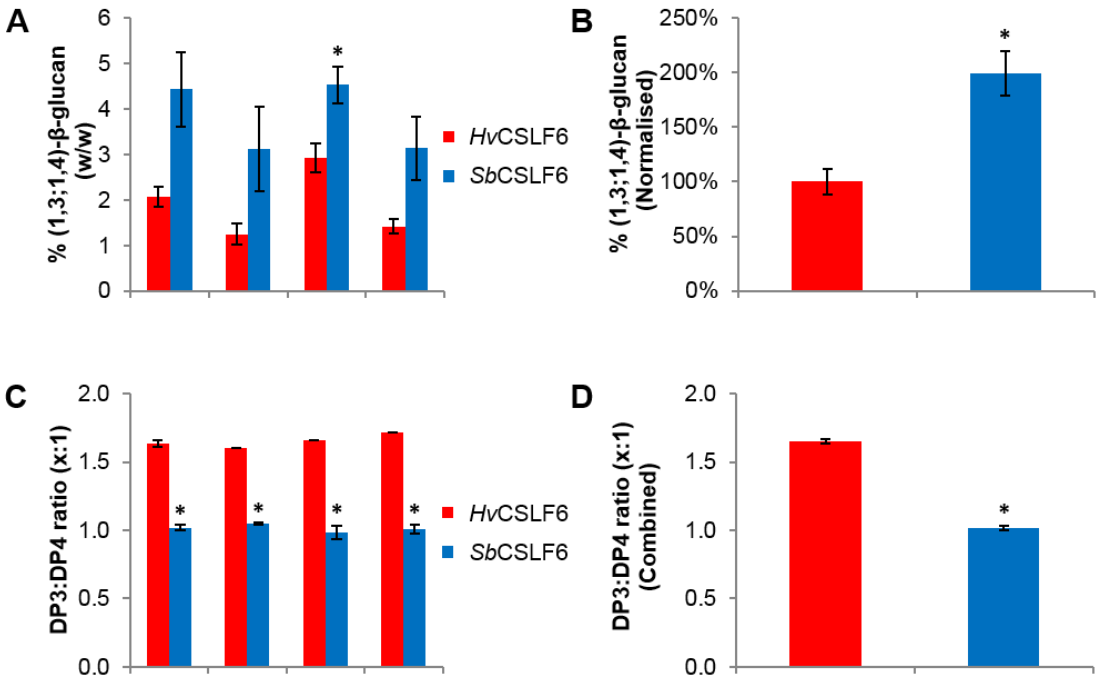


**Figure 2-3. Differences in (1,3;1,4)-β-glucan amounts and fine structure produced by CSLF6 orthologs across four individual experiments.**

Levels of (1,3;1,4)-β-glucan % w/w (**a**) and normalised (**b**) produced by *Hv*CSLF6 (red) and *Sb*CSLF6 (blue) when expressed in *N. benthamiana* leaves. Polysaccharide DP3:DP4 ratios produced by *Hv*CSLF6 (red) and *Sb*CSLF6 (blue) when expressed in *N. benthamiana* leaves in four separate experiments (**c**) and combined (**d**). Error bars in each graph represent the standard error (n = 3). Asterisk above columns denote statistical significance (P≤0.05).

### 2.2.3 The $NH_2$-Terminal Region Influences (1,3;1,4)-β-Glucan Levels but not DP3:DP4 Ratios

A series of chimeric *Hv*CSLF6 and *Sb*CSLF6 constructs was developed in which the barley enzyme was progressively replaced by the sorghum enzyme (**Figure 2-4a**). In this experiment, *Sb*CSLF6 again produced larger amounts of (1,3;1,4)-β-glucan than *Hv*CSLF6 but the DP3:DP4 ratios remained at 1.02±0.02:1 and 1.64±0.03:1, respectively (**Figure 2-4 a** and **b**). When the entire *Hv*CSLF6 $NH_2$-terminal region upstream of the first two transmembrane helices was replaced with the equivalent region from *Sb*CSLF6 (*Sbα:Hv*) (**Figure 2-4a**), the amount of (1,3;1,4)-β-glucan produced increased by 48% compared with *Hv*CSLF6, without altering the DP3:DP4 ratio (**Figure 2-4 a** and **b**). Similarly, when the entire *Sb*CSLF6 $NH_2$-terminal region was replaced with that from *Hv*CSLF6 (*Hvα:Sb*), the amount of (1,3;1,4)-β-glucan produced increased by 60% compared with *Sb*CSLF6, without altering the DP3:DP4 ratio. As similar increases in (1,3;1,4)-β-glucan production were observed when this region was reciprocally exchanged (**Figure 2-4g**), it can be concluded that the $NH_2$-terminal region does not explain the differences between species, but has an apparent interaction with the rest of the sequence affecting amounts of (1,3;1,4)-β-glucan synthesised by the native *Hv*CSLF6 and *Sb*CSLF6 enzymes.

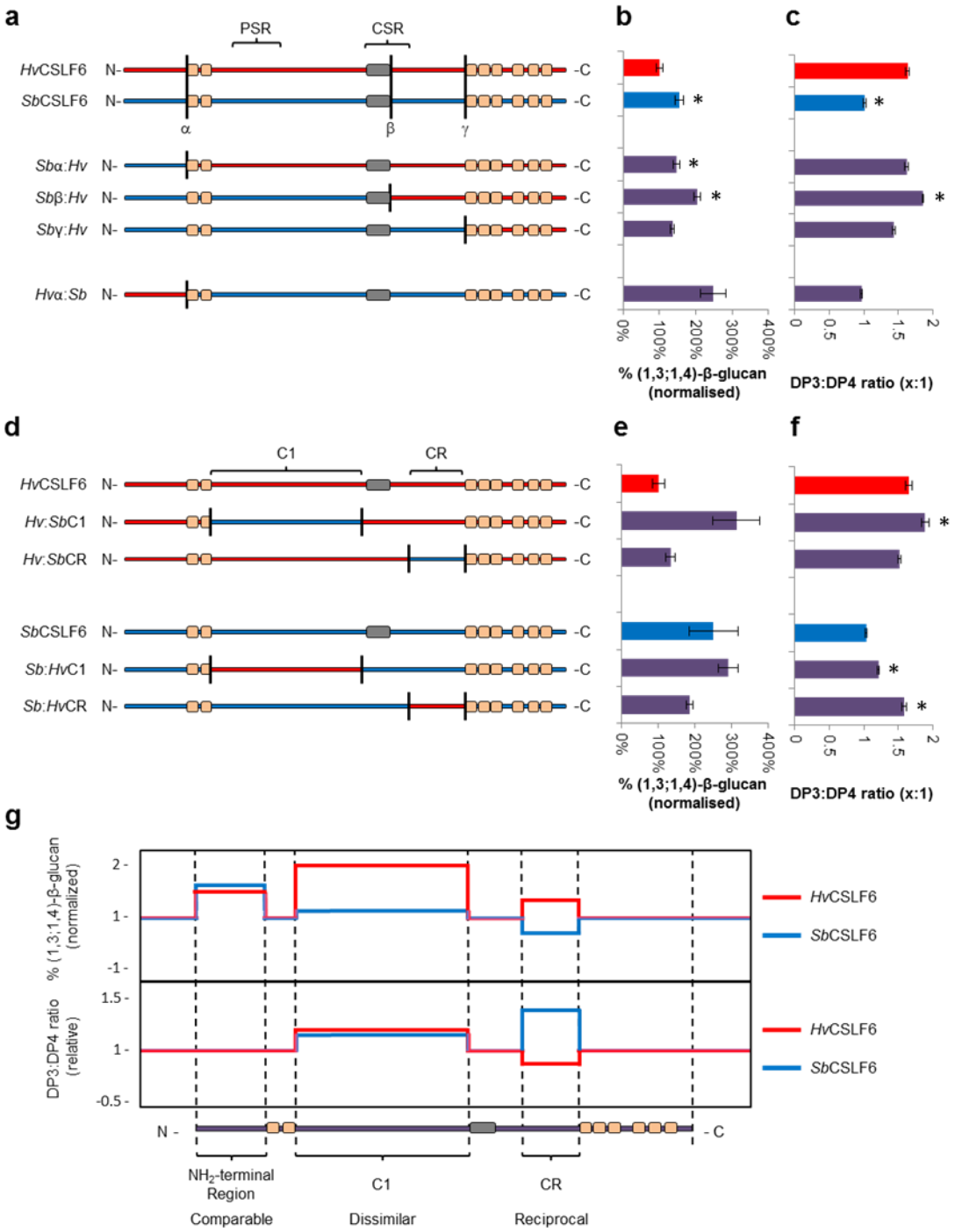
a
PSR
CSR
HvCSLF6 N-
SbCSLF6 N-
-C
α
β
γ
Sbα:Hv N-
Sbβ:Hv N-
Sbγ:Hv N-
Hvα:Sb N-
b
0%
100%
200%
300%
400%
% (1,3;1,4)-β-glucan (normalised)
c
0
0.5
1
1.5
2
DP3:DP4 ratio (x:1)
d
C1
CR
HvCSLF6 N-
Hv:SbC1 N-
Hv:SbCR N-
SbCSLF6 N-
Sb:HvC1 N-
Sb:HvCR N-
e
% (1,3;1,4)-β-glucan (normalised)
f
DP3:DP4 ratio (x:1)
g
% (1,3;1,4)-β-glucan (normalized)
2
1
-1
DP3:DP4 ratio (relative)
1.5
1
-0.5
HvCSLF6
SbCSLF6
N -
- C
NH2-terminal Region
Comparable
C1
Dissimilar
CR
Reciprocal

**Figure 2-4. Chimeric CSLF6 constructs, amounts of (1,3;1,4)-β-glucan synthesised in *N. benthamiana* leaves and fine structures of the (1,3;1,4)-β-glucans produced.**

(**a**) *Hv*CSLF6 (red) and *Sb*CSLF6 (blue) structures showing positions of predicted transmembrane helices (brown boxes), the 'extra region of 55 amino acid residues' (grey box), the Class Specific Region (CSR), the Plant Specific Region (PSR). Sites for recombination between *Hv*CSLF6 and *Sb*CSLF6 are shown with black vertical lines (α, β and γ). (**b**) (1,3;1,4)-β-Glucan (% normalised) produced by recombinant CSLF6 proteins in *N. benth*amiana leaves. (**c**) DP3:DP4 ratios produced by recombinant CSLF6 proteins. (**d**) Black vertical lines mark the boundaries where C1 and CR have been interchanged between *Hv*CSLF6 and *Sb*CSLF6. (**e**) (1,3;1,4)-β-Glucan (% w/w) produced by these C1/CR chimeras. (**f**) DP3:DP4 ratios produced by these C1/CR chimeras. (**g**) Schematic summary showing normalized (1,3;1,4)-β-glucan levels and DP3:DP4 ratios. In all cases, error bars represent standard errors (n = 3). Asterisk above columns denote statistical significance (P≤0.05).

## 2.2.4 The Cytoplasmic Region Influences Both (1,3;1,4)-β-Glucan Amounts and DP3:DP4 Ratios

As the chimeric construct series progressed from *Sb*α*:Hv* to *Sb*β*:Hv*, a considerable portion of the cytoplasmic region of *Hv*CSLF6 was replaced by *Sb*CSLF6 (**Figure 2-4a**). This led to a 37% increase in (1,3;1,4)-β-glucan production for *Sb*β:*Hv* compared to *Sb*α:*Hv*, and an increase in DP3:DP4 ratio from 1.64±0.03:1 to 1.86±0.01:1 (**Figure 2-4 a** and **b**). The section between the second amphipathic helix and the CSR, labelled C1, was exchanged between *Hv*CSLF6 and *Sb*CSLF6 (**Figure 2-4d**), generating *Hv*:*Sb*C1 and *Sb*:*Hv*C1, respectively. Like *Sb*β*:Hv*, expression of *Hv*:*Sb*C1 resulted in the synthesis of (1,3;1,4)-β-glucan with an elevated DP3:DP4 ratio of 1.89±0.05:1 (**Figure 2-4**Figure 2-4**f**), and a 212% increase in (1,3;1,4)-β-glucan production compared with the native *Hv*CSLF6 enzyme (**Figure 2-4e**). However, the *Sb*:*Hv*C1 construct displayed no difference in (1,3;1,4)-β-glucan production but did synthesise a (1,3;1,4)-β-glucan that had an increased DP3:DP4 ratio relative to *Sb*CSLF6 (**Figure 2-4e** and **f**). The dissimilar effect seen for both *Hv*:*Sb*C1 and *Sb*:*Hv*C1 (**Figure 2-4g**) suggests that the C1 region is unlikely to be responsible for the observed differences between *Hv*CSLF6 and *Sb*CSLF6. It is important to note that the insert of approximately 55 amino acid residues that is found exclusively in CSLF6 enzymes is located within the CSR (**Figure 2-4a**).

In the *Sb*γ*:Hv* construct, the remaining section of the major cytoplasmic region of *Hv*CSLF6 was replaced with that of *Sb*CSLF6 (**Figure 2-4a**). This led to a 32% decrease in (1,3;1,4)-β-glucan production, in addition to a decrease in DP3:DP4 ratio from 1.86±0.01:1 to 1.44±0.02:1, relative to the *Sb*β*:Hv* construct (**Figure 2-4 a** and **b**). To further narrow the region of interest, a small section containing the conserved TED and QxxRW motifs, termed the catalytic region (CR), was interchanged between *Hv*CSLF6 and *Sb*CSLF6 (**Figure 2-4d**), generating *Hv*:*Sb*CR and *Sb*:*Hv*CR, respectively. Compared with *Hv*CSLF6, *Hv*:*Sb*CR expression resulted in a 33% increase in (1,3;1,4)-β-glucan production and a decrease in DP3:DP4 ratio from 1.63±0.05:1 to 1.52±0.02:1 (**Figure 2-4 e** and **f**). Conversely, compared to *Sb*CSLF6, *Sb*:*Hv*CR expression resulted in a 26% decrease in (1,3;1,4)-β-glucan production, and an increase in DP3:DP4 ratio from 1.03±0.01:1 to 1.59±0.03:1. The reciprocal effects seen for *Hv*:*Sb*CR and *Sb*:*Hv*CR (**Figure 2-4g**) therefore suggest that the

CR region is important for the observed differences between *Hv*CSLF6 and *Sb*CSLF6.

### 2.2.5 Amino Acid Substitutions Affect (1,3;1,4)-β-Glucan Amounts and DP3:DP4 Ratios

Across the eighty amino acids of the CR, only six substitutions differentiate *Hv*CSLF6 from *Sb*CSLF6 (**Figure 2-5 a** and **d**). As the *Sb*:*Hv*CR construct showed the greatest effect on (1,3;1,4)-β-glucan production and DP3:DP4 ratio (**Figure 2-4**), six individual amino acid substitution constructs were developed from *Sb*CSLF6, namely *Sb*:S631K, *Sb*:D632E, *Sb*:G638D, *Sb*:Y680F, *Sb*:R696K and *Sb*:F705Y (**Figure 2-5a**). The *Sb*:Y680F construct showed a 72% decrease in (1,3;1,4)-β-glucan production compared with *Sb*CSLF6 (**Figure 2-5b**). While five of the six *Sb*CSLF6 point mutants retained the wild type DP3:DP4 ratio of approximately 1:1 (**Figure 2-5c**), the *Sb*:G638D construct displayed an increase in DP3:DP4 ratio from about 1:1 to mirror the *Hv*CSLF6 ratio at 1.62±0.06:1. The corresponding *Hv*CSLF6 point mutant, *Hv*:D629G (**Figure 2-5d**), resulted in a reciprocal yet smaller reduction in DP3:DP4 ratio from 1.60±0.01:1 to 1.50±0.02:1 with an increase in (1,3;1,4)-β-glucan production (**Figure 2-5 e** and **f**) that was akin to the previous observation with *Hv*:*Sb*CR (**Figure 2-4**).

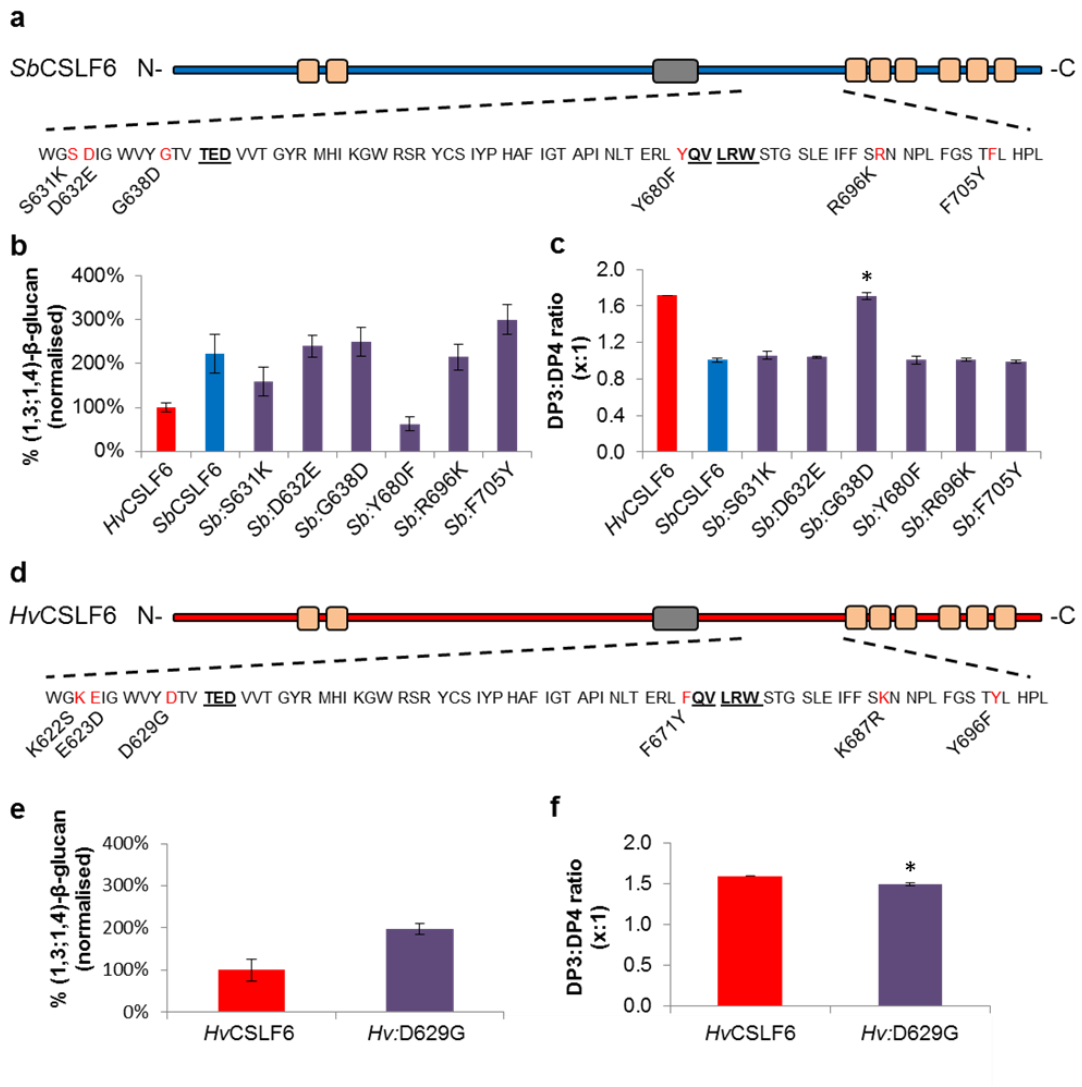


**Figure 2-5. Amounts and fine structures of (1,3;1,4)-β-glucan synthesised in *N. benthamiana leaves* by specific amino acid mutation constructs in the 'catalytic region' of CSLF6.**

(**a**) The primary structure of the CR region of *Sb*CSLF6. Conserved residues are in bold and underlined, and red residues indicate amino acid substitutions analysed below. (**b**) (1,3;1,4)-β-Glucan (% normalised) produced by *Sb*CSLF6 point mutant constructs. (**c**) DP3:DP4 ratios produced by *Sb*CSLF6 point mutant constructs. (**d**) The primary sequence of the CR region of *Hv*CSLF6. Conserved residues are in bold and underlined, red residues highlight specific amino acid substitutions. (**e**) (1,3;1,4)-β-Glucan (% w/w) and (**f**) DP3:DP4 ratios produced by the *Hv*CSLF6 point mutation construct. Error bars represent standard errors (n = 3). Asterisk above columns denote statistical significance (P≤0.05).

### 2.2.6 Three-dimensional Dispositions of Amino Acid Residues That Affect (1,3;1,4)-β-Glucan Amounts and Fine Structure

To identify the spatial positioning of *Sb*CSLF6 Y680 and G638, we constructed a homology model based on the *Rhodobacter sphaeroides* BCSA cellulose synthase subunit crystal structure (Morgan et al., 2013). The locations of Y680 and G638 are indicated in **Figure 2-6**. Y680 is present on the helix homologous to the BCSAs amphipathic interface helix, IF2, which is adjacent to the core QxxRW catalytic motif. The G638 residue is located just upstream of the 'finger helix' and adjacent to the TED motif that is predicted to interact with the acceptor end of the nascent polysaccharide (Morgan et al., 2014).

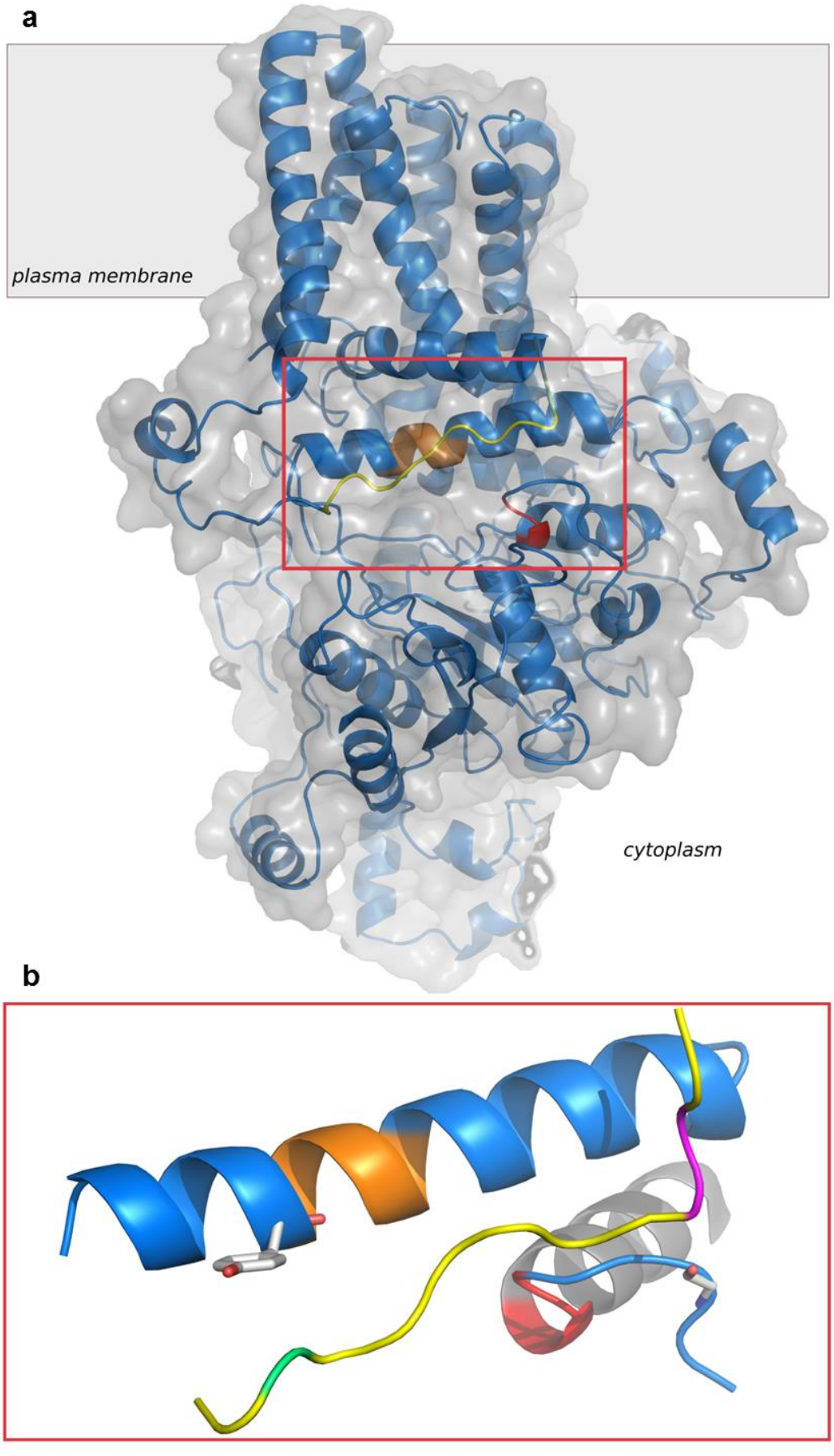
a
plasma membrane
cytoplasm
b

**Figure 2-6. An *in silico* protein threaded model of *Sb*CSLF6.**

(**a**) The model of *Sb*CSLF6 contains a cytoplasmic region and membrane spanning helices that are predicted to form a pore for the extrusion of nascent (1,3;1,4)-β-glucan chains. The long helix (IF2) in the boxed region includes the QxxRW motif (orange) while the shorter helix in the lower right corner of the boxed region contains the TED motif (red). The putative gating loop of CSLF6 is coloured yellow. (**b**) Magnification of the boxed region of **Figure 2-6a** shows the predicted locations of the Y680F and G638D mutations. The IF2 helix is in blue, with the QxxRW motif shown in orange. The predicted position of the Y680 residue is shown in stick conformation. The G638 residue is shown on the blue loop close to the TED motif (red). The putative gating loop is shown in yellow. Within the gating loop the green section indicates the position of the conserved FxLTxK motif, which is close to the Y680 residue, and the magenta section of the gating loop shows the position of R810 and R811, both of which are close to the G638 residue (shown in stick conformation).

## 2.3 Discussion

The CSLF6 enzyme, which is encoded by one of ten *CslF* genes in barley (Schreiber et al., 2014), has emerged as the synthase responsible for producing the majority of (1,3;1,4)-β-glucan in developing cereal grain (Burton et al., 2008; Nemeth et al., 2010; Burton et al., 2011; Taketa et al., 2011; Vega-Sάnchez et al., 2012). Substantial variation in (1,3;1,4)-β-glucan content and fine structure is evident across different grass species, but until now it was unclear if different CSLF6 orthologs were functionally equivalent with respect to this variation. The heterologous expression of different *CslF6* cDNAs in a *N. benthamiana* system was chosen to test this possibility and to identify regions or specific amino acids that influence how much (1,3;1,4)-β-glucan is synthesised and the DP3:DP4 ratios of the synthesised polysaccharides.

Transient expression of three CSLF6 orthologs, *Os*CSLF6, *Hv*CSLF6 and *Sb*CSLF6 in *N. benthamiana* revealed significant differences in (1,3;1,4)-β-glucan production between the three synthases. Whilst *Hv*CSLF6 produced more (1,3;1,4)-β-glucan than *Os*CSlF6, *Sb*CSLF6 consistently produced the greatest amount of (1,3;1,4)-β-glucan in the heterologous system (**Figure 2-2a**). Similar differences in (1,3;1,4)-β-glucan production between the synthases were observed in *P. vulgaris* leaves and in stably transformed rice callus tissues (**Figure 2-2b** and **c**), indicating that the observed differences were not specific to the *N. benthamiana* expression system.

It has been suggested that individual CSLF enzymes may synthesise (1,3;1,4)-β-glucans with different fine structures (Burton et al., 2011). Expression of the three CSLF6 orthologs in *N. benthamiana* clearly showed that *Os*CSLF6 and *Hv*CSLF6 produced (1,3;1,4)-β-glucan with DP3:DP4 ratios of 1.57±0.01:1 and 1.68±0.03:1, respectively, whilst the ratio of the *Sb*CSLF6 product was noticeably lower at 0.98±0.01:1 (**Figure 2-2a**). These ratios remained constant across experimental replicates, despite considerable differences in (1,3;1,4)-β-glucan production by the respective synthases (**Figure 2-3 c** and **d**). This suggests that amino acid differences between the synthases are specifically influencing the DP3:DP4 ratio, irrespective of how much (1,3;1,4)-β-glucan is produced. As reported previously for *Hv*CSLF6 expression in *N. benthamiana* (Taketa et al., 2011), the DP3:DP4 ratios obtained in this heterologous background are lower than the endogenous ratios of *Poaceae* species.

For example, the DP3:DP4 ratio of (1,3;1,4)-β-glucans in barley grain is 2.6:1 (Fincher and Stone, 2004), but the value obtained in the *N. benthamiana* system is close to 1.65:1 (**Figure 2-2**). This therefore suggests that one or more factors such as ancillary proteins or cofactors that are normally associated with CSLF6 expression and (1,3;1,4)-β-glucan biosynthesis are not present in the *N. benthamia*na leaves. Nevertheless, the consistent differences in DP3:DP4 ratios obtained in the *N. benthamiana* system allowed us to identify regions and amino acid residues that were important determinants of polysaccharide fine structure.

When the $NH_2$-terminal regions were reciprocally interchanged between *Hv*CSLF6 and *Sb*CSLF6 (**Figure 2-4a**), both synthases displayed increased (1,3;1,4)-β-glucan production without influencing the polysaccharide's DP3:DP4 ratio (**Figure 2-4 b** and **c**). The disconnected effects on the DP3:DP4 ratio and production levels of (1,3;1,4)-β-glucan suggests that there are independent mechanisms regulating these properties. The effect of interchanging the $NH_2$-terminal region of *Hv*CSLF6 and *Sb*CSLF6 suggests that this region plays a regulatory role in (1,3;1,4)-β-glucan biosynthesis. At this stage we are not able to explain these effects, but they could be attributable to a conformational change in the protein, resulting in the alteration of an intramolecular interaction between the $NH_2$-terminal region and another part of the CSLF6 protein, or between the $NH_2$-terminal region and an ancillary protein/substrate. Thus, the changes might result in a loss of enzyme inhibition (Morgan et al., 2014). The subsequent decrease in (1,3;1,4)-β-glucan levels observed between chimeras *Sb*β*:Hv* and *Sb*γ*:Hv* (**Figure 2-4**) suggests that in the *Sb*γ*:Hv* chimera, the $NH_2$-terminal region may once again be able to interact with the CSLF6 core, leading to a return of normal CSLF6 function. This suggests that either the $NH_2$-terminal region is binding to the CSLF6 cytoplasmic region between points β and γ, or that the *Sb*γ*:Hv* chimera has the correct structural conformation which allows the $NH_2$-terminal region to bind to another undefined region or protein.

Reciprocal effects on the amount of (1,3;1,4)-β-glucan synthesis were observed when the catalytic region (CR) was interchanged between *Hv*CSLF6 and *Sb*CSLF6 (**Figure 2-4g**). Six amino acid polymorphisms within this region were investigated by site-directed mutagenesis. Of the six targeted point mutation constructs, five showed no significant differences in the amount of (1,3;1,4)-β-glucan production, compared with *Sb*CSLF6 (**Figure**

**2-5**). However, the *Sb*:Y680F construct resulted in a 72% decrease in (1,3;1,4)-β-glucan production compared with *Sb*CSLF6. The Y680 residue is located immediately upstream of the QxxRW motif and is predicted to interact with the putative gating loop of CSLF6, which contains an FxLTxK motif similar to that of BCSA (**Figure 2-6** and **Supplementary Figure 7-1**, p128) (Morgan et al., 2014). The gating loop of the bacterial BCSA is observed in two positions. In the resting state, the gating loop is some distance from the IF2 helix and the enzyme retains an auto-inhibitory conformation, in which the UDP-Glc binding cleft is closed. When cyclic-di-GMP binds to the bacterial enzyme, the gating loop is re-positioned close to the IF2 helix and the attendant opening of the UDP-Glc binding pocket leads to the activation of the enzyme (Morgan et al., 2014). If a similar mechanism operates in the CSLF6 enzyme, the Y680 residue is situated in a position that might be important in holding the gating loop against the adjacent helix IF2 (Morgan et al., 2014) during opening of the UDP-Glc binding site (**Figure 2-6**) and in the accompanying activation of the enzyme from its resting state (Morgan et al., 2014). The interaction presumably involves the hydroxyl group of Y680, which is absent in the lower activity *Sb*:Y680F construct but which is within hydrogen bonding distance of the T818 residue of the conserved FxLTxK motif in the gating loop of the CSLF6 enzyme model (**Figure 2-6**).

When the DP3:DP4 ratios produced by the six *Sb*CSLF6 CR point mutation constructs were examined, five retained the wild type (1,3;1,4)-β-glucan DP3:DP4 ratio of approximately 1:1 (**Figure 2-5c**). However, the *Sb*:G638D mutation caused a noticeable shift in DP3:DP4 ratio, to a value close to that observed with the native *Hv*CSLF6 construct, namely 1.62±0.06:1. The G638 amino acid residue is located three residues upstream from the TED motif and, based on the predicted structure, appears to be close to the gating loop (**Figure 2-6**). Inserting an Asp residue in the sorghum model at position 638 suggests that its carboxyl group would be within ionic bonding distance from the guanidinium groups of either R810 or R811 at the $NH_2$-terminal region of the gating loop (**Figure 2-6**).

There is considerable debate over whether the CSLF6 enzyme is able to catalyse the formation of both the (1,3)- and (1,4)-β-glycosidic linkages present in (1,3;1,4)-β-glucan chains, or if an ancillary protein or enzyme is required to introduce the (1,3)-linkages. Thus, the CSLF6 enzyme might synthesise (1,4)-β-oligoglucosides that are subsequently linked

through (1,3)-linkages by an ancillary transferase enzyme (Burton et al., 2010) or a single CSLF6 synthase enzyme might synthesise both (1,3)- and (1,4)-linkages in the nascent polysaccharide chain (Buckeridge et al., 1999; Kim et al., 2015). At this stage we are not able to predict just exactly how the *Sb*:G638D single amino acid substitution caused such a profound effect on DP3:DP4 ratio. In contrast to the *Sb*:G638D construct, the corresponding mutation in *Hv*CSLF6 (*Hv*:D629G) resulted in an increase in (1,3;1,4)-β-glucan production and only a subtle decrease in the DP3:DP4 ratio (**Figure 2-5 e** and **f**). The fact that this single amino acid substitution did not result in a shift in DP3:DP4 ratio to mirror that of *Sb*CSLF6 at approximately 1:1 indicates that G638D variants are not the sole determinants of changes in the DP3:DP4 ratios.

Since this chapter has been written, Jobling (2015) showed that one polymorphism in the fourth predicted transmembrane helix of CSLF6 was influencing the polysaccharide DP3:DP4 ratio across several species. This was done by generating a series of chimeric constructs between four *CslF6* cDNAs and expressing them *N. benthamiana* leaves. CSLF6 enzymes possessing the Ile polymorphism typically displayed a DP3:DP4 ratio above 1.4:1, whilst those with the Leu polymorphism were below 1.4:1 (**Supplementary Figure 7-4**, p132). Here, in the *Sbγ:Hv* chimera, the Ile/Leu polymorphism identified by Jobling (2015) is present in the remaining *Hv*CSLF6 section of the chimera. The corresponding increase in DP3:DP4 ratio compared with the remaining *Sb*CSLF6 core, 1.4:1 compared with 1.0:1, therefore supports the findings of Jobling (2015) that CSLF6 enzymes possessing the Ile polymorphism typically display a DP3:DP4 ratio above 1.4:1. This finding therefore indicates that CSLF6 pore architecture is one factor contributing to the DP3:DP4 ratio of the polysaccharide produced. Of the seven CSLF6 orthologs analysed by Jobling (2015), the G638D polymorphism also appears to be distinguishing those with high or low DP3:DP4 ratios (**Supplementary Figure 7-4**, p132). Orthologs possessing the Asp typically displayed a high DP3:DP4 ratio whilst those with the Gly polymorphism were low. Cumulatively, the evidence indicates that a number of CSLF6 polymorphisms are capable of influencing the DP3:DP4 ratio of the polysaccharide produced.

In summary, we have used a chimeric approach to define the effects of sequence differences between CSLF6 orthologs on enzyme function. This takes another step towards

unravelling the complex mechanism of (1,3;1,4)-β-glucan biosynthesis in higher plants. The data generated here have identified specific amino acid residues and regions of the CSLF6 enzyme that significantly affect the amounts and fine structures of (1,3;1,4)-β-glucans synthesised by the enzyme and, using genetic or mutagenesis approaches, can now be applied to generate tailor-made CSLF6 enzymes that produce defined amounts of (1,3;1,4)-β-glucan with defined fine structures that would deliver physicochemical properties adapted to a desired application. For example, increased levels of (1,3;1,4)-β-glucan with lower DP3:DP4 ratios in cereal grains would result in increased levels of soluble dietary fibre that would benefit human health by reducing the risk of developing diseases such as type II diabetes, cardiovascular disease and colorectal cancer (Collins et al., 2010).

## 2.4 Methods

### 2.4.1 TEM Immunocytochemistry

Detection of (1,3;1,4)-β-glucan in *N. benthamiana* leaves was carried out using fixation and embedding procedures described by Burton et al. (2011) and with sectioning and imaging procedures described by Wilson et al (2006). Here, a 1:500 dilution of the (1,3;1,4)-β-glucan specific mouse primary antibody BG-1 (Biosupplies, Melbourne, Australia) (Meikle et al., 1994), and a 1:30 dilution of Aurion goat IgG/IgM (Aurion, Wageningen, The Netherlands) anti-mouse secondary antibody conjugated to 10 nm gold particles were used.

### 2.4.2 RNA isolation, cDNA synthesis and Q-PCR

RNA isolation and cDNA synthesis was performed according to Burton et al (2008) on freeze-dried and ground *N. benthamiana* tissue, initially prepared for the analysis of (1,3;1,4)-β-glucan content. Primers for *CslF6* and *N. benthamiana* control genes were designed according to standard guidelines, and real-time quantitative PCR (Q-PCR) was performed according to Burton et al. (2008). Primers, PCR fragment sizes and optimal acquisition temperatures are shown (**Supplementary Table 7-4**, p136).

## 2.4.3 Total Protein Quantification

Total protein quantification was performed using the Plant Total Protein Extraction Kit (Sigma-Aldrich, Missouri, USA) as per manufacturer's instructions. Samples were taken from freeze-dried and ground *N. benthamiana* tissue, initially prepared for the analysis of (1,3;1,4)-β-glucan content.

## 2.4.4 DNA Constructs

The *HvCslF6* ('Sloop') cDNA sequence has been previously isolated (Burton et al., 2008) and was available in house in the pCR8/GW/TOPO vector of the Gateway™ cloning system (Curtis and Grossniklaus, 2003). *S. bicolor* ('Texas white TX623') leaf tissue was used to isolate RNA and generate cDNA using the methods described in Burton et al. (2008). The full length *SbCslF6* cDNA was obtained by PCR (**Supplementary Table 7-1**, p133) using Phusion® high fidelity DNA polymerase (New England Biolabs, Massachusetts, USA) as per the manufacturer's instructions. The *OsCslF6* ('Nipponbare') (J013002J18) cDNA was obtained from Riken (Riken, 2011) and PCR amplified (**Supplementary Table 7-1**, p133) as previously described. PCR fragments of correct size were excised from the gel, purified using NucleoSpin® Gel and PCR Clean-up kit (Machery-Nagel, Amtsgericht Düren, Germany) and inserted into the pCR8/GW/TOPO vector (Life Technologies, Carlsbad, USA) as per the manufacturer's instructions, and sequenced (Australian Genome Research Facility Ltd, Queensland, Australia). Correct constructs were transferred to the pEAQ-HT-DEST-1 vector carrying the Gateway™ cloning system (Curtis and Grossniklaus, 2003; Sainsbury et al., 2009) using LR Clonase (Life Technologies, Carlsbad, USA) as per manufacturer's instructions.

Chimeric constructs were developed using the Geneart™ Seamless cloning and assembly kit (Life Technologies, Carlsbad, USA) as per manufacturer's instructions (**Supplementary Table 7-1**, p133 and **Supplementary Table 7-2**, p134). A similar approach was used to generate the amino acid substitution constructs where the modified codon sequence was incorporated into the fifteen base pair overlap region of the primer (**Supplementary Table 7-3**, p135). Constructs were sequenced (Australian Genome Research Facility Ltd) before being transferred to the pEAQ-HT-DEST-1 binary expression vector (Sainsbury et al., 2009)

for transient expression in *N. benthamiana*. DNA sequence comparisons were performed using Geneious software (version 8.1.3, available from http://www.geneious.com).

## 2.4.5 Transient Transformation of *Nicotiana benthamiana*

All *N. benthamiana* plants were grown with 22°C day and 15°C night temperatures without supplemented light in the Plant Accelerator® (University of Adelaide). *Agrobacterium tumefaciens* preparation and transformation procedures were adapted from Wydro et al. (2006). *Agrobacterium* strains (AGL1) harbouring the insert and vector of interest were grown with shaking for 48 hours at 28˚C in 10 mL tubes containing 2 mL Luria Broth (LB) supplemented with 50µg/mL kanamycin and 50µg/mL rifampicin. An aliquot of 200 µL was spread onto two LB Agar plates supplemented with identical antibiotics and incubated overnight at 28˚C. *Agrobacterium* was scraped off plates and diluted to an $OD_{600}$ of 1.0 with MMA (0.01M $MgCl_2$ and 0.01M MES). After 3 hour incubation at room temperature with 0.1 µM acetosyringone, entire intact leaves were infiltrated using a 10 mL syringe without a needle. Tissue was harvested six days post infiltration for analysis unless stated otherwise. Data shown is based on three biological replicates with two technical replicates of each sample.

## 2.4.6 Transient transformation of *Phaseolus vulgaris* leaves

*P. vulgaris* leaf *Agro*-infiltrations were performed as per 'transient transformation of *Nicotiana benthamiana*', using the first true leaves in fifteen day old seedlings. Plants were grown with 22°C day and 15°C night temperatures without supplemented light in the Plant Accelerator® (University of Adelaide).

## 2.4.7 Stable rice callus transformation

The transformation procedure was adapted from Nishimura et al. (2007) with the following minor changes. Autoclaved filter paper replaced stainless steel sieves. Callus induction media (CIM) was composed of 3.99g Chu's N6 salts and vitamins, 100mg myo-inositol, 2.8g proline, 30g sucrose, 2.5µg/ml 2,4-D, 2.6g phytagel, water to 1000mL, pH 5.8. Infection media was composed of 1.99g Chu's N6 salts and vitamins, 350mg proline, 34.2g sucrose, 1.25µg/mL 2,4-D, 10µM acetosyringone, water to 500mL, pH 5.2. Co-cultivation media was

composed of 3.99g Chu's N6 salts and vitamins, 30g sucrose, 2.5µg/mL 2,4-D, 10µM acetosyringone, 7g type 1 agarose (low electroendosmosis (EEO), water to 1000mL, pH 5.2. Selection media was composed of 3.99g Chu's N6 salts and vitamins, 2.8g proline, 30g sucrose, 2.5µg/mL 2,4-D, 400µg/mL cefotaxime, 100µg/mL vancomycin, 7g type 1 agarose (low EEO), water to 1000mL, pH 6. For solid media, 500mL water with agarose or phytagel was prepared in a 1L bottle and autoclaved. The remaining chemicals were prepared in 500ml water, pH adjusted and filtered into the autoclaved bottle using a Millipore 0.2µm, 500mL filter. Post co-cultivation, calli were washed with infection media supplemented with 400µg/mL cefotaxime and 100µg/mL vancomycin. All incubation steps were carried out in darkness at 28˚C. For all transformations, cDNAs were expressed from the pMDC32 vector of the Gateway™ cloning system (Curtis and Grossniklaus, 2003; Sainsbury et al., 2009). All chemicals were sourced from either Sigma-Aldrich (Missouri, USA), Life Technologies (Carlsbad, USA), Austratec (Victoria, Australia) or Phytotechnology Laboratories (Kansas, USA).

Rather than re-generating transformed plants, the method was also modified to amplify transformed calli instead. Secondary calli were separated from primary calli and subjected to an additional two weeks of selection. These calli were transferred to individual CIM plates and left to grow until ~1/3 of the plate was covered before harvesting.

## 2.4.8 (1,3;1,4)-β-Glucan Assay

Analysis of (1,3;1,4)-β-glucan content was performed using commercially available reagents (Megazyme International Ireland Ltd, Bray, Ireland) and a scaled down protocol (Burton et al., 2011) based on McCleary and Codd (1991). *N. benthamiana* tissue was snap frozen, freeze dried, ground with metal ball bearings and 20 mg of ground tissue was weighed into individual tubes. Method modifications included two washes with 1 mL of 50% ethanol and two washes with 1 mL of 100% ethanol at 97˚C for 10 min to remove sugars and chlorophyll. After lichenase [EC 3.2.1.73; (1,3;1,4)-β-glucan endohydrolase] digestion, aliquots were taken for high performance liquid chromatography (HPLC) analysis of the amount of product and the DP3:DP4 ratios. (1,3;1,4)-β-Glucan is reported as mg of (1,3;1,4)-β-glucan per mg of freeze-dried matter and expressed as a percentage % (w/w).

### 2.4.9 Measurement of Polysaccharide DP3:DP4 Ratios

The DP3:DP4 ratios of lichenase-digested samples were determined according to Lazaridou and Biliaderis (Lazaridou and Biliaderis, 2007). Derivatization followed Rozaklis et al. (Rozaklis et al., 2002) and samples were fractionated on an Agilent 1200 LC (Agilent Technologies, USA) at 40˚C using a Phenomenex Kinetex XB-C18 2.6 µm 3x100 mm column (Phenomenex Inc, California, USA) and detected at 250 nm.

### 2.4.10 CSLF6 Homology Model

The CSLF6 amino acid sequences were aligned to the BCSA crystal structure (Morgan et al., 2013) glycosyl transferase 2 PFAM domain (PF00535) and their two flanking transmembrane helices (TMH) using Clustal Omega (Sievers et al., 2011) and manually edited to ensure alignment of homologous catalytic motifs and TMHs. Gap regions longer than 11 residues were modelled *de novo* using I-TASSER (Yang et al., 2015). Modeller (Šali and Blundell, 1993) was used to construct homology models of CSLF6 using BCSA and de novo predictions as templates. Modeller DOPE functions, ProSA (Sippl, 1993) and Procheck (Laskowski et al., 1996) was used to assess the reliability of candidate models. High scoring models were passed through a Modeller loop refinement script and final models chosen using Modeller DOPE, Modeller GA32, ProSA and Procheck assessments.

## 2.5 Acknowledgements

This work was supported by grants from the Australian Research Council. GD and JGS acknowledge the receipt of Graduate Research Scholarships from the Grains Research and Development Corporation. We thank Vincent Bulone for his invaluable advice during the preparation of this manuscript.

# 3. CSLF6 Synthesises (1,3;1,4)-β-Glucan in Complexes Mediated by the Class-Specific and $NH_2$-Terminal Regions.

## 3.0 Abstract

*CELLULOSE SYNTHASE-LIKE F6* (*CslF6*) genes have been shown to encode the synthase responsible for producing the majority of (1,3;1,4)-β-glucan present in barley and many other cereals. Given the difficulties associated with expressing and purifying membrane-bound glycosyltransferase protein complexes in an active form, it has proven challenging to understand the process by which the CSLF6 protein is regulated. By co-expressing a variety of chimeric, truncated and mutated *CslF6* constructs in a heterologous model system, we have demonstrated that CSLF6 complex formation is required for (1,3;1,4)-β-glucan synthetic activity. Both the class specific region (CSR) and the $NH_2$-terminal region of CSLF6 are involved in intermolecular and intramolecular binding *in vivo.* This interaction mimics the de-repression mechanism of the bacterial cellulose synthase *A* (BCSA) subunit where the COOH-terminal region releases the gating loop upon binding of the secondary messenger, cyclic-di-GMP, to the PilZ domain. An inverted PilZ motif was identified in the CSLF6 $NH_2$-terminal region and subsequent site-directed mutagenesis to disable this domain indicates that synthase activity may be regulated by the binding of the plant secondary messenger, cyclic-GMP.

## 3.1 Introduction

The *CslF* (Burton et al., 2006), *CslH* (Doblin et al., 2009) and *CslJ* (unpublished data) gene families have been implicated in the biosynthesis of (1,3;1,4)-β-glucan in cereals. CSLF6 has emerged as the synthase responsible for producing the bulk of the (1,3;1,4)-β-glucan in cereals. This is based on high *HvCslF6* transcript abundances in developing barley endosperm (Burton et al., 2008), increased (1,3;1,4)-β-glucan levels in barley grain when *Hv*CSLF6 is overexpressed (Burton et al., 2011), the lack of (1,3;1,4)-β-glucan in *betaglucanless* barley lines with mutations in the *CSLF6* gene (Taketa et al., 2011) and the decreased (1,3;1,4)-β-glucan levels when *CslF6* transcripts are reduced in wheat (Nemeth et al., 2010) and *CslF6* is knocked out in rice (Vega-Sάnchez et al., 2012). One noticeable feature differentiates CSLF6 from CSLH, CSLJ and the remaining CSLF members; that is the presence of additional amino acid residues in the region designated here as the 'extra-

region' (Burton et al., 2011), and is believed to be one feature that has enhanced the (1,3;1,4)-β-glucan synthase activity of CSLF6.

Recently, Kim et al. (2015) were able to express a catalytically active CSLF6 from *Brachypodium distachyon* (*Bd*) in *Pichia pastoris*, enabling the synthase to be purified in microsomal fractions and examined for membrane topology. Using protease treatments, Kim et al. (2015) showed that the catalytic domain, and the $NH_2$- and COOH- termini of *Bd*CSLF6 were all exposed to the cytoplasm. By attaching yellow fluorescent protein to *Bd*CSLF6 and expressing the construct in *Nicotiana benthamiana* leaves, they were also able to show that the synthase is located in Golgi-stacks. This contrasts with work by Wilson et al. (2015) who defined the locations of CSLF6 proteins from various *Poaceae* species using an anti-CSLF6 antibody and concluded that the enzyme is located at the endoplasmic reticulum, Golgi, secretory vesicles and plasma membrane (PM). Using the (1,3;1,4)-β-glucan specific antibody BG1 (Meikle et al., 1994), Wilson et al. (2015) also showed in various *Poaceae* species that (1,3;1,4)-β-glucan was evident only in the wall and not in the Golgi, suggesting that final synthesis of a form recognized by BG1 occurs at the PM. Clearly our understanding of the location of (1,3;1,4)-β-glucan biosynthesis requires further analysis and will be debated for some time.

As with other members of the *CELLULOSE SYNTHASE* superfamily (Richmond and Somerville, 2000), CSLF6 is an integral membrane protein consisting of numerous putative amphipathic helixes. This has made the synthase extremely difficult to express and purify in an active form, hindering our understanding of how CSLF6 synthesises (1,3;1,4)-β-glucan and how it is regulated at the protein level. Comparative studies of CSLF6 are now possible based on sequence and three-dimensional structural similarities with the better understood *cellulose synthases* of plants (CESA) and bacteria (BCSA). This is largely due to the definition of the crystal structure of the membrane-integrated bacterial cellulose synthase A (BCSA) subunit, together with the periplasmic membrane-associated BCSB subunit from the bacterium *Rhodobacter sphaeroides* (Morgan et al., 2013; Morgan et al., 2014). The BCSA subunit shows many structural similarities to a plant CESA *in silico* predicted model (Sethaphong et al., 2013) and has been used to develop an *in silico* threaded model of CSLF6 (Chapter 2). Conserved amongst all members of the plant

*CELLULOSE SYNTHASE* superfamily and bacterial *cellulose synthases* are the D, D, TED and QxxRW motifs (Richmond and Somerville, 2000). These motifs are located at the active site of BCSA (Morgan et al., 2013) and include the nucleotide sugar binding and catalytic residues. The motifs are believed to perform a similar role in members of the *cellulose synthase* superfamily from plants (Richmond and Somerville, 2000). Two features of plant CESA and CSLF6 enzymes that are not present in the bacterial BCSA structure are the plant-conserved region (P-CR) and the highly variable class-specific region (CSR). In plant CESA enzymes the P-CR and CSR are predicted to fold into subdomains, contributing to oligomerization of CESA subunits and rosette formation (Sethaphong et al., 2013). As CSLF6 is not known to form large complexes, it remains unclear as to the roles the P-CR and CSR may play in CSLF6 function.

Using chimeric approaches, two studies have recently taken steps toward unravelling the mechanism of (1,3;1,4)-β-glucan biosynthesis. Jobling (2015) was able to identify a small section of CSLF6 responsible for much of the difference in DP3:DP4 ratio observed between synthases from several species. A Leu to Ile polymorphism in the fourth predicted transmembrane helix was identified to be responsible. With the Ile present, CSLF6 enzymes typically displayed a DP3:DP4 ratio above 1.4:1 whilst those with the Leu were below 1.4:1. This result demonstrated how CSLF6 pore architecture does influence DP3:DP4 ratio. In chapter 2 we were able to define the effect of sequence differences between two CSLF6 orthologs. Principally we demonstrated that two individual amino acid substitutions in the catalytic region, adjacent to the TED and QxxRW motifs, were able to significantly influence polysaccharide amount and structure (Chapter 2**, Figure 2-5**, p42). However in the absence of a crystal structure, it remains unknown precisely how the process of (1,3;1,4)-β-glucan biosynthesis has been altered by the above mentioned CSLF6 mutations.

In chapter 2 there is also the suggestion that the $NH_2$-terminal region of CSLF6 could play a role in regulating enzyme activity. Under normal conditions, the $NH_2$-terminal region may have been binding and repressing the main catalytic region of the CSLF6 protein. When the $NH_2$-terminal region was exchanged between the two CSLF6 orthologs, the putative regulatory mechanism was disrupted due to an incompatible binding site on the chimeric synthase. This resulted in the de-repression of both synthases, increasing (1,3;1,4)-β-glucan

production by 50% in the *N. benthamiana* expression system. The mechanism that controls this intramolecular binding *in vivo* is currently unknown and could hold the key to increasing (1,3;1,4)-β-glucan production *in planta*. As the CSLF6 $NH_2$-terminal region contains four cysteine residues, the region may function similarly to CESA enzymes, where the $NH_2$-terminal region is believed to regulate enzyme activity via oxidative dimerisation of zinc-binding domains (Kurek et al., 2002). Alternatively, the CSLF6 $NH_2$-terminal region may function by binding a secondary messenger that mediates enzyme activity, as observed in BCSA. In the COOH-terminal region of BCSA, a PilZ domain has been shown to bind c-di-GMP, which modulates enzyme activation/repression via the gating loop (Morgan et al., 2014).

Here, co-expression analyses in the model heterologous expression system of *N. benthamiana* has been performed using a variety of synthetic CSLF6 constructs to investigate the regulation of the CSLF6 enzyme in the process of (1,3;1,4)-β-glucan biosynthesis. We have demonstrated that CSLF6 activity is dependent on complex formation and involves the binding of a secondary messenger in a similar fashion to BCSA.

## 3.2 Results

### 3.2.1 (1,3;1,4)-β-Glucan Production by Full-length CSLF6 Increases when Co-expressed with the CSLF6 $NH_2$-Terminal Region.

As the $NH_2$-terminal region of CSLF6 has previously been shown to influence enzyme activity (Chapter 2, section 2.2.3, p32), truncated CSLF6 constructs were generated to further investigate the regulatory mechanism via transient co-expression analyses (**Figure 3-2a**). Constructs were infiltrated into whole *N. benthamiana* leaves either individually or in pairs at a total *Agrobacterium* optical density at 600nm ($OD_{600}$) of 1.0, consistent with chapter 2 (Section 2.4.5, p48). Since individual constructs were infiltrated at an $OD_{600}$ level of 0.5, notably lower levels of (1,3;1,4)-β-glucan were produced compared to those reported in chapter 2 (**Figure 2-2a**, p28). *Sb*CSLF6 and *Hv*CSLF6 expression resulted in the production of 1.8% and 0.9% (1,3;1,4)-β-glucan (w/w) respectively. The chimeric constructs with the $NH_2$-terminal regions interchanged, *Sb*-N:*Hv* and *Hv*-N:*Sb* (**Figure 3-2a**), each displayed ~50% increases in (1,3;1,4)-β-glucan production compared with their parent synthases (**Figure 3-2b**), again consistent with chapter 2 (**Figure 2-4a**, p3535). It should be noted that in each of the following co-expression experiments, DP3:DP4 ratios remained at ~1.65:1 when full length *Hv*CSLF6 was expressed and ~1.0:1 when full length *Sb*CSLF6 was expressed.

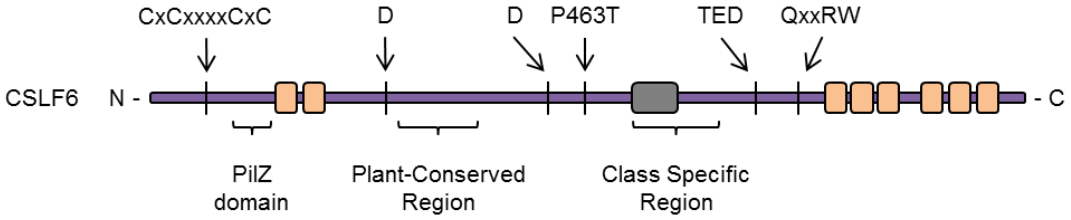


**Figure 3-1. CSLF6 primary structure and locations of conserved motifs.**

CSLF6 primary structure highlighting relative positions of predicted amphipathic helices (brown boxes), the 'extra region' (grey box), the class specific region, plant-conserved region, putative PilZ domain, the CxCxxxxCxC, D, D, TED and QxxRW motifs and the P463T mutation.

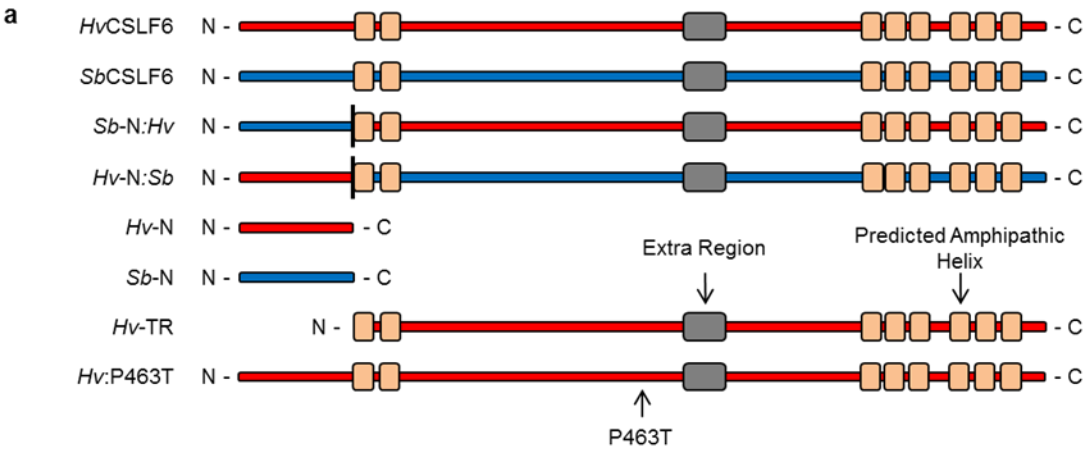
a
HvCSLF6 N - - C
SbCSLF6 N - - C
Sb-N:Hv N - - C
Hv-N:Sb N - - C
Hv-N N - - C
Sb-N N - - C
Hv-TR N - - C
Hv:P463T N - - C
Extra Region
Predicted Amphipathic Helix
P463T

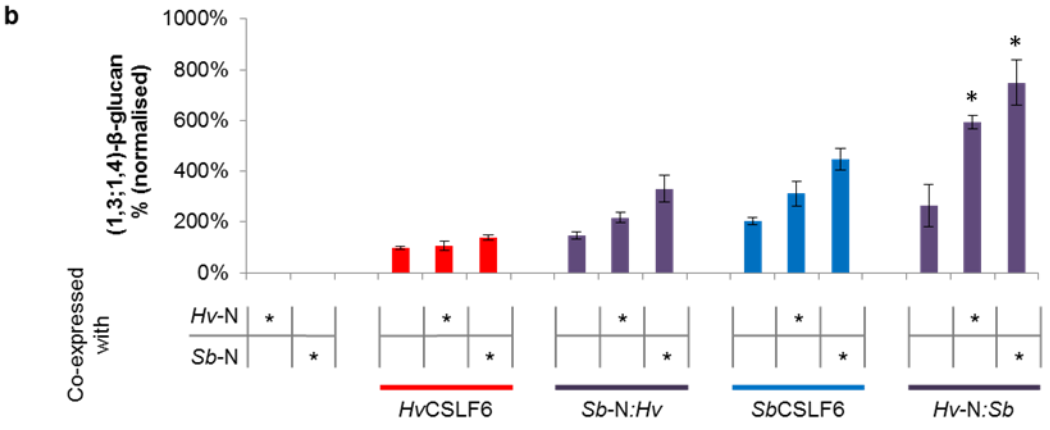
b
(1,3;1,4)-β-glucan % (normalised)
1000%
800%
600%
400%
200%
0%
Co-expressed with
Hv-N
Sb-N
HvCSLF6
Sb-N:Hv
SbCSLF6
Hv-N:Sb

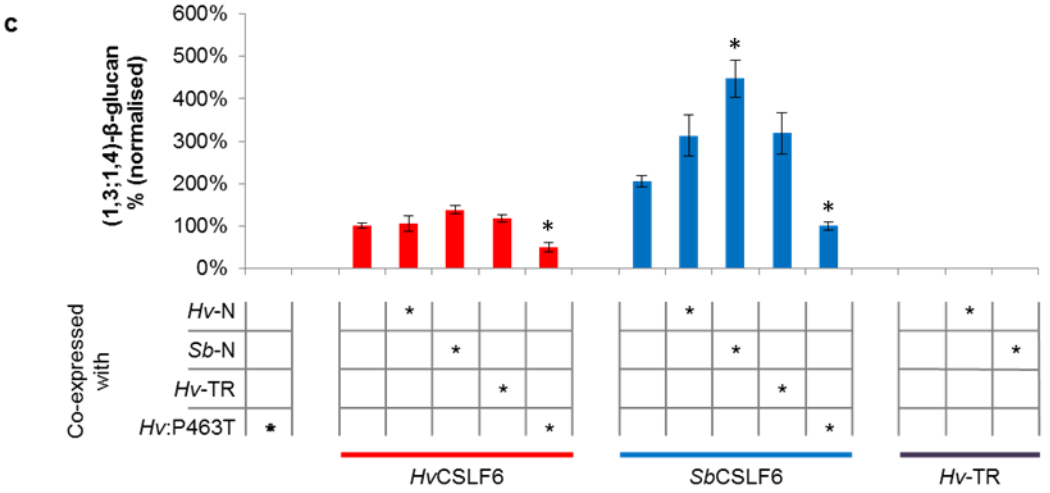
c
(1,3;1,4)-β-glucan % (normalised)
600%
500%
400%
300%
200%
100%
0%
Co-expressed with
Hv-N
Sb-N
Hv-TR
Hv:P463T
HvCSLF6
SbCSLF6
Hv-TR

**Figure 3-2. Chimeric, truncated and mutated CSLF6 proteins and the amounts of (1,3;1,4)-β-glucan produced after individual and combined expression in *N. benthamiana* leaves.**

(**a**) *Hv*CSLF6 (red) and *Sb*CSLF6 (blue) schematics showing relative positions of the predicted amphipathic helices (brown boxes), the 'extra region' (grey box) and the location of the P463T mutation. Chimeric, truncated and mutated constructs derived from *Hv*CSLF6 and *Sb*CSLF6 are also shown with black lines defining borders where gene sections have been exchanged. (**b and c**) (1,3;1,4)-β-Glucan (% normalised against *HvCslF6* levels) produced by CSLF6 constructs when expressed in *N. benth*amiana leaves. Asterisks indicate when the construct below has been co-expressed with the construct to the left. Error bars represent the standard error (n = 3). Asterisk above columns denote statistical significance (P≤0.05).

When the $NH_2$-terminal regions, *Hv*-N or *Sb*-N alone were expressed, no (1,3;1,4)-β-glucan was detected (**Figure 3-2b**), indicating that this region alone is insufficient for biosynthesis. When a full-length synthase was co-expressed with *Hv*-N or *Sb*-N, in each case, (1,3;1,4)-β-glucan production by the full-length synthase increased compared to when it was expressed by itself. This result raises the possibility that *Hv*-N and *Sb*-N may be interacting with and activating the full length synthases, leading to increased biosynthesis (**Figure 3-3a** and **Figure 3-11b**).

When co-expressed with *Hv*-N and *Sb*-N, (1,3;1,4)-β-glucan production by *Hv*CSLF6 increased by 6% and 37% respectively (**Figure 3-2b**). When *Sb*CSLF6 was co-expressed with *Hv*-N or *Sb*-N, (1,3;1,4)-β-glucan production by *Sb*CSLF6 increased by 53% and 119% respectively. When *Sb*-N:*Hv* was co-expressed with *Hv*-N or *Sb*-N, (1,3;1,4)-β-glucan production by *Sb*-N:*Hv* increased by 47% and 124% respectively. When *Hv*-N:*Sb* was co-expressed with *Hv*-N or *Sb*-N, (1,3;1,4)-β-glucan production by *Hv*-N:*Sb* increased by 125% and 185% respectively (**Figure 3-2b**).

For each combination, co-expression with *Sb*-N resulted in a greater increase in (1,3;1,4)-β-glucan production by the full-length synthase than co-expression with *Hv*-N. When co-expressed with *Hv*-N or *Sb*-N, *Sb*CSLF6 displayed a greater increase in (1,3;1,4)-β-glucan production than *Hv*CSLF6, and the chimeric constructs (*Sb*-N:*Hv* and *Hv*-N:*Sb*) displayed even greater increases in (1,3;1,4)-β-glucan production than their wild-type parent synthases.

### 3.2.2 The $NH_2$-Terminal Region of CSLF6 is Required for Enzyme Function.

Expression of the $NH_2$-terminally truncated *Hv*-TR construct (**Figure 3-2a**) resulted in no detectable (1,3;1,4)-β-glucan being produced (**Figure 3-2c**), indicating that the presence of this $NH_2$-terminal region is absolutely required for (1,3;1,4)-β-glucan biosynthesis in the *N. benthamiana* system. When *Hv*-TR was co-expressed in *trans* with the $NH_2$-terminal constructs *Hv*-N and *Sb*-N, (1,3;1,4)-β-glucan production by *Hv*-TR was not restored. When *Hv*CSLF6 and *Sb*CSLF6 were co-expressed with *Hv*-TR, (1,3;1,4)-β-glucan production by the full length synthases increased by 18% and 56% respectively compared with individual

expression. This result suggests that *Hv*-TR may be interacting with and activating the full length synthases, leading to increased (1,3;1,4)-β-glucan production (**Figure 3-3b** and **Figure 3-11b**).

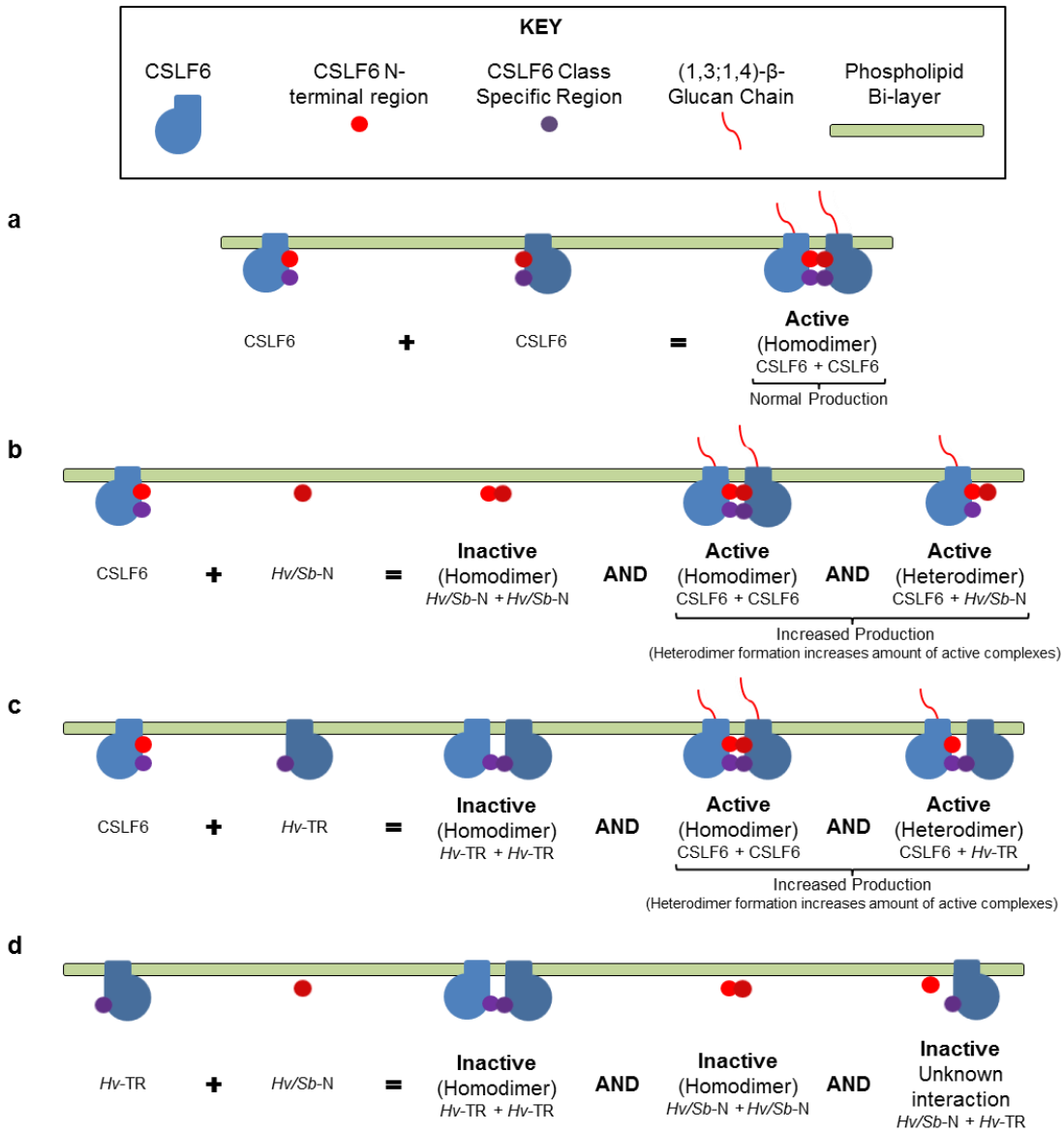


**Figure 3-3. Model of CSLF6 complex formation and interactions with truncated constructs.**

A model showing how CSLF6 might become active when in a homodimeric complex (**a**), and the theoretical complexes formed when CSLF6 is co-expressed with *Hv*-N or *Sb*-N (**b**), or with *Hv*-TR (**c**). In **b** and **c** heterodimeric complexes may form in addition to the active CSLF6 homodimer, resulting in more active complexes and increased (1,3;1,4)-β-glucan production. No active complexes form when *Hv*-TR is co-expressed with *Hv*-N or *Sb*-N (**d**).

### 3.2.3 A P463T Mutated *Hv*CSLF6 Enzyme Reduces (1,3;1,4)-β-Glucan Biosynthesis.

Complex formation has been shown to be required for activity within the CESA family through the use of dominant negative mutations. This was shown by the substitution of a conserved Pro residue in CESA3 (*thanatos*) and CESA7 (*fra5*) in *Arabidopsis,* which led to a negative effect on cellulose synthesis (Zhong et al., 2003; Daras et al., 2009). The mutant enzymes were believed to be inactive themselves, yet were still able to form complexes with other functional CESA subunits but would inhibit their activity or interfere with the formation or function of the rosette complex, reducing cellulose synthesis. As the Pro residue is conserved across all CSLF6 enzymes (**Figure 3-1**), it may also influence complex formation by CSLF6 and mutating it may provide a means to investigate this possibility. When the conserved Pro residue was mutated to a Thr in *Hv*CSLF6 (*Hv*:P463T) and the construct was expressed in *N. benthamiana*, no detectable (1,3;1,4)-β-glucan was produced (**Figure 3-2c**). When co-expressed with *Hv*:P463T, both wild-type *Hv*CSLF6 and *Sb*CSLF6 displayed a ~50% reduction in (1,3;1,4)-β-glucan biosynthesis compared with their individual expression. This result also raises the possibility that *Hv*:P463T is able to form heterodimeric complexes with the wild-type synthases and inhibit their activity (**Figure 3-4** and **Figure 3-11c**).

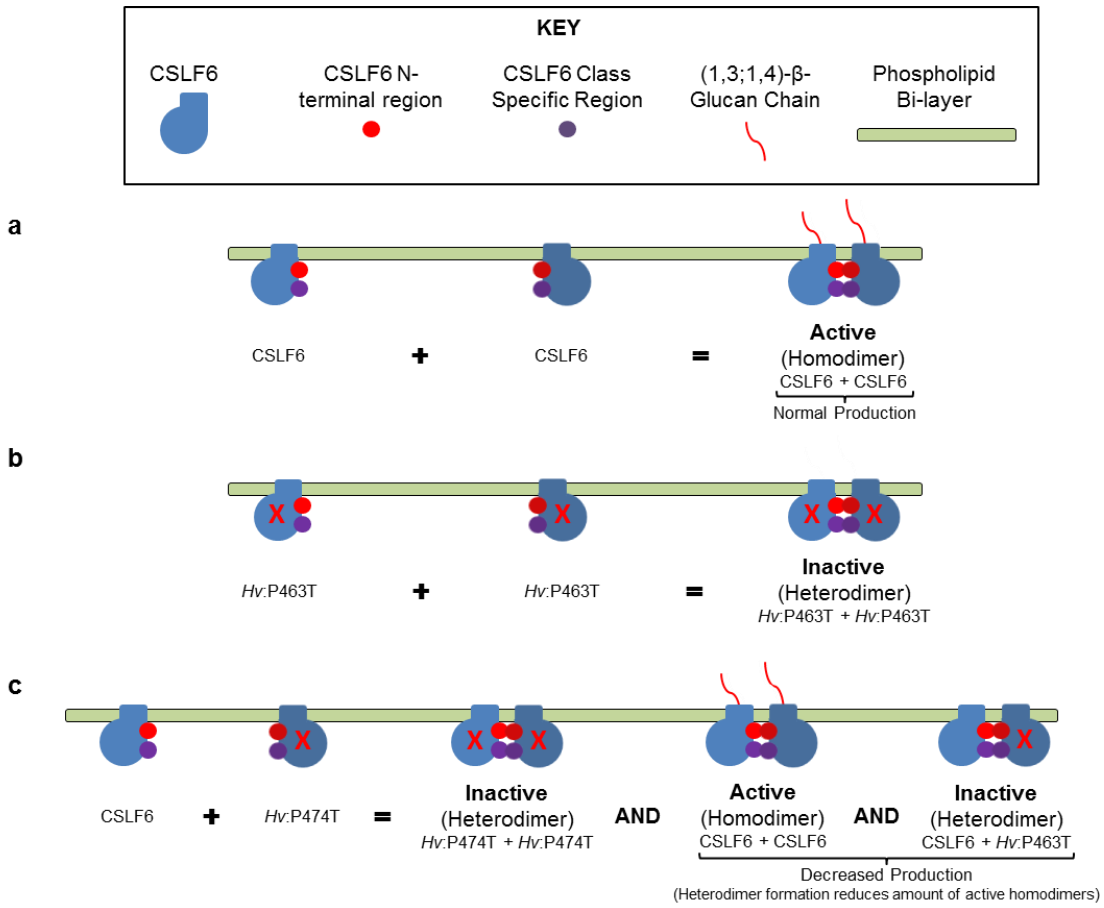


**Figure 3-4. Model of CSLF6 complex formation and interactions with a P463T mutated construct.**

A model showing CSLF6 becoming active when in a homodimeric complex (**a**), and *Hv*:P463T (marked with a red cross) forming an inactive homodimer (**b**). When CSLF6 is co-expressed with *Hv*:P463T (**c**), in addition to the two homodimeric complexes, heterodimeric complexes also form that are inactive. This pool of heterodimers decreases the amount of active CSLF6 homodimers, decreasing (1,3;1,4)-β-glucan production.

### 3.2.4 The CSLF6 Class Specific Region is not Required for Enzyme Function.

To investigate the role of the CSLF6 'Extra Region' (ExR) and 'Class Specific Region' (CSR) in (1,3;1,4)-β-glucan biosynthesis, several internally deleted and chimeric constructs were made and tested in the transient expression system (**Figure 3-5a**). *Sb*CSLF6 produced 30% more (1,3;1,4)-β-glucan than *Hv*CSLF6, with DP3:DP4 ratios at 1.05±0.06:1 and 1.55±0.03:1, respectively (**Figure 3-5b**). When the *Hv*CSLF6 CSR was replaced with that from *Sb*CSLF6, generating *Hv*:*Sb*CSR, (1,3;1,4)-β-glucan production increased by 33% compared with *Hv*CSLF6, and the DP3:DP4 ratio increased to 1.69±0.08:1. The opposite effect, namely decreased (1,3;1,4)-β-glucan production with a lower DP3:DP4 ratio, was observed for the *Sb*CSLF6 reciprocal construct, *Sb*:*Hv*CSR. Constructs with an internally deleted ExR failed to produce any detectable (1,3;1,4)-β-glucan, as did *Hv*CSLF6 with the CSR internally deleted (*Hv*:ΔCSR). However, *Sb*:ΔCSR produced the same amount of (1,3;1,4)-β-glucan with the same DP3:DP4 ratio as wild-type *Sb*CSLF6. Based on the *in silico* threaded model of CSLF6, the two ends of the CSR are predicted to be in relatively close proximity in three dimensional space (**Figure 3-6**). Thus, removing this region from *Sb*CSLF6 and "splicing" the ends does not appear to have unduly perturbed the remaining structure and its function was maintained.

For the internally deleted *Hv*CSLF6 protein however, "splicing" the ends does appear to have generated a non-functional protein and the artificial joining of the two ends may have caused more of a topological perturbation. The persistent activity of the Sb:ΔCSR enzyme suggests that the CSR is not essential for CSLF6 activity but this observation does not preclude a functional or regulatory role of the CSR in CSLF6.

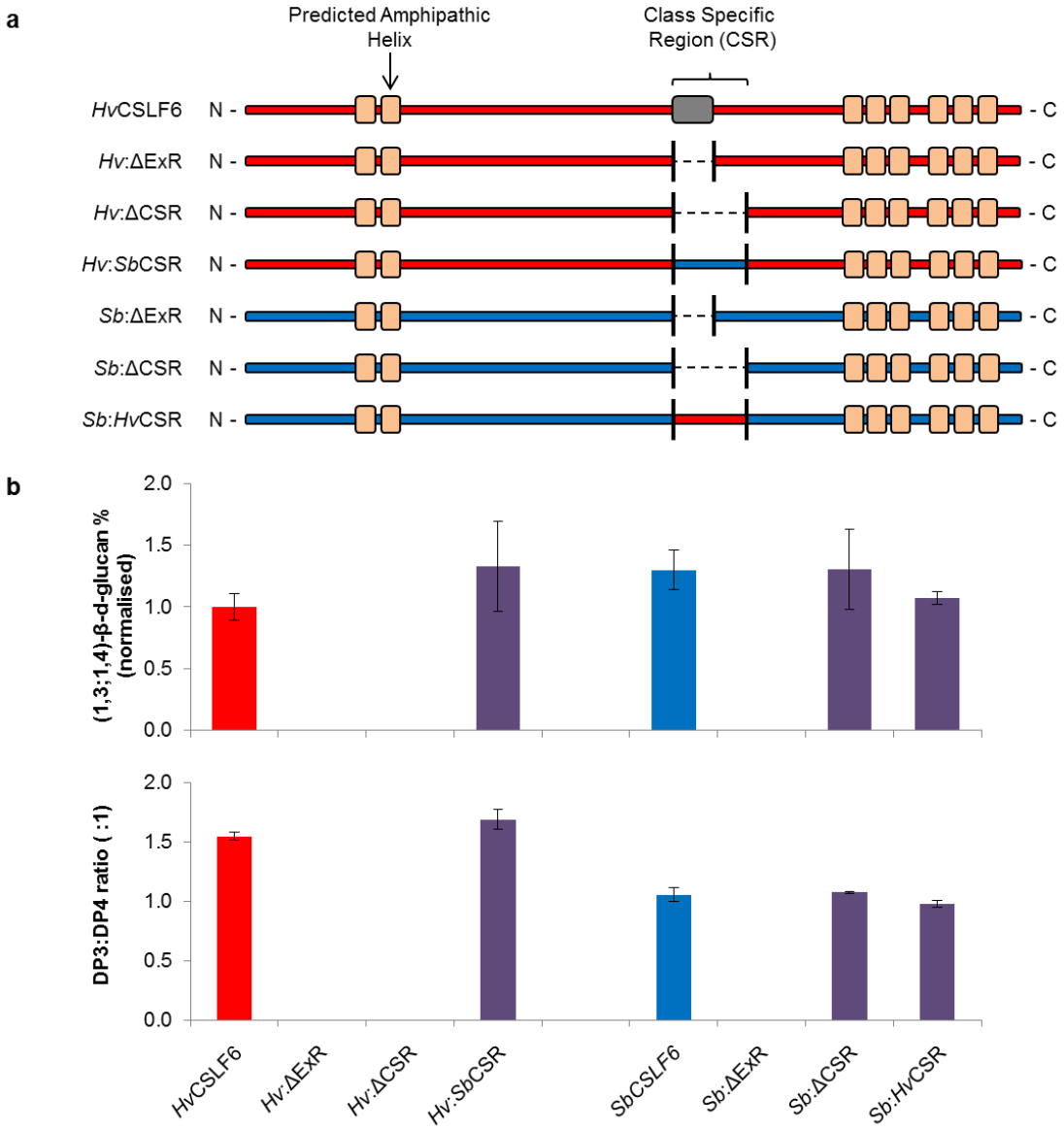


**Figure 3-5. Internally deleted and chimeric CSLF6 proteins with their associated amounts and DP3:DP4 ratios of (1,3;1,4)-β-glucan produced in *N. benthamiana* leaves.**

(**a**) *Hv*CSLF6 (red) and *Sb*CSLF6 (blue) schematics highlight the relative positions of predicted amphipathic helices (brown boxes), the CSR and the 'extra region' (grey box). Chimeric and internally deleted constructs derived from *Hv*CSLF6 and *Sb*CSLF6 are also shown with black lines marking boundaries. (**b**) Amounts (% normalised) and DP3:DP4 ratios (x :1) of (1,3;1,4)-β-glucan produced by *CslF6* constructs. Error bars represent the standard error (n = 3).

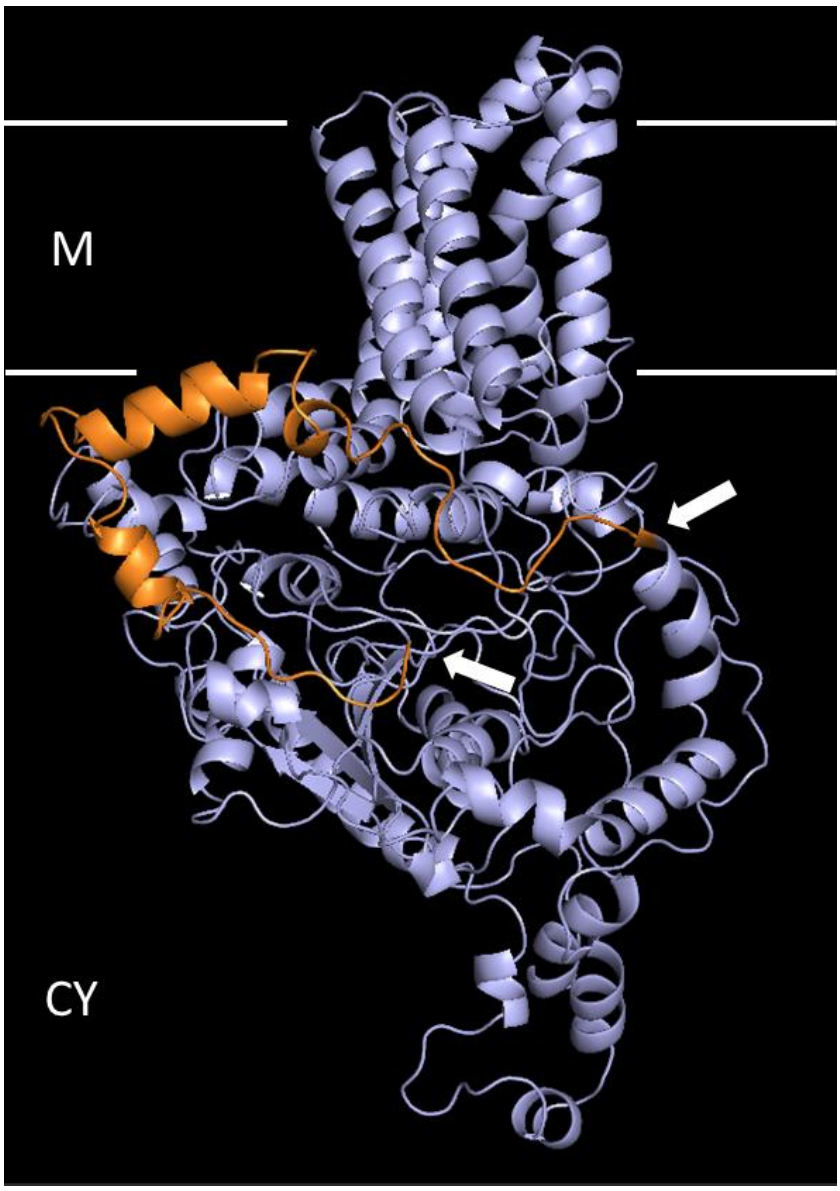


**Figure 3-6. An *in silico Sb*CSLF6 protein threaded model.**

The *Sb*CSLF6 model contains a cytoplasmic region (CY) and a membrane (M) spanning pore which (1,3;1,4)-β-glucan chains are believed to extrude through. In orange is the class specific region (CSR) with white arrows indicating where the CSR termini are located.

### 3.2.5 The CSLF6 Extra and Class Specific Regions do not Enhance (1,3;1,4)-β-Glucan Production when Inserted into CSLJ, CSLH or Other CSLF Members.

To determine if the ExR or CSR enable CSLF6 to produce more (1,3;1,4)-β-glucan than other related synthases, chimeric constructs were developed with the ExR or CSR of *Hv*CSLF6 replacing the equivalent wild-type regions of *Hv*CSLF3, *Hv*CSLF4, *Hv*CSLF7, *Hv*CSLF9, *Hv*CSLF10, *Hv*CSLJ and *Hv*CSLH (**Supplementary Table 8-1**, p138). As there is sufficient sequence homology between all of these synthases in the regions flanking the ExR and CSR, identical boundaries were used to incorporate the *CslF6* sequences. If CSLJ, CSLH or the other CSLF members are modelled based on the bacterial BCSA structure (Morgan et al., 2013), as shown in chapter 2 (section 2.2.6, p39), then their equivalent ExR and CSR would not be predicted to form part of the core synthase (data not shown). Instead, the regions may form distinct structures, and replacing these with the equivalent region from CSLF6 could alter the synthase activity via an unknown mechanism.

When transiently expressed in *N. benthamiana* leaves, *Hv*CSLF7, *Hv*CSLF9, *Hv*CSLJ and *Hv*CSLH produced low levels of (1,3;1,4)-β-glucan (**Supplementary Table 8-1**, p138), indicating that the synthases were weakly active in the expression system. None of the chimeric constructs produced any detectable (1,3;1,4)-β-glucan, suggesting that ExR and CSR replacements have knocked out activity of the synthases. It may be concluded that the CSLF6 ExR and CSR do not enhance the synthetic abilities of related synthases and are not solely responsible for the higher production levels catalysed by CSLF6.

### 3.2.6 The Cysteine-rich Motif in the $NH_2$-Terminal Region of CSLF6 is not Required for (1,3;1,4)-β-Glucan Biosynthesis or Complex Formation in *N. benthamiana*.

The $NH_2$-terminal region of CSLF6 contains a 'CxCxxxxCxC' motif (**Figure 3-1**), which is similar to, but smaller than, the Cys rich zinc-binding domains found in CESA enzymes. In other systems, this motif is believed to be involved in dimerization (Kurek et al., 2002). As the results presented thus far suggest that CSLF6 also forms dimers or higher order complexes, the four Cys residues of the 'CxCxxxxCxC' motif were mutated to Ser residues (*Sb*:(C-S)) to investigate their influence on CSLF6 function (**Figure 3-7 a** and **b**). When expressed in *N. benthamiana*, *Sb*:(C-S) produced similar amounts of (1,3;1,4)-β-glucan as the wild type *Sb*CSLF6 (**Figure 3-7c** and **Supplementary Table 8-2**, p139), suggesting that the motif does not influence the synthesis of (1,3;1,4)-β-glucan by CSLF6. When co-expressed with *Hv*:P463T, *Sb*:(C-S) displayed a 77% reduction in (1,3;1,4)-β-glucan biosynthesis (**Figure 3-7c**). This implies that the 'CxCxxxxCxC' motif is not essential for CSLF6 complex formation if the *Hv*:P463T protein is still able to form a heterodimeric complex with *Sb*:(C-S) and repress its activity. To support this observation, the four Cys of the 'CxCxxxxCxC' motif in the *Sb*-N (**Figure 3-2a**) construct were also all mutated to Ser (*Sb*-N:(C-S)) (**Figure 3-7a**). As with the *Sb*-N construct (**Figure 3-2a**), individual expression of *Sb*-N:(C-S) in *N. benthamiana* leaves resulted in no (1,3;1,4)-β-glucan production (data not shown). Co-expression of *Sb*-N:(C-S) with *Hv*CSLF6 and *Sb*CSLF6 however resulted in increased (1,3;1,4)-β-glucan biosynthesis by the full length-synthases, compared with their expression alone (**Figure 3-7d**). The increase in biosynthesis resulting from the co-expression of *Sb*-N:(C-S) is approximately equal to that resulting from co-expression with *Sb*-N, indicating that the functionality of the $NH_2$-terminal region is not dependent on the presence of the four Cys residues.

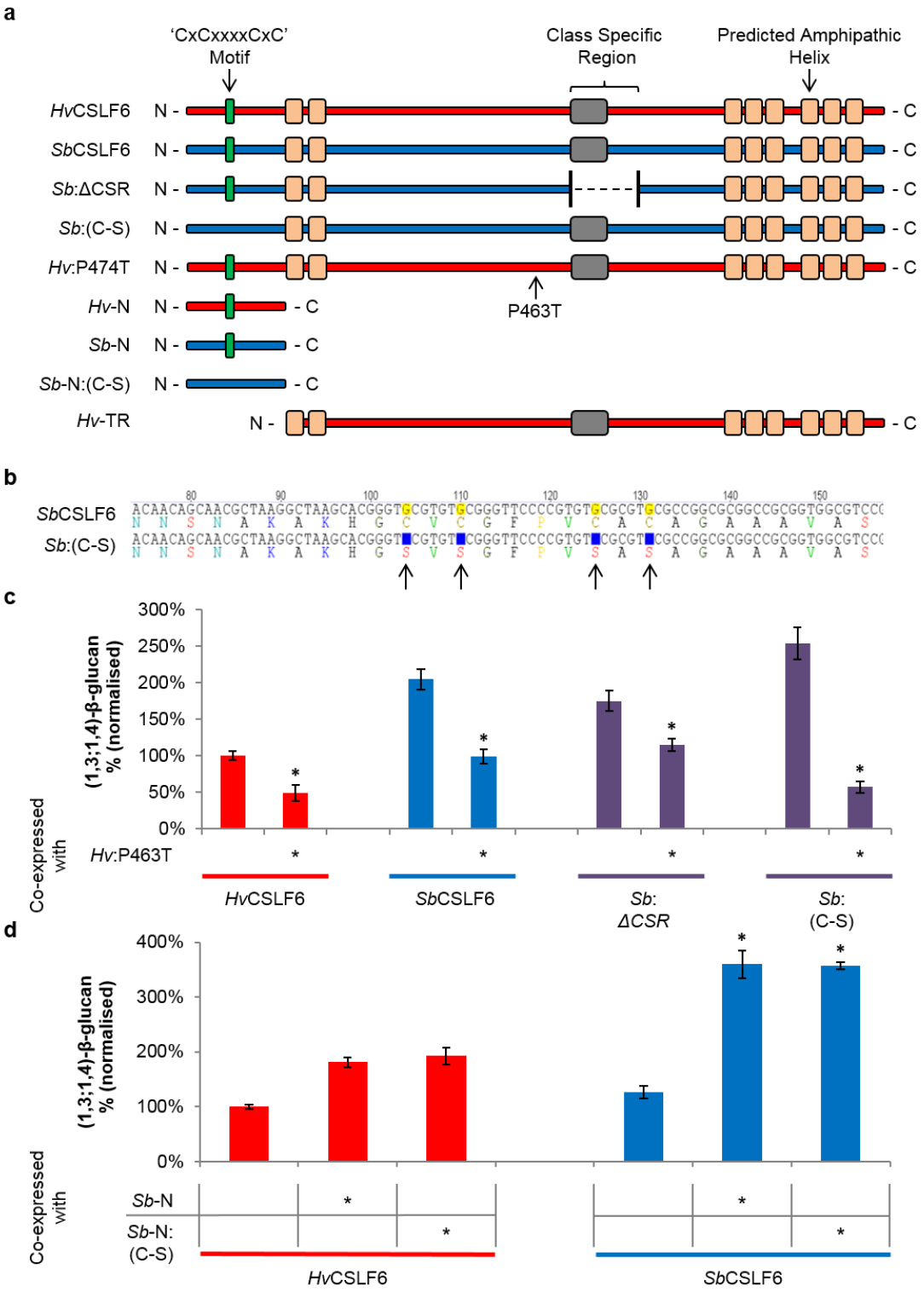
a
'CxCxxxxCxC' Motif
Class Specific Region
Predicted Amphipathic Helix
HvCSLF6
SbCSLF6
Sb:ΔCSR
Sb:(C-S)
Hv:P474T
Hv-N
Sb-N
Sb-N:(C-S)
Hv-TR
N -
- C
P463T
b
SbCSLF6
Sb:(C-S)
c
(1,3;1,4)-β-glucan % (normalised)
300%
250%
200%
150%
100%
50%
0%
Co-expressed with
Hv:P463T
HvCSLF6
SbCSLF6
Sb: ΔCSR
Sb: (C-S)
d
(1,3;1,4)-β-glucan % (normalised)
400%
300%
200%
100%
0%
Co-expressed with
Sb-N
Sb-N: (C-S)
HvCSLF6
SbCSLF6

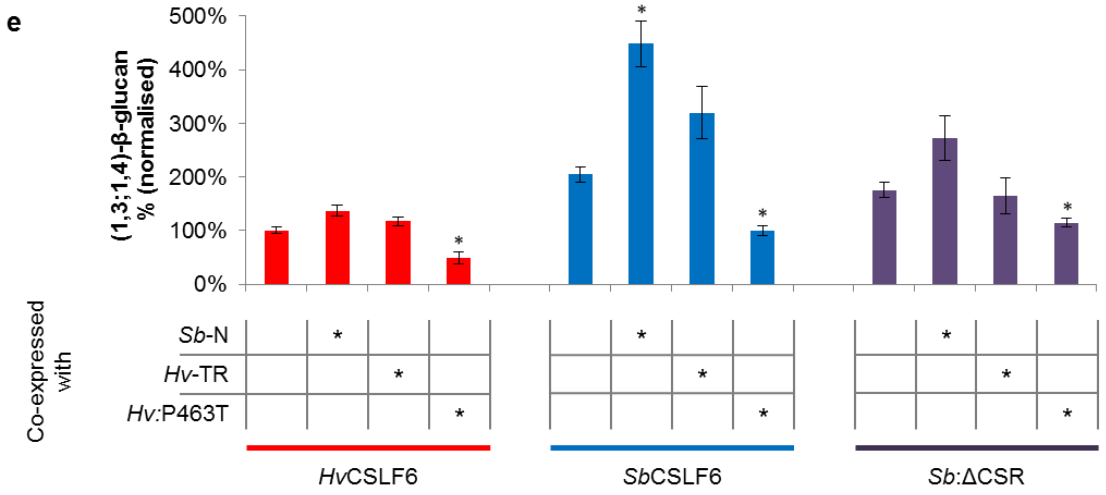


**Figure 3-7. Internally deleted, truncated and mutated CSLF6 proteins and the amounts of (1,3;1,4)-β-glucan produced after individual and combined expression in *N. benthamiana* leaves.**

(**a**) *Hv*CSLF6 (red) and *Sb*CSLF6 (blue) schematics showing the relative positions of predicted amphipathic helices (brown boxes), the 'extra region' (grey box), the Class Specific Region (CSR), the 'CxCxxxxCxC' motif and the P463T mutation. Internally deleted, truncated and mutant forms of *Hv*CSLF6 and/or *Sb*CSLF6 are shown with black lines marking boundaries. (**b**) Sequence alignments (DNA above with translation below) of a section of the *Sb*CSLF6 $NH_2$-terminal region with arrows showing where the four Cys residues of the 'CxCxxxxCxC' motif have been mutated to Ser residues in the *Sb*:(C-S) protein. (**c**, **d** and **e**) (1,3;1,4)-β-Glucan (% normalised) produced by CSLF6 constructs when expressed in *N. benthamiana* leaves. Asterisks indicate when the construct below has been co-expressed with the construct to the left. Error bars represent the standard error (n = 3). Asterisk above columns denote statistical significance (P≤0.05)

### 3.2.7 The CSLF6 CSR may be Involved in Complex Formation.

When expressed individually, *Sb*CSLF6 and *Sb*:ΔCSR produced similar levels of (1,3;1,4)-β-glucan, at 1.8% and 1.6% w/w, respectively. *Sb*:ΔCSR can still be repressed using the dominant negative mutant *Hv*:P463T and activated by co-expression with *Sb*-N (**Figure 3-7e** and **Figure 3-8**). However, when co-expressed with *Hv*-TR, *Sb*:ΔCSR displayed no change in production levels, unlike the wild type *Sb*CSLF6 which produced 56% more (1,3;1,4)-β-glucan compared with its individual expression (**Figure 3-7e**). This result suggests that *Sb*CSLF6 and *Hv*-TR may be able to interact via their CSRs (**Figure 3-11b**). *Sb*:ΔCSR however cannot be activated with *Hv*-TR, as one protein is missing the CSR, and the other is missing the $NH_2$-terminal region (**Figure 3-8** and **Figure 3-11d**). Given that the loss of the $NH_2$-terminal region or the CSR region alone is not sufficient to prevent complex formation, it is interesting to observe that the combination of an $NH_2$-terminal deletion in one protein and a CSR deletion in another results in altered complex formation.

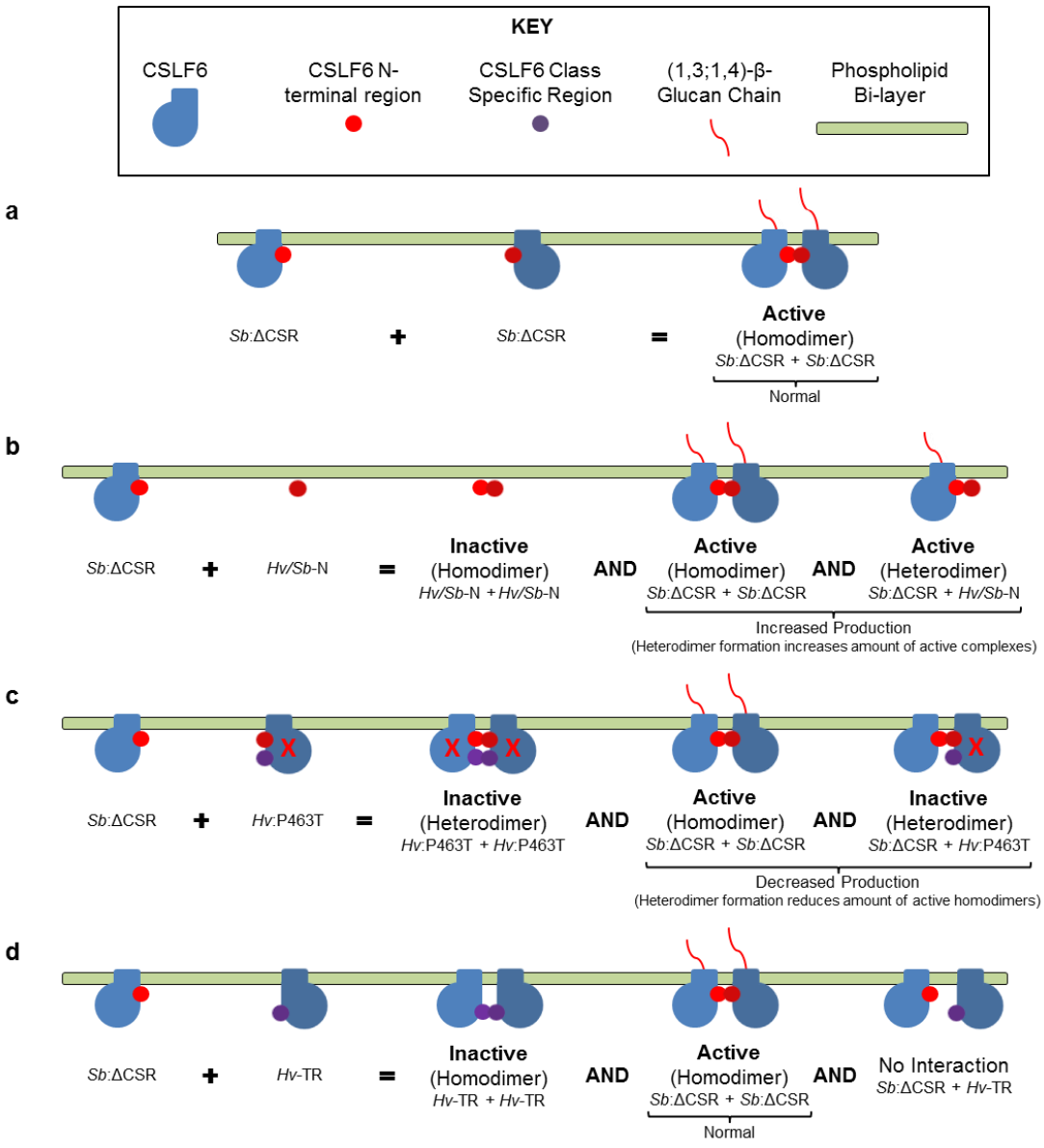


**Figure 3-8. Model of *Sb*:ΔCSR complex formation and interactions with truncated and mutated constructs.**

A model showing *Sb*:ΔCSR becoming active when in homodimeric complexes (**a**). When co-expressed with *Hv*-N or *Sb*-N (**b**), heterodimeric complexes form in addition to the active CSLF6 homodimer, resulting in more active complexes and increased (1,3;1,4)-β-glucan production. When co-expressed with *Hv*:P463T (**c**), inactive heterodimeric complexes also form which decrease the amount of active CSLF6 homodimers, decreasing (1,3;1,4)-β-glucan production. When co-expressed with *Hv*-TR (**d**), heterodimeric complexes do not form and (1,3;1,4)-β-glucan production remains unaltered.

### 3.2.8 A Thirty Amino Acid Stretch of the CSLF6 $NH_2$-Terminal Region May Regulate CSLF6.

To identify which part of the $NH_2$-terminal region was responsible for the regulation of CSLF6 activity, fourteen additional *Hv*CSLF6 and *Sb*CSLF6 chimeric constructs were designed with exchanges of every possible combination of three sections of the $NH_2$-terminal region, labelled A, B and C (**Figure 3-9a** and **Supplementary Table 8-2**, p139). The boundaries of these sections are stretches of identical sequence that naturally separate three regions of high dissimilarity.

Expression in *N. benthamiana* revealed considerable variation in (1,3;1,4)-β-glucan production from the different constructs (**Supplementary Table 8-2**, p139). The DP3:DP4 ratios however remained constant at ~1.65:1 for *HvCslF6* constructs, and ~1.0:1 for *SbCslF6* constructs (**Supplementary Table 8-2**, p139). (1,3;1,4)-β-Glucan expression levels were adjusted to 100% for the wild-type synthases, allowing the values from each of the chimeric *Hv*CSLF6 and *Sb*CSLF6 constructs to be normalised against them (**Figure 3-9b**). Once normalised, it became clear that constructs of both *Hv*CSLF6 and *Sb*CSLF6 with the same section exchanged, such as AC (**Figure 3-9b**), displayed similar differences in (1,3;1,4)-β-glucan levels compared with the wild-type synthases. To show the overall influence of the separate sections when exchanged between *Hv*CSLF6 and *Sb*CSLF6, the normalised results were combined and averaged (**Figure 3-9c**). For example, for section C, normalised (1,3;1,4)-β-glucan levels from each of the C, AC, BC and ABC constructs were combined and averaged. Overall, the greatest effect on (1,3;1,4)-β-glucan levels was observed when section C was exchanged between *Hv*CSLF6 and *Sb*CSLF6, increasing (1,3;1,4)-β-glucan production by 70%.

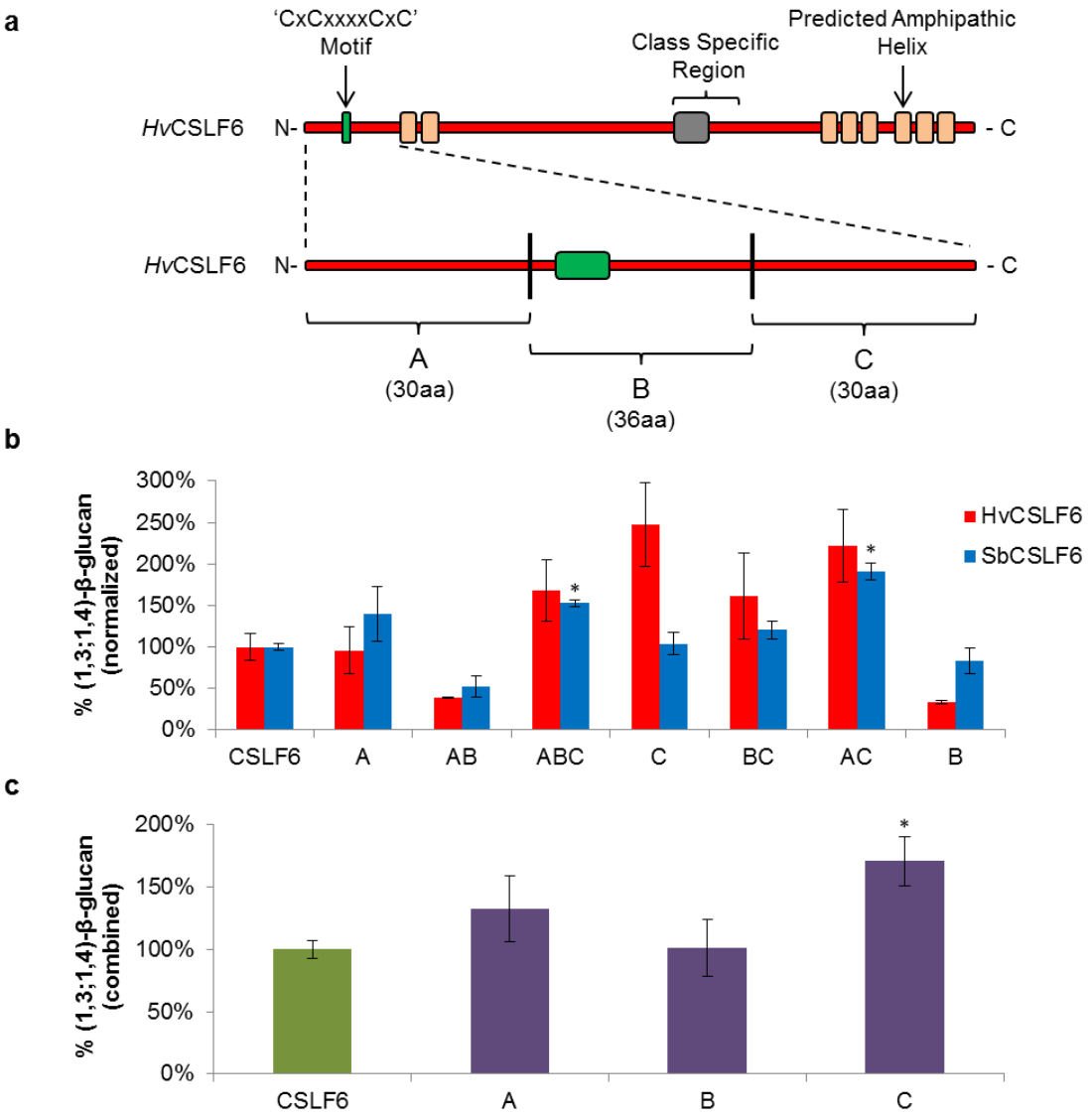
a
'CxCxxxxCxC' Motif
Class Specific Region
Predicted Amphipathic Helix
HvCSLF6 N-
- C
HvCSLF6 N-
- C
A (30aa)
B (36aa)
C (30aa)
b
% (1,3;1,4)-β-glucan (normalized)
300%
250%
200%
150%
100%
50%
0%
HvCSLF6
SbCSLF6
CSLF6
A
AB
ABC
C
BC
AC
B
c
% (1,3;1,4)-β-glucan (combined)
200%
150%
100%
50%
0%
CSLF6
A
B
C

**Figure 3-9. The influence of separate sections of the CSLF6 $NH_2$-Terminal region on (1,3;1,4)-β-glucan synthesis in *N. benthamiana* leaves.**

(**a**) *Hv*CSLF6 schematics highlighting relative positions of predicted amphipathic helices (brown boxes), the 'extra region' (grey box), the Class Specific Region and the 'CxCxxxxCxC' motif. Sections exchanged between *Hv*CSLF6 and *Sb*CSLF6 are also shown (A, B and C) with black lines marking the boundaries. (**b**) (1,3;1,4)-β-Glucan levels produced by *Hv*CSLF6 and *Sb*CSLF6 were adjusted to 100% (CSLF6) when expressed in *N. benth*amiana leaves. (1,3;1,4)-β-Glucan levels produced by the chimeric constructs were normalised against the wild-type synthases. The red column labelled AB represents the normalised (1,3;1,4)-β-glucan levels produced by the *Hv*CSLF6 construct which has had sections A and B exchanged with the equivalent regions from *Sb*CSLF6. Error bars represent the standard error. (**c**) The normalised (1,3;1,4)-β-glucan levels have been combined and averaged for both wild-type synthases, and every construct with sections A, B or C exchanged between *Hv*CSLF6 and *Sb*CSLF6. Error bars represent the standard error (n = 3). Asterisk above columns denote statistical significance ($P \leq 0.05$)

### 3.2.9 Point Mutations in the CSLF6 PilZ Motif Alter (1,3;1,4)-β-Glucan Production and DP3:DP4 Ratio.

The sequence of Section C in the CSLF6 $NH_2$-terminal region varies greatly between different CSLF6 orthologs (**Figure 3-10a**). Two motifs, 'DxSxxG' and 'RxxxR', are present in this region and are inverted but identical in sequence to the PilZ domain of BCSA, which has the 'RxxxR' motif followed by 'DxSxxG' (Morgan et al., 2014) (**Figure 3-10b**). As the PilZ domain is involved in the c-di-GMP mediated regulation of BCSA activity, it is predicted that the PilZ motif in CSLF6 may regulate enzyme activity via a similar mechanism, by binding an activator. Directly mutating these motifs in CSLF6 may therefore result in a reduction in (1,3;1,4)-β-glucan production. Three *Sb*CSLF6 point mutation constructs were developed to investigate the role of the PilZ motif in CSLF6 activity. The 'DxSxxG' motif was mutated to 'AxAxxA' (*Sb*:AxAxxA), and the 'RxxxR' motif was mutated to 'AxxxR' (*Sb*:R104A) and 'RxxxA' (*Sb*:R108A). As predicted, upon infiltration each of the three constructs displayed reduced (1,3;1,4)-β-glucan levels (**Figure 3-10c**), indicating that the residues are somehow influencing CSLF6 activity. As with all other manipulations of the $NH_2$-terminal region (**Supplementary Table 8-2**, p139), the *Sb*:AxAxxA and *Sb*:R104A constructs displayed wild-type DP3:DP4 ratios at ~1.05:1. The *Sb*:R108A construct however generated an elevated DP3:DP4 ratio of 1.29±0.03:1.

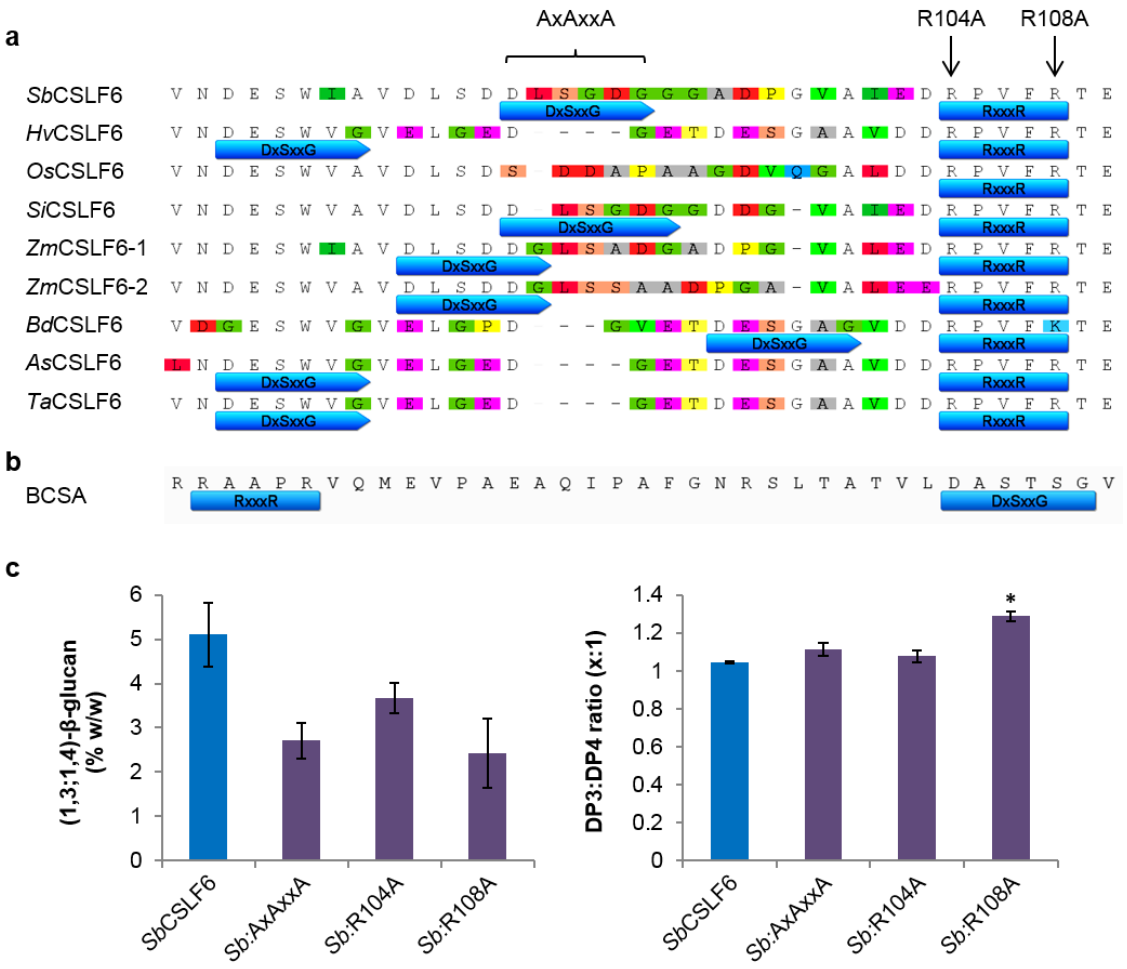
a
AxAxxA
R104A
R108A
SbCSLF6
HvCSLF6
OsCSLF6
SiCSLF6
ZmCSLF6-1
ZmCSLF6-2
BdCSLF6
AsCSLF6
TaCSLF6
DxSxxG
RxxxR
b
BCSA
RxxxR
DxSxxG
c
(1,3;1,4)-β-glucan (% w/w)
DP3:DP4 ratio (x:1)
SbCSLF6
Sb:AxAxxA
Sb:R104A
Sb:R108A
*

**Figure 3-10. The PilZ motifs of CSLF6 orthologs and BCSA, and the amount and structure of (1,3;1,4)-β-glucan produced by specific *Sb*CSLF6 mutant constructs in *N. benthamiana* leaves.**

(**a**) Amino acid comparisons between CSLF6 orthologs of the $NH_2$-terminal region immediately upstream of the first predicted amphipathic helix. CSLF6 orthologs include *Sb* (sorghum; *Sorghum bicolor*), *Hv* (barley, *Hordeum vulgare*), *Os* (rice; *Oryza sativa*), *Si* (foxtail millet; *Setaria italica*), *Zm* (corn; *Zea mays*), *Bd* (Purple false brome; *Brachypodium distachyon*), *As* (oat; *Avena sativa*) and *Ta* (wheat; *Triticum aestivum*). Coloured residues highlight amino acid differences between the orthologs. Predicted PilZ motifs ('DxSxxG' and 'RxxxR') are shown as blue bars immediately underneath individual sequences. Specific amino acids mutated in *Sb*CSLF6 constructs ('AxAxxA', 'R104A' and 'R108A') are also shown. (**b**) A section of the COOH-terminal region of BCSA from *Rhodobacter sphaeroides*, with the 'RxxxR' and 'DxSxxG' motifs of the PilZ domain highlighted with blue bars. (**c**) Amounts (% w/w) and DP3:DP4 ratios (x:1) of (1,3;1,4)-β-glucan produced by mutant *Sb*CSLF6 constructs when expressed in *N. benthamiana* leaves. Error bars represent the standard error (n = 3). Asterisk above columns denote statistical significance ($P \leq 0.05$)

## 3.3 Discussion

In chapter 2 the $NH_2$-terminal regions of wild type *Hv*CSLF6 and *Sb*CSLF6 were exchanged, resulting in increased (1,3;1,4)-β-glucan production by both chimeric synthases. It was therefore suggested that a conformational change may have occurred that resulted in the change of activity, indicating that the $NH_2$-terminal region of CSLF6 may be involved in the regulation of enzymic activity. The experiments presented here further investigated this observation through the coexpression of various CSLF6 constructs with modifications that affect putative complex formation and/or regulation of (1,3;1,4)-β-glucan production. However, as with each of the following theoretical explanations, direct biochemical evidence is required to support such theories. The proteins expressed may interact with and influence protease action, substrates, inhibitors or activators, each of which could influence (1,3;1,4)-β-glucan production independent of CSLF6 complex formation. Principally, each of the wild type, chimeric, truncated and mutated constructs must be purified in an active form such that specific activity, stability and protein-protein interactions can be assayed quantitatively.

Nevertheless, a model has been devised whereby the $NH_2$-terminal region of CSLF6 exists in equilibrium between two conformational states, open and closed (**Figure 3-11a**). The enzyme is suggested to be inactive in the closed state and active in the open state. We have used this model to help simplify and explain the behaviour of each of the CSLF6 constructs, consistent with the data. For example, one possible explanation for the increase in (1,3;1,4)-β-glucan production when the $NH_2$-terminal region is exchanged between CSLF6 enzymes may lie in the stability of the open and closed state of the $NH_2$-terminal region. Exchanging this region may have reduced putative binding of the $NH_2$-terminus with the core of the CSLF6 protein, destabilising the closed confirmation and shifting the equilibrium towards the open state, resulting in a greater number of active synthase complexes and increased (1,3;1,4)-β-glucan production.

Alternatively, (1,3;1,4)-β-glucan production may have increased when the $NH_2$-terminal regions were exchanged between CSLF6 enzymes because the region was more available to bind an allosteric activator or an interacting enzyme. If the $NH_2$-terminal regions were regulating CSLF6 activity by such a means, then co-expressing *Hv*-N or *Sb*-N (**Figure 3-2a**)

with a full length synthase would theoretically result in a decrease in (1,3;1,4)-β-glucan production due to sequestration of a key factor. However, when *Hv*CSLF6 and *Sb*CSLF6 were co-expressed with either *Hv*-N or *Sb*-N, increases in (1,3;1,4)-β-glucan production were observed from both wild-type synthases (**Figure 3-2b**). We therefore suggest that the $NH_2$-terminal region constructs were modulating CSLF6 activity either by directly interacting with and activating the full length synthases; or by sequestering an inhibitory factor.

If CSLF6 were indeed bound in *N. benthamiana* leaves by an inhibitory factor interacting with the $NH_2$-terminal region, then removing this region from CSLF6 should have abolished the negative regulation, causing (1,3;1,4)-β-glucan production to increase. When *Hv*-TR was expressed however, no (1,3;1,4)-β-glucan was produced, nor was activity restored when *Hv*-TR was co-expressed with *Hv*-N or *Sb*-N (**Figure 3-2c**). The evidence therefore suggests that CSLF6 is not regulated by an inhibitory factor in *N. benthamiana* through an interaction with the $NH_2$-terminal region. Rather it appears possible that CSLF6 activity may be modulated by dimerisation or the formation of higher order complexes, which is in part mediated by the $NH_2$-terminal region (**Figure 3-11**). When *Hv*-N or *Sb*-N were co-expressed with *Hv*CSLF6 and *Sb*CSLF6, the $NH_2$-terminal fragments may have been able to interact with the full-length synthases, mimicking normal complex formation and increasing (1,3;1,4)-β-glucan production (**Figure 3-11b** and **Figure 3-11b**). Similarly, when *Hv*-TR was co-expressed with *Hv*CSLF6 and *Sb*CSLF6, increased (1,3;1,4)-β-glucan production was observed by both wild-type synthases (**Figure 3-2c**). This result suggests that *Hv*-TR may have also been able to interact with the full-length synthases, mimicking wild type complex formation and enhancing (1,3;1,4)-β-glucan production (**Figure 3-11c** and **Figure 3-11b**).

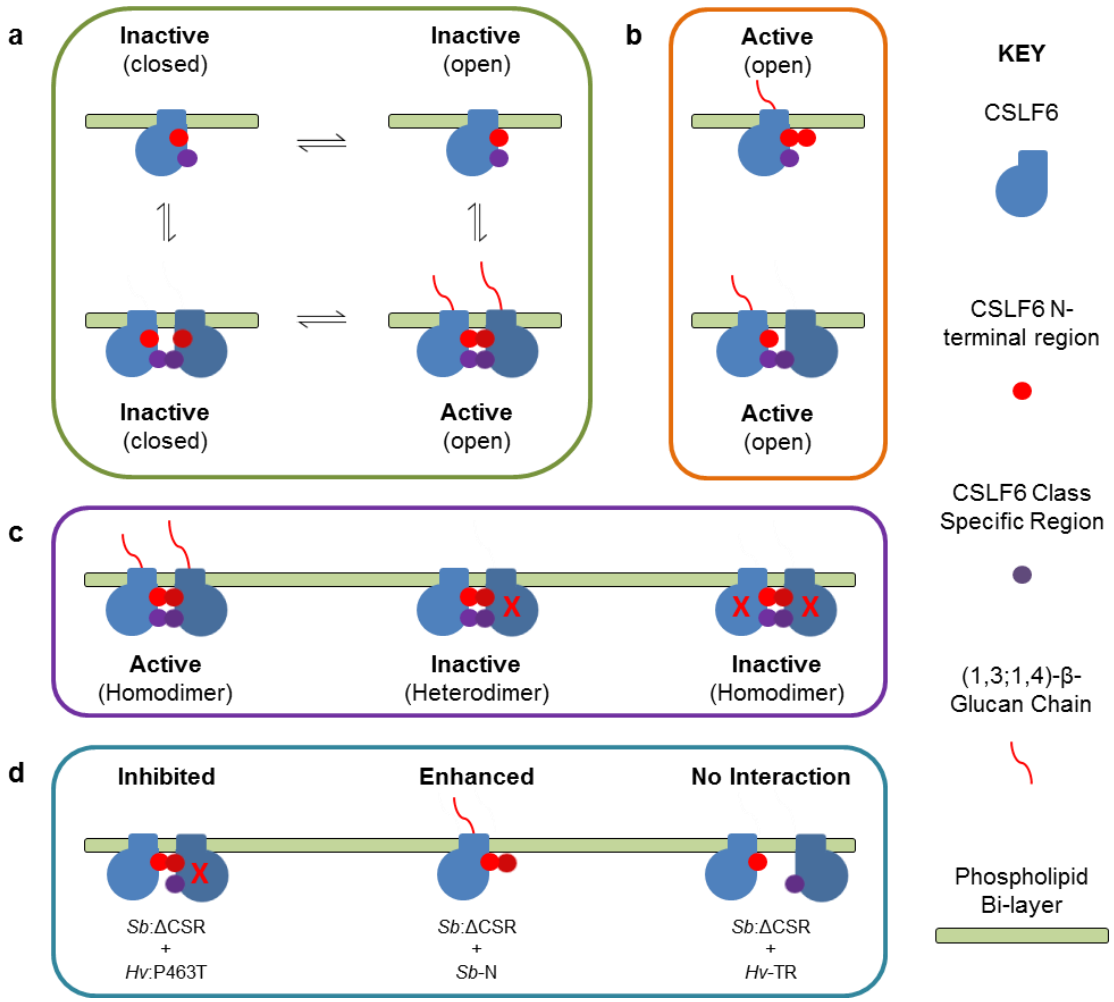


**Figure 3-11. Model of CSLF6 regulation and the effect of co-expressing internally deleted, truncated and mutated constructs.**

(**a**) Four theoretical states in which CSLF6 enzymes may exist based on the conformation of the $NH_2$-terminal region (closed or open) and the monomeric or dimeric status of CSLF6. (**b**) Theoretical states of the CSLF6 enzyme when co-expressed with *Hv*-N or *Sb*-N (above) or the *Hv*-TR (below). (**c**) A representation of the three theoretical dimeric forms of CSLF6 when co-expressed with the mutated *Hv*:P463T construct (marked with a red cross) which acts in a dominant negative manner to repress activity. (**d**) A representation of how *Sb*:ΔCSR may be affected by the co-expression of *Hv*:P463T (left), *Sb*-N (centre) and *Hv*-TR (right).

To further support a model where CSLF6 is active as a dimer or higher order complex, a

mutated *Hv:*P463T construct was generated based on two *CESA* dominant negative mutants, *thanatos* (Daras et al., 2009) and *fra5* (Zhong et al., 2003). In *Arabidopsis*, these mutated synthases were predicted to form complexes with other CESA members. In doing so, they inhibited their activity, leading to reduced cellulose production and plant growth abnormalities. The CSLF6 equivalent, *Hv:*P463T, also exhibited a dominant negative effect on (1,3;1,4)-β-glucan production when co-expressed with *Hv*CSLF6 or *Sb*CSLF6 (**Figure 3-7**), causing a ~50% reduction in biosynthesis. This result suggests that like the CESA mutants, *Hv*:P463T may also capable of forming complexes and inactivating wild-type synthases (**Figure 3-11c**), supporting the theory that CSLF6 is active in a complex. The *Hv:*P463T protein therefore provides an opportunity to identify regions of *Hv*CSLF6 that are required for oligomerisation. By co-expressing wild type *Hv*CSLF6 with *Hv:*P463T constructs that have additional mutations, it would be possible to find regions of the protein that interfere with complex formation and abolish the dominant negative effect.

Two further regions of CSLF6, which are similar to CESA enzymes, were investigated, because they have been postulated to be involved in CESA oligomerisation. These regions are a highly conserved 'CxCxxxxCxC' motif similar to a zinc-binding domain (Kurek et al., 2002) and the highly variable CSR (Sethaphong et al., 2013). When each of the four Cys residues of the 'CxCxxxxCxC' motif at the $NH_2$-terminal region were replaced with Ser (*Sb*:(C-S)), no difference in (1,3;1,4)-β-glucan production was observed (**Figure 3-7c** and **Supplementary Table 8-2**, p139); *Hv:*P463T could still inhibit synthesis and the mutated $NH_2$-terminal fragment (*Sb*-N:(C-S)) caused the same increase in (1,3;1,4)-β-glucan biosynthesis by the full-length synthases as the wild-type fragment (*Sb*-N) (**Figure 3-7d**). Overall, it appears that in the *N. benthamiana* system, the highly conserved 'CxCxxxxCxC' motif has no effect on enzyme activity or the ability of the protein to form putative higher order complexes.

The second region of CSLF6 predicted to contribute to complex formation, the CSR, showed little effect when exchanged between *Hv*CSLF6 and *Sb*CSLF6, and no effect when it was removed from *Sb*CSLF6 (**Figure 3-5**). It was not unexpected that CSLF6 remained capable of (1,3;1,4)-β-glucan biosynthesis without the CSR, given that the CSR is not present in bacterial cellulose synthases (Morgan et al., 2013) and it is not predicted to be structurally

required for catalysis in CESA enzymes (Sethaphong et al., 2013). Therefore to investigate the role of the CSR in CSLF6 complex formation, *Sb*:ΔCSR was co-expressed separately with *Sb*-N, *Hv*:P463T and *Hv*-TR in *N. benthamiana* leaves (**Figure 3-7e**). When co-expressed, *Sb*:ΔCSR responded very differently from wild-type *Sb*CSLF6 to the presence of *Sb*-N, *Hv*:P463T and *Hv*-TR (**Figure 3-11d**). *Sb*CSLF6 displayed a greater increase in (1,3;1,4)-β-glucan production when co-expressed with *Sb*-N, and a greater decrease when co-expressed with *Hv*:P463T, compared with *Sb*:ΔCSR. When co-expressed with *Hv*-TR, *Sb*CSLF6 displayed an increase in (1,3;1,4)-β-glucan production, whilst *Sb*:ΔCSR showed no change, suggesting that *Sb*CSLF6 and *Hv*-TR are able to interact via their CSRs (**Figure 3-11b**). *Sb*:ΔCSR was not activated by *Hv*-TR however, as one protein was missing the CSR, and the other was missing the $NH_2$-terminal region (**Figure 3-8**and **Figure 3-11d**). Cumulatively, the results presented here suggest that CSLF6 activity is dependent on the formation of higher order complexes. Complex formation can occur when either the $NH_2$-terminal region or CSR is missing, but cannot occur when one enzyme is missing the $NH_2$-terminal region and another is missing the CSR. To support the hypotheses presented here, work is underway to investigate complex formation *in vitro*, to develop an *in silico* model of complex formation and to understand its significance *in vivo*.

One question remains however; if in the absence of the $NH_2$-terminal, the CSR is sufficient for complex formation and activation of a full-length synthase, then why is *Hv*-TR inactive (**Figure 3-2**)? This suggests that the CSLF6 $NH_2$-terminal region is indeed involved in enzyme activation, a process that may, or may not, be associated with complex formation. In order to pinpoint functional residues, the $NH_2$-terminal region was divided into three sections and constructs with every possible swap were made between *Hv*CSLF6 and *Sb*CSLF6 (**Figure 3-9a** and **Supplementary Table 8-2**, p139). Transient expression in *N. benthamiana* indicated that the section at the COOH-terminal end (Section C) affects the greatest change in (1,3;1,4)-β-glucan production when exchanged between the two synthases, at an average of 70% (**Figure 3-9c**). This section contains the 'DxSxxG' and 'RxxxR' motifs that are identical, but in the opposite order to the BCSA PilZ domain (**Figure 3-10b**) (Morgan et al., 2014), which is involved in c-di-GMP mediated enzyme activation. To date, no cyclic-di-nucleotides have been found in plants or shown to influence plant enzymes. Cyclic nucleotides such as cGMP, on the other hand, are abundant in plants and are known to

function as secondary messengers (Martinez-Atienza et al., 2007). Therefore it is feasible that cGMP may be responsible for CSLF6 activation in a similar manner to the c-di-GMP activation of BCSA.

If the PilZ motif of CSLF6 functioned similarly to that of BCSA (Morgan et al., 2014), to bind a regulatory molecule and activate the synthase, then why was an increase in (1,3;1,4)-β-glucan production observed when the section was exchanged between *Hv*CSLF6 and *Sb*CSLF6 (**Figure 3-10a**)? Sequence differences across this region may have caused a loss or reduction in intramolecular interactions between the region and the downstream protein sequence, impacting the inhibitory mechanism. This could possibly render the area more accessible to $NH_2$-terminal mediated dimerisation and/or activator binding, leading to increased activation and (1,3;1,4)-β-glucan production.

If the 'DxSxxG' and 'RxxxR' motifs of CSLF6 were involved in binding a secondary messenger, then mutating the conserved residues would presumably decrease binding affinity and lead to reduced (1,3;1,4)-β-glucan production? This was the case for each of the three *Sb*CSLF6 PilZ mutant constructs (**Figure 3-10b**), which mimicked the loss of activity resulting from mutations in the BCSA PilZ domain. However, when the first Arg of the 'RxxxR' motif was mutated in BCSA, the enzyme exhibited constitutive activity (Morgan et al., 2014). In BCSA this Arg was predicted to be directly involved in enzyme repression and its mutation led to the abolition of the negative regulatory mechanism. The same effect was not observed in *Sb*CSLF6 when the second Arg of the 'RxxxR' motif was mutated, however there was an increase in the DP3:DP4 ratio of the (1,3;1,4)-β-glucan from 1.05±0.01:1 to 1.29±0.03:1 (**Figure 3-10b**). This suggests that the R108 residue of *Sb*CSLF6 could be interacting with the active site in a similar manner to the Arg in approximately the equivalent position in BCSA, but the mutagenesis may not have led to a complete disassociation, instead resulting in a conformational change at the active site, causing the altered DP3:DP4 ratio. Nevertheless, the conserved residues of the CSLF6 PilZ motif do appear to influence enzyme activity. The regulatory mechanism appears to function similarly to BCSA and it may be binding an unknown factor that affects enzyme activation/de-repression. In addition, the increase in (1,3;1,4)-β-glucan production by *Hv*CSLF6 and *Sb*CSLF6 when co-expressed with the $NH_2$-terminal fragments (**Figure 3-2c**) suggests that secondary

messenger binding may also be coupled to CSLF6 dimerisation. In order to confirm the role of a secondary messenger in CSLF6 activation/de-repression, experiments are underway to purify wild-type and PilZ mutated CSLF6 $NH_2$-terminal regions to measure the kinetics of secondary messenger binding *in-vitro*.

By taking a co-expression approach to investigate CSLF6 regulation, and by using a variety of chimeric, internally deleted, truncated and mutated constructs, measurable progress has been made towards understanding the way in which (1,3;1,4)-β-glucan biosynthesis is controlled in cereals. Useful tools have also been generated to help understand the functional role of CSLF6 complex formation and to determine the mode of enzyme activation. With an enhanced biochemical understanding of (1,3;1,4)-β-glucan biosynthesis and regulation it may be possible to control the deposition of (1,3;1,4)-β-glucan and its rate of synthesis *in planta*, enhancing the human health benefits and industrial value of cereal tissues.

## 3.4 Materials and Methods

### 3.4.1 Construct Development

The *HvCslF6* ('Sloop') (Burton et al., 2008), *SbCslF6* ('BTx623'), *HvCslF6:Sb-N* and *SbCslF6:Hv-N* (Chapter 2) sequences were available in the pCR8/GW/TOPO and pEAQ-HT-DEST-1 vectors of the Gateway™ cloning system (Curtis and Grossniklaus, 2003; Sainsbury et al., 2009). *Hv-N* and *Sb-N* truncation constructs were isolated by PCR (**Supplementary Table 8-3**, p140) from *HvCslF6* and *SbCslF6* sequences respectively using a reverse primer that introduced a stop (TGA) codon at the 3' end. All other constructs were generated by PCR (**Supplementary Table 8-3**, p140, **Supplementary Table 8-4**, p141 and **Supplementary Table 8-5**, p142) prior to cloning using the Geneart™ Seamless cloning and assembly kit (Life Technologies, Carlsbad, USA) according to the manufacturer's instructions. $NH_2$-terminal region fragments with sections interchanged were synthesised prior to PCR by GeneArt® Gene Synthesis (Life Technologies, Carlsbad, USA). *HvCslF3*, *HvCslF4*, *HvCslF7*, *HvCslF9*, *HvCslF10*, *HvCslJ* and *HvCslH* cDNA sequences were available in-house (RA Burton, unpublished data). Each construct was sequenced (Australian Genome Research Facility Ltd) before being transferred to the pEAQ-HT-DEST-1 binary expression vector (Sainsbury et al., 2009) for transient expression in *N. benthamiana*. DNA sequence comparisons were performed on Geneious software (version 8.1.3, available from http://www.geneious.com).

### 3.4.2 Transient Transformation of *Nicotiana benthamiana*

All *N. benthamiana* plants were grown with 22°C day and 15°C night temperatures without supplemented light in the Plant Accelerator® (University of Adelaide). *Agrobacterium tumefaciens* preparation and transient transformation was adapted from Kapila et al. (1997) and Wydro et al. (2006) and performed according to chapter 2 (Section 2.4.5, p48) with the following changes. For experiments where combinations of constructs were co-infiltrated, an *Agrobacterium* optical density at 600nm ($OD_{600}$) of 0.5 per construct was used. An empty vector *Agrobacterium* control was combined with singly expressed constructs in such experiments to ensure that each infiltration event contained the same concentration of *Agrobacterium* and the p19 silencing suppressor (Voinnet et al., 2003)

present in pEAQ-HT-DEST-1 (Sainsbury et al., 2009). In experiments where constructs were infiltrated individually, final $OD_{600}$ levels of 1.0 were used. Data shown is based on three biological replicates with two technical replicates of each sample.

### 3.4.3 (1,3;1,4)-β-Glucan Assay

Analysis of (1,3;1,4)-β-glucan content was performed according to chapter 2 (Section 2.4.8, p49) using commercially available reagents (Megazyme International Ireland Ltd, Bray, Ireland), with a protocol based on McCleary and Codd (1991).

### 3.4.4 High Performance Liquid Chromatography (HPLC) Analysis

Analysis was performed according to Ermawar et al. (2015) using high pH anion exchange chromatography with pulsed amperometric detection (HPAEC-PAD) on a Dionex ICS-5000.

# 4. Analysis of the *HvCslF6* Promoter.

## 4.0 Introduction

Members of the *CslF* and *CslH* gene families have been implicated in the biosynthesis of (1,3;1,4)-β-glucan in gain of function experiments conducted in *Arabidopsis thaliana*, which is a dicot devoid of (1,3;1,4)-β-glucan (Burton et al., 2006; Doblin et al., 2009). Although expression was driven by the constitutive 35S promoter, only a small quantity of (1,3;1,4)-β-glucan was synthesised and only in specific cell types. One or more additional factors that interact with the CSLF and CSLH enzymes may therefore be required for high levels of synthesis to occur, and these are missing, limiting or poorly equivalent in the dicot cells (Burton et al., 2006).

In barley, Q-PCR analysis has shown that each *CslF* gene exhibits distinct patterns of transcript abundance (Burton et al., 2008; Schreiber et al., 2014). Most *CslF* genes displayed low transcript levels across all examined tissues. *HvCslF6* was the exception, however, displaying a high transcript abundance across most tissues, suggesting that it may be responsible for producing the majority of the (1,3;1,4)-β-glucan in barley. The central role of *CslF6* has subsequently been supported by Nemeth et al. (2010), who transformed wheat (*Ta*) with a *TaCslF6* RNA interference construct. RNAi lines showed a fourfold decrease in *TaCslF6* transcripts in wheat grain at 14 days post anthesis, resulting in a 42.2% reduction of grain (1,3;1,4)-β-glucan at maturity. Taketa et al. (2011) investigated three independent *betaglucanless* barley mutants, which exhibited no detectable (1,3;1,4)-β-glucan in any of the tissues tested. Supporting earlier findings by Burton et al. (2008) and Nemeth et al. (2010), mutations in *Hv*CSLF6 near highly conserved motifs were likely to have abolished CSLF6 activity. This hypothesis was confirmed by the lack of (1,3;1,4)-β-glucan production by the mutated enzymes when expressed heterologously in *N. benthamiana* leaves (Taketa et al. (2011).

In a study by Burton et al. (2011), gene and promoter-specific effects were observed when selected *Hv*CSLF enzymes were overexpressed with the constitutive 35S and the grain-specific *As*GLO promoters. Mature grain from 35S:*HvCslF4* transgenic plants showed elevated (1,3;1,4)-β-glucan levels, 35S:*HvCslF6* plants showed elevated leaf (1,3;1,4)-β-glucan levels, and *As*GLO:*HvCslF6* plants showed elevated grain (1,3;1,4)-β-glucan levels. For the 35S:*HvCslF6* lines, where the use of a strong, supposedly constitutive promoter was

likely to have increased *CslF6* transcript levels in most tissues, (1,3;1,4)-β-glucan levels were not elevated in any of the tissue types. This result therefore supported earlier work in *A. thaliana* (Burton et al., 2006) suggesting that one or more other factors are required for efficient (1,3;1,4)-β-glucan biosynthesis. Therefore, in order to better control biosynthesis and increase (1,3;1,4)-β-glucan in specific cell types, it is necessary to identify any other factors that might contribute to biosynthesis. Thus far, Q-PCR and barley Affymetrix microarray datasets (Close et al., 2004) have provided few co-expressed candidate genes and these techniques seem limited in their capabilities to identify such genes (Burton and Fincher, 2009).

The identification of regulatory elements such as those that might potentially allow the binding of transcription factors to the *CslF6* promoter may prove more successful than previously outlined techniques. Such regulatory elements may also modulate the expression of unknown genes associated with (1,3;1,4)-β-glucan biosynthesis, potentially enabling candidate genes to be identified. Typically, promoter binding assays are performed to pinpoint the binding sites of such regulatory elements. The promoter sequences are inserted into a vector and drive the expression of a reporter gene such as Green-Fluorescent Protein (GFP) (Chiu et al., 1996) or GUS (Jefferson et al., 1987) in stably transformed plants (Matzke et al., 1990). By using a 5' or 3' deletion series of the promoter of interest the regions containing the binding sites can be identified.

As barley is our target species and it requires approximately one year to generate mature transgenic plants, a transient *Agrobacterium*-mediated vacuum infiltration system was developed. This procedure was performed using barley roots, coleoptiles and first leaf bases, each of which have been shown to exhibit high levels of *HvCslF6* transcript abundance (Burton et al., 2008). Three Kb of putative promoter sequence upstream of the *HvCslF6* open reading frame (ORF) was isolated and a 5' deletion series was generated. Promoter activity was quantified using the Dual-Luciferase reporter system because it contains an embedded positive control of *Renilla* luciferase, increasing the accuracy of measurements by minimising the effect of experimental variables such as transformation efficiency (**Figure 4-1**).

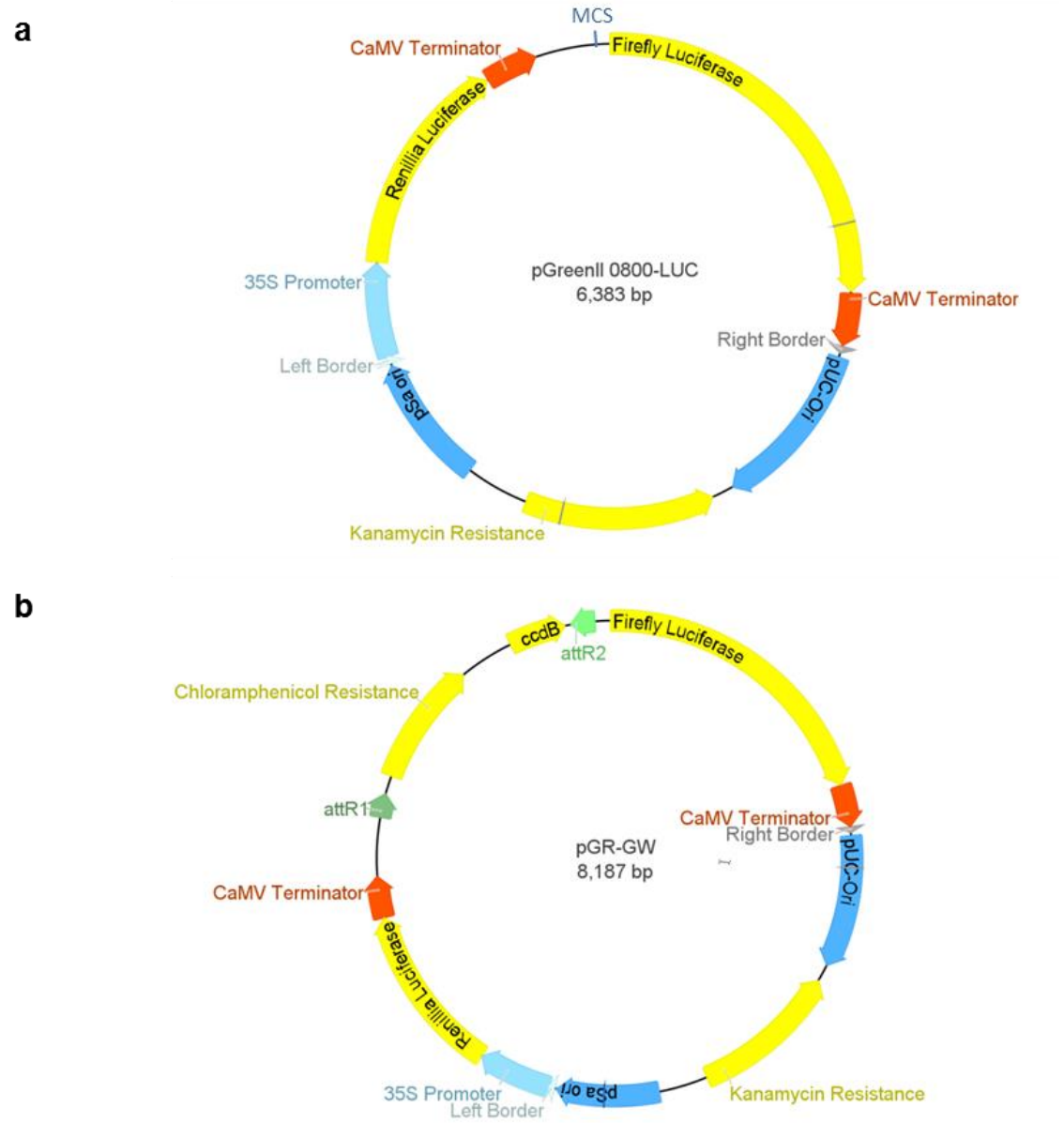


**Figure 4-1. Expression vectors used to transiently transform *N. benthamiana* leaves and barley tissues for the Dual Luciferase Assay.**

(**a**) The pGreenII-0800-LUC vector contains both firefly and *Renilla* luciferases, CaMV transcriptional terminators, one 35S promoter, Kanamycin resistance, both the pUC and pSa origins of replication and a right and left border. Immediately upstream of the firefly luciferase lies a multiple cloning site (MCS) for the insertion of promoter fragments. (**b**) pGR-GW differs from pGreenII-0800-LUC as it has a Gateway™ sequence inserted into the multiple cloning site, consisting of two attR sites, chloramphenicol resistance and a cell death gene (ccdB).

## 4.1 Results

### 4.1.1 The Putative *HvCslF6* Promoter is not active in *Nicotiana benthamiana* Leaves.

Promoter fragments were first assayed for activity in *N. benthamiana* leaves three days post infiltration. With the exception of the un-infiltrated blank, each construct displayed considerable expression of the embedded positive control, *Renilla* luciferase (**Figure 4-3a**). When the 35S promoter was driving firefly luciferase expression, significant chemiluminescence was observed. The low firefly:*Renilla* (F:R) ratio of 0.05:1 (**Figure 4-3b**) for the empty vector pGreen-0800-LUC (pGR-0800) indicated that in the absence of a promoter fragment, there was only a low degree of background firefly luciferase expression. The Gateway-enabled empty vector construct (pGR-GW) displayed an elevated F:R ratio of 0.22:1, suggesting that the Gateway sequence may be driving weak expression of firefly luciferase. With the full putative *HvCslF6* promoter inserted into the pGR-GW construct (*Hv*PrA) (**Figure 4-2**), no change in F:R ratio was observed compared with pGR-GW (**Figure 4-3**). Therefore the putative *HvCslF6* promoter does not appear to be able to drive firefly luciferase expression in the *N. benthamiana* system.

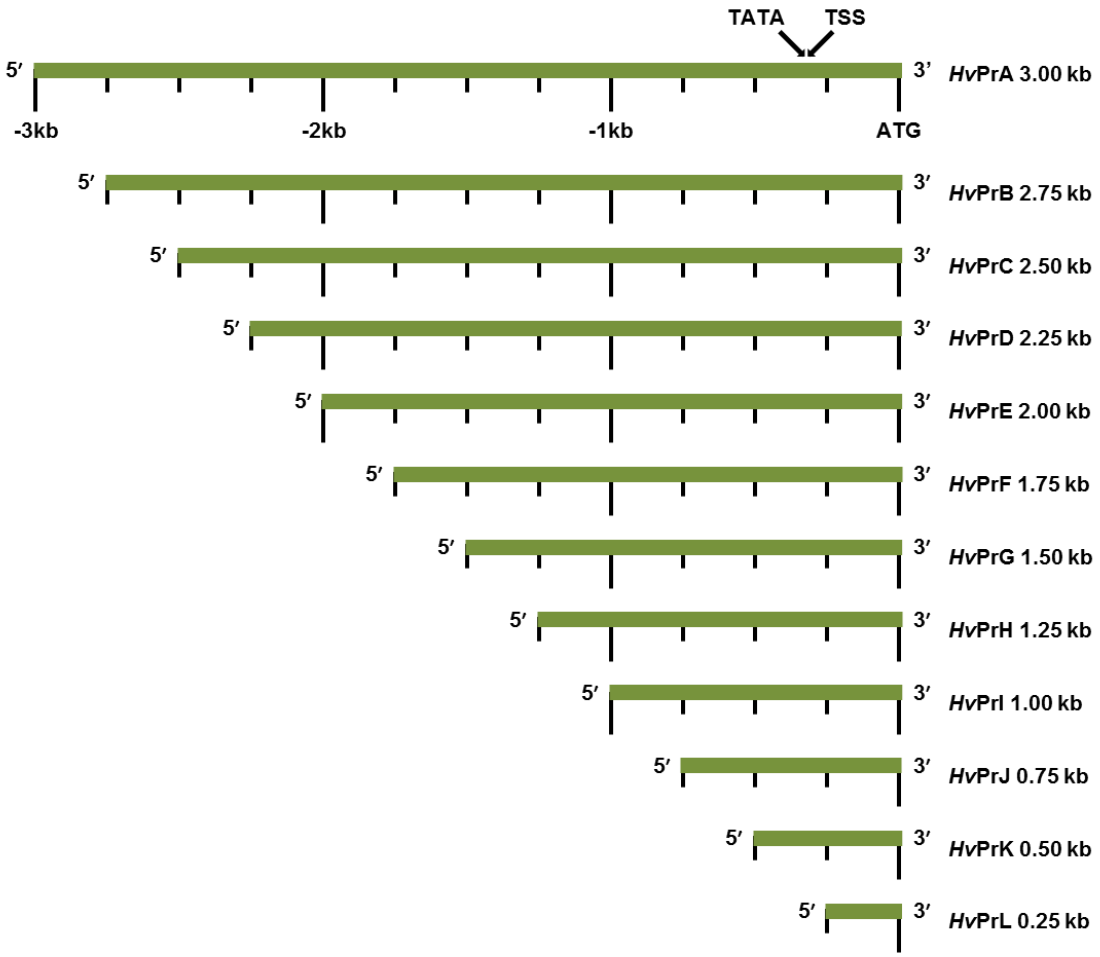


**Figure 4-2. Deletion series of the putative *HvCslF6* promoter.**

Three Kb of genomic DNA immediately upstream of the *HvCslF6* ORF was defined as the putative *HvCslF6* promoter. The 'TATA' box and transcriptional start site (TSS) are predicted to be located within the first four hundred bases upstream of the 'ATG' site. Twelve constructs labelled *Hv*PrA to *Hv*PrL are progressively shorter at the 5′ end by approximately two hundred and fifty bases and have been inserted into the Gateway enabled pGR-GW expression vector.

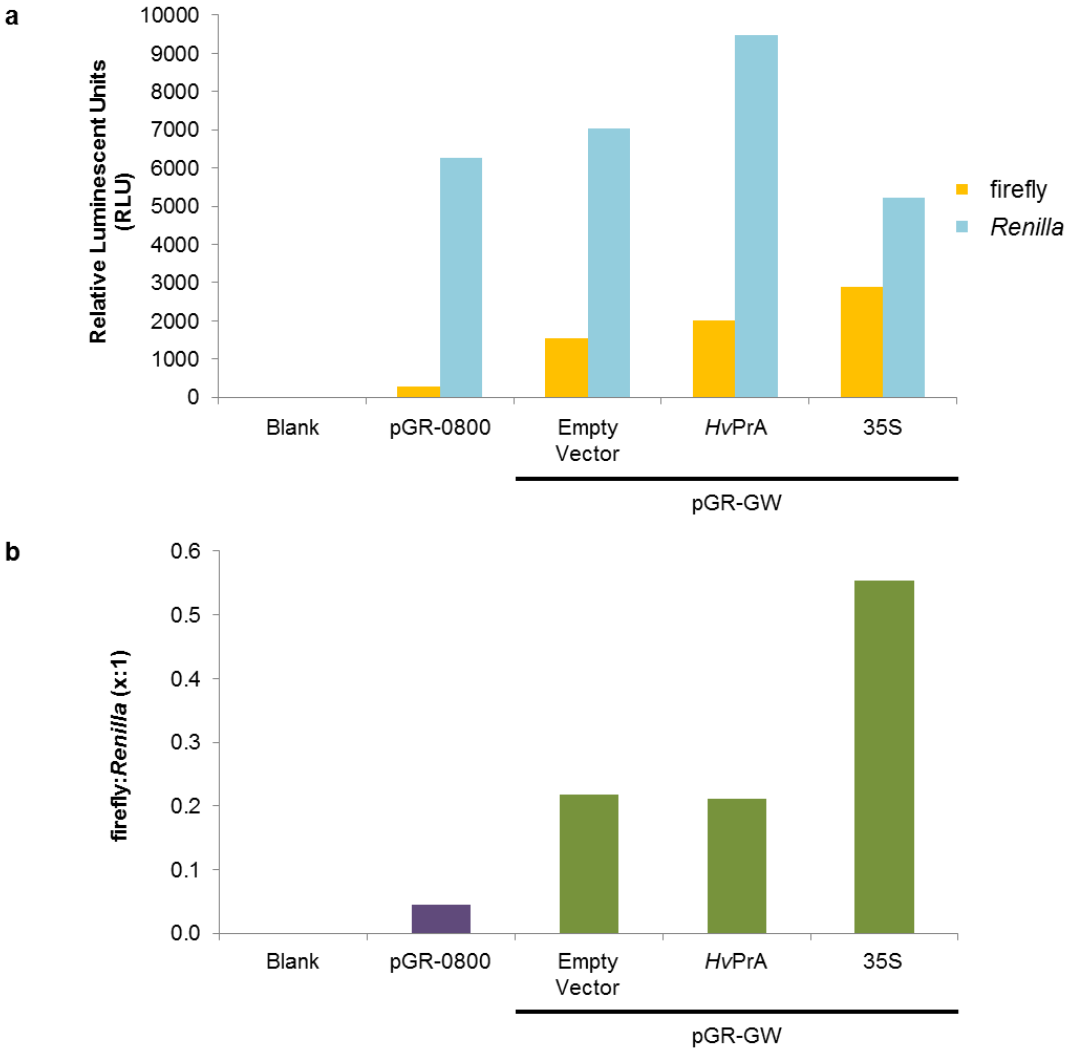


**Figure 4-3. Firefly and *Renilla* luciferase activity post-transient infiltration of promoter fragments in *N. benthamiana* leaves.**

(**a**) Quantification of firefly and *Renilla* luciferase levels via chemiluminescent measurement of enzyme activity post construct infiltration of *N. benthamiana* leaves. (**b**) The ratio of enzyme activity of firefly luciferase, driven by the promoter fragments, against the *Renilla* luciferase internal standard, driven by the 35S promoter, when constructs were infiltrated into *N. benthamiana* leaves. pGR-0800 is an empty vector construct, pGR-GW is derived from pGR-0800 and has been Gateway-enabled, *Hv*PrA is the full-length *HvCslF6* promoter fragment, and 35S is a constitutive promoter fragment. (n = 1)

### 4.1.2 Transient *Agrobacterium-m*ediated Expression can be Performed in Barley Tissues

A barley expression system was tested in place of the *N. benthamiana* system so that cereal-specific regulatory sites in the putative *HvCslF6* promoter could be identified. Four day old roots and coleoptiles, and ten day old first leaf bases were selected based on Burton et al. (2008), as these tissues exhibit high levels of *HvCslF6* transcript abundance. As a robust transient expression system has not yet been developed for cereal systems, an *Agrobacterium*-mediated vacuum infiltration method was used. Overall, luciferase expression was considerably lower in the barley tissues than in *N. benthamiana*, requiring the addition of three hundred times more of the crude protein preparation into the assay for reliable chemiluminescent analysis (**Figure 4-4**). Nevertheless, the procedure allowed adequate detection of the signal.

In each tissue type comparable F:R ratios were observed (**Figure 4-4b**); the 35S promoter generated the highest ratio whilst the negative control (NosT), *Hv*PrA and *Hv*PrF generated similar, but lower, ratios. Since the first leaf base tissues were the most simple to prepare and manipulate, and generally displayed the highest luciferase expression levels (**Figure 4-4a**), this tissue was selected for further examination of the promoter deletion series.

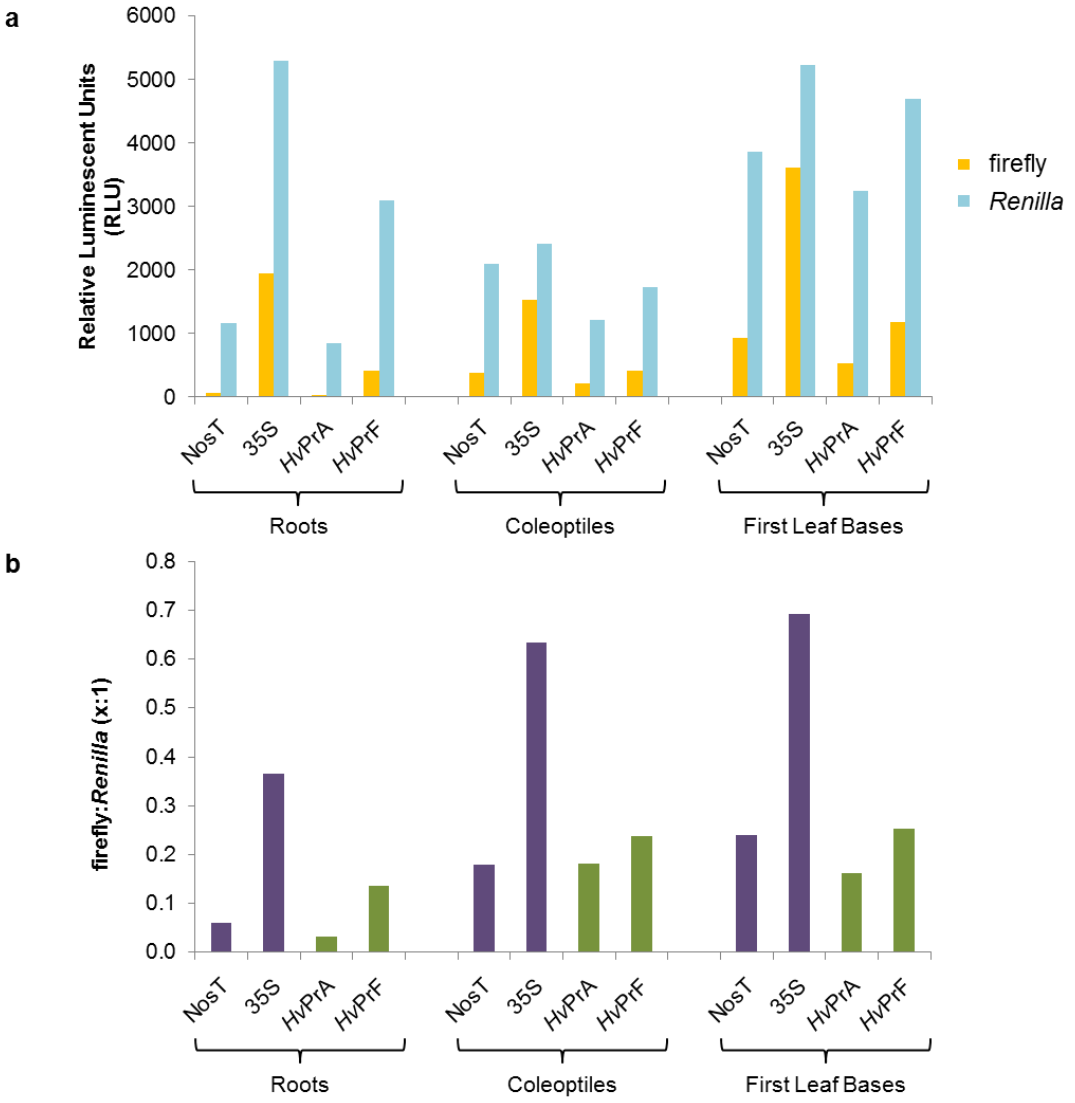


**Figure 4-4. Firefly and *Renilla* luciferase activity in barley tissues.**

(**a**) Quantification of firefly and *Renilla* luciferase expression levels via chemiluminescent measurement of enzyme activity in barley roots, coleoptiles and first leaf bases. (**b**) The ratio of enzyme activity of firefly luciferase, driven by the promoter fragments, against the *Renilla* luciferase internal standard. Negative control (NosT), constitutive 35S promoter and *HvCslF6* promoter deletion series fragments (*Hv*PrA and *Hv*PrF) were each present in the pGR-GW vector. (n = 1)

### 4.1.3 A Repressor Element in the *HvCslF6* Promoter Inhibits Transient Luciferase Expression.

Excluding *Hv*PrE, each construct of the *HvCslF6* promoter deletion series (**Figure 4-2**) was transiently expressed in barley first leaf bases for a period of three days. Expression levels of the embedded control *Renilla* luciferase varied considerably between the constructs (**Figure 4-5a**), suggesting that the *Agrobacterium* infiltration method may be less than optimal. Consistent with earlier results however (**Figure 4-3**), pGR-GW generated a higher F:R ratio than pGR-0800 (**Figure 4-5b**), whilst many of the deletion series constructs generated a similar F:R ratio to pGR-GW of ~0.3:1. This indicates that either the region is not actively driving expression of firefly luciferase, or that the construct is not being expressed in cell types that support high *HvCslF6* expression levels. Firefly luciferase expression was dramatically reduced when the *Hv*PrC and *Hv*PrD constructs were tested. It is possible that a repressor element can bind to a motif somewhere in the 1750bp and 2500bp upstream region.

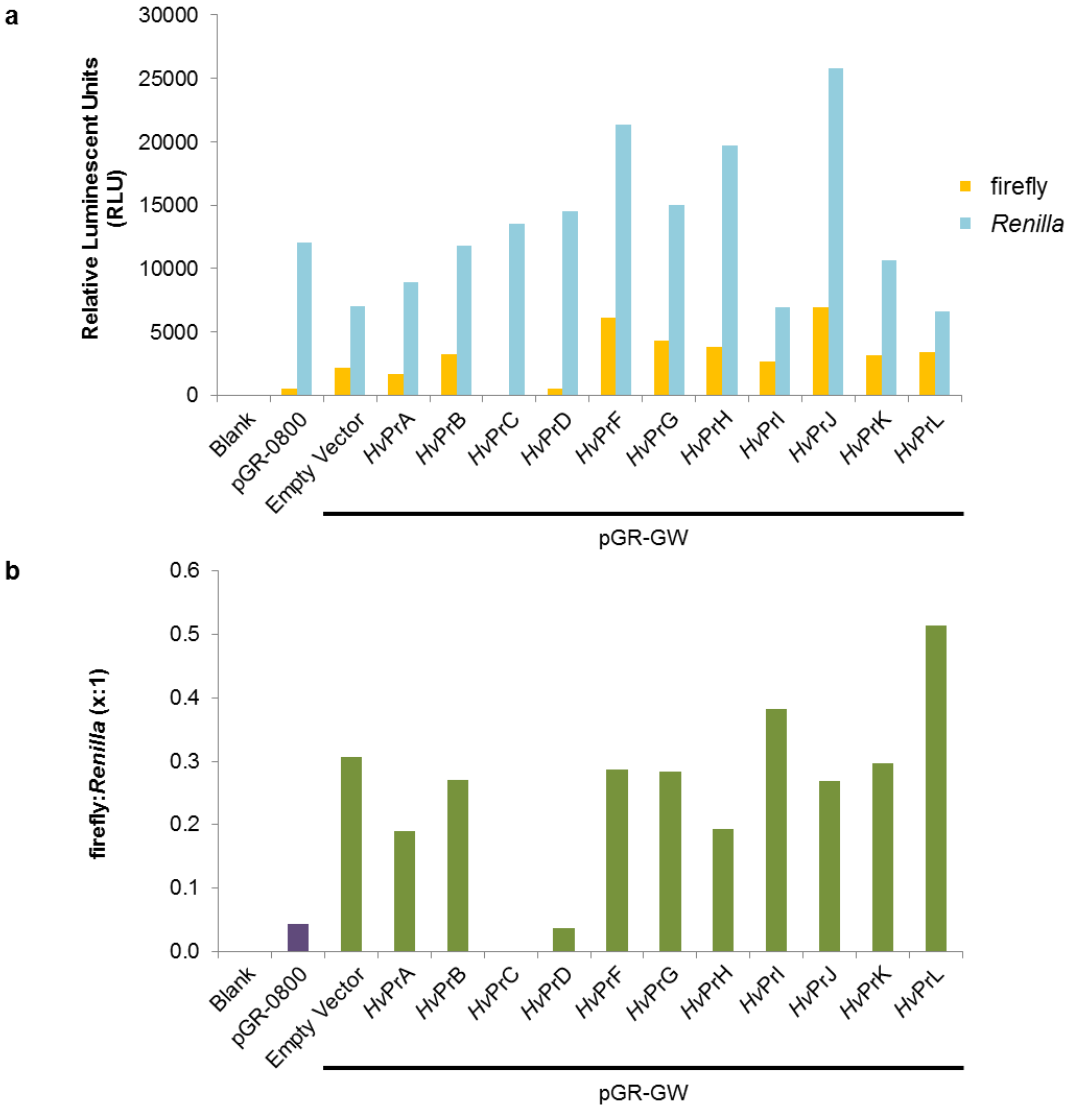


**Figure 4-5. Firefly and *Renilla* luciferase activity in barley first leaf bases.**

(**a**) Quantification of firefly and *Renilla* luciferase expression levels in first leaf bases via chemiluminescent measurement of enzyme activity driven by the *HvCslF6* promoter deletion series. (**b**) The ratio of enzyme activity of firefly luciferase, driven by the promoter fragments, against the embedded *Renilla* luciferase standard, driven by the 35S promoter. pGR-0800 is an empty vector construct, pGR-GW is derived from pGR-0800 and has been Gateway-enabled, *Hv*PrA to *Hv*PrL are *HvCslF6* promoter deletion series fragments. (n = 1)

### 4.1.4 Numerous regulatory elements are predicted to interact with the *HvCslF6* promoter.

In order to identify conserved regulatory elements that govern *CslF6* expression, 3 kb of sequence immediately upstream from the barley, sorghum and rice *CslF6* ORF was aligned using Geneious software. The three sequences shared 33% sequence identity and contained only 13 regions where 5 or more consecutive residues were conserved, 12 of which were within 1kb of the start codon. None of the 13 conserved regions fell between 1750bp and 2500bp upstream of *HvCslF6* where a putative negative regulator binds. Running these 13 conserved sequences on the Database of Plant Cis-acting Regulatory DNA Elements (PLACE database) (Higo et al., 1999) revealed 37 putative motifs which may influence *CslF6* regulation in each of the three species (**Supplementary Table 9-1**, p144). In order to identify putative regulatory elements that may have repressed luciferase activity in the *Hv*PrC and *Hv*PrD constructs (**Figure 4-5**), the sequence between 1750bp and 2500bp upstream of *HvCslF6* was analysed against the PLACE database (Higo et al., 1999), identifying 68 potential regulatory elements (**Supplementary Table 9-2**, p146).

## 4.2 Discussion and Future Directions

Numerous lines of evidence now suggest that one or more factors other than the CSLF or CSLH proteins by themselves influence the biosynthesis of (1,3;1,4)-β-glucan (Burton et al., 2006; Burton et al., 2008; Doblin et al., 2009; Burton et al., 2011). As CSLF6 appears to be responsible for the synthesis of the vast majority of (1,3;1,4)-β-glucan present in cereals (Burton et al., 2008; Nemeth et al., 2010; Taketa et al., 2011), its promoter is an ideal candidate for the investigation of regulatory elements such as transcription factors. Such transcription factors may also influence the expression of other genes involved in a biosynthesis network where such genes carry common regulatory motifs.

Three kb of sequence immediately upstream from the *HvCslF6* ORF was isolated and a deletion series developed whereby the promoter fragment was made progressively shorter from the 5′ end (**Figure 4-2**). Initial experiments conducted in the *N. benthamiana* model system suggest that the *HvCslF6* promoter does not drive reporter expression in the dicot system (**Figure 4-3**). As an alternative Li et al. (2009) published an *Agrobacterium*-mediated method that reported considerable GUS expression using rice and switchgrass seedlings. A similar experimental approach was therefore taken using barley roots, coleoptiles and first leaf bases, which each exhibit high endogenous *HvCslF6* transcript levels (Burton et al., 2008). Initial experiments showed that luciferase activity could be detected in each tissue type (**Figure 4-4**), but the controls were at considerably reduced levels compared with the *N. benthamiana* system (**Figure 4-3**). It would therefore be useful to investigate the potential of an *Agrobacterium* infiltration system that employs an alternative reporter system such as GUS (Jefferson et al., 1987). This process would allow *Agrobacterium* penetration and distribution throughout the tissues to be observed visually, confirming if sufficient cells were expressing the construct of interest and allowing the infiltration method to be optimised.

Similar chemiluminescence levels were obtained in the roots, coleoptiles and first leaf bases (**Figure 4-4**), with the constitutive 35S promoter displaying a much greater F:R ratio than the negative control as shown in *N. benthamiana*. The pGR-GW construct also produced a higher F:R ratio than pGR-0800, suggesting that the Gateway sequence was weakly driving background firefly luciferase expression. These results need to be confirmed

using the *HvCslF6* promoter deletion series fragments in the pGR-0800 vector.

Most of the *HvCslF6* promoter deletion series constructs displayed no difference in F:R ratio from the empty vector pGR-GW (**Figure 4-5**). As barley first leaf bases have been shown to exhibit particularly high *HvCslF6* transcript abundances (Burton et al., 2008), the results here therefore suggest that either the construct is not being expressed in the intended cell types, or that the regulatory element leading to elevated expression has not been captured within the 3kb of genomic DNA upstream of the *HvCslF6* ORF. Nevertheless this approach has identified one putative regulatory region; a repressor element appears to bind between 1750bp and 2500bp upstream of the *HvCslF6* ORF.

Promoter sequences from three species were analysed using the PLACE database (Higo et al., 1999) to identify putative regulatory elements that might regulate *CslF6* transcription levels. In particular, the aim was to identify global *CslF6* regulators that should be conserved across different cereal species, and which may also regulate the transcription of other components in the (1,3;1,4)-β-glucan biosynthetic pathway or network. In the 3 kb of sequence immediately upstream from barley, sorghum and rice *CslF6,* there were 13 regions where 5 or more consecutive residues were conserved. Regulatory elements do not necessarily require large stretches of conserved residues across species to allow consistent DNA binding, nevertheless, these regions were searched using PLACE. Accordingly, 37 putative regulatory elements were identified (**Supplementary Table 9-1**, p144). However none of the 13 conserved promoter regions coincided with the region between 1750bp and 2500bp upstream of the start codon. This region was therefore specifically used to query the PLACE database (Higo et al., 1999), which identified a further 68 putative regulatory elements (**Supplementary Table 9-2**, p146). Clearly with such a large set of regulatory elements potentially influencing *CslF6* transcription, further experimentation is required to hone in on the very small section of DNA where the putative negative regulatory element binds. When this is done, more confident predictions of putative regulators can be made.

The results presented here investigating the *HvCslF6* promoter have been useful for the design of further experiments in this area. Future experiments should focus on narrowing the regions where the two putative regulatory factors are interacting with the *HvCslF6*

promoter and a non-Gateway enabled vector should be used to reduce background expression levels of a suitable reporter gene. Once defined, the specific binding sequences may be used to isolate DNA binding factors; some of which may have been identified as putative regulatory elements when queried against the PLACE database (**Supplementary Table 9-1**, p144 and **Supplementary Table 9-2**, p146) (Higo et al., 1999). Once obtained, the DNA binding factors could be overexpressed in stable transgenic barley plants to observe their effect on (1,3;1,4)-β-glucan biosynthesis, and RNA could be isolated from several tissue types for microarray or next generation sequencing. Such RNA analyses could identify genes with altered expression patterns that may correlate with *HvCslF6,* and therefore may be linked to (1,3;1,4)-β-glucan biosynthesis. In time, such an approach may lead to the discovery of factors regulating and directly influencing (1,3;1,4)-β-glucan biosynthesis in cereals. These could then be manipulated to better control the production and distribution of (1,3;1,4)-β-glucan in cereal tissues to benefit applications in human health and industry, without adverse effects on plant health or yield.

## 4.3 Methods

### 4.3.1 Vector Construction

The pGreenII 0800-LUC vector (pGR-0800) (**Figure 4-1**) (Hellens et al., 2005), was kindly provided by Dr. Roger Hellens (Plant and Food Research, Auckland). To streamline the insertion of promoter fragments, pGR-0800 was Gateway™ enabled (pGR-GW) by digesting the plasmid with the restriction enzyme EcoRV (New England Biolabs Inc) and inserting the Gateway™ region including the attR sites using the GENEART™ seamless cloning and assembly kit (Life Technologies, Carlsbad, USA) as per manufacturer's instructions (Curtis and Grossniklaus, 2003), and sequenced (Australian Genome Research Facility Ltd). The DNA comparisons were performed using Geneious software (version 8.1.3, available from http://www.geneious.com).

### 4.3.2 Promoter Fragment Isolation

Promoter fragments up to 3kb immediately upstream of *HvCslF6* were amplified from genomic DNA ('SloopSA') (**Supplementary Table 9-3**, p148). Positive control 35S and negative control NosT sequences were PCR amplified from the pMDC32 vector of the Gateway™ cloning system (Curtis and Grossniklaus, 2003; Sainsbury et al., 2009). All PCR reactions were performed using Phusion® High-Fidelity DNA Polymerase (New England Biolabs Inc) as per manufacturer's instructions. Fragments of correct size were gel-excised, purified using the NucleoSpin® Gel and PCR Clean-up kit (Machery-Nagel, Amtsgericht Düren, Germany) and inserted into the pCR8 vector (Life Technologies, Carlsbad, USA) as per manufacturer's instructions, then sequenced (Australian Genome Research Facility Ltd). Correct constructs were transferred to the pGR-GW vector using LR Clonase (Life Technologies, Carlsbad, USA) as per manufacturer's instructions.

### 4.3.3 Transient *N. benthamiana* Expression

*Agrobacterium* preparation and *N. benthamiana* leaf infiltration was performed as per chapter 2 (Section 2.4.5, p48) using an *Agrobacterium* strain (AGL1) that contained the binary helper plasmid pSoup (Hellens et al., 2005), kindly provided by Dr. Roger Hellens (Plant and Food Research, Auckland), which allowed the pGR-0800 and pGR-GW vectors to

replicate.

### 4.3.4 Preparation of Barley Tissues for Transient Expression

All grains were soaked in water overnight at 4˚C in complete darkness. When leaf bases were to be harvested, pre-soaked grains were transferred to soil and grown for a further nine days with 22°C day and 15°C night temperatures without supplemented light. First leaves were cut at the grain-leaf junction, coleoptile sheaths were removed and the 2cm leaf bases collected. For other samples, pre-soaked grain were placed on wet filter paper for a further three days in darkness. Whole coleoptiles and roots were collected separately.

### 4.3.5 Transient Barley Tissue Expression

*Agrobacterium* (AGL1) preparation was based on chapter 2 (Section 2.4.5, p48) with cultivation techniques adapted from Li et al. (2009). *Agrobacterium* was scraped off plates using 10 mM $MgCl_2$ into 50 mL tubes, and 0.005% Silwet L77 (LEHLE SEEDS, USA) was added to the *Agrobacterium* suspension immediately prior to vacuum infiltration.

Barley tissues were infiltrated using a vacuum infiltration method adapted from Simmons et al. (2009) as follows. Tissues were immersed in *Agrobacterium* suspensions in open vessels and placed in a small vacuum chamber. A vacuum pump was attached and allowed to pull a vacuum for 1 min. The vacuum was held for one minute before being rapidly released, and this was repeated once more. Tissues were placed on filter paper in Petri dishes pre-wet with co-cultivation media consisting of 1x Murashige and Skoog basal medium with vitamins (*Phyto*Technologies, USA) and 1% sucrose (Sigma-Aldrich, USA). Roots and coleoptiles were incubated in darkness, and first leaf bases were incubated with 22°C day and 15°C night temperatures without supplemented light, each for a period of three days.

### 4.3.6 Dual Luciferase Reporter (DLR) Assay

The DLR assay was performed using commercially available reagents (Promega, Madison, USA), and a method based on Gretton and Harris (2008). *N. benthamiana* leaf pieces $2cm^2$ were ground in 500 µL Passive Lysis Buffer (PLB) (Promega), and diluted 100 fold in PLB. A 10 µL aliquot was loaded onto a black 96 well plate (BMG Labtechnologies, Ortenberg,

Germany) and read on a FLUOstar OPTIMA microplate reader (Optima, BMG LABTECH) over a period of 24 sec. Chemiluminescent measurements were taken at 0.5 sec intervals. An aliquot of 40 µL of Luciferase Assay Reagent II (LarII) (Promega) was injected and firefly luciferase activity was recorded as an average from 1.5 sec to 11.5 sec. An aliquot of 40 µL of Stop & Glo Reagent (S&GR) (Promega) was injected at 12 sec and *Renilla* luciferase activity was recorded as an average from 13.5 sec to 23.5 sec.

For barley tissues, five roots, eight coleoptiles or two first leaf bases were each ground in 500 µL PLB and 30 µL undiluted sample loaded onto a black plate. Aliquots of 150 µL of LarII and S&GR were separately injected in order to quantify firefly and *Renilla* luciferase activity.

### 4.3.7 *CslF6* Promoter Comparisons

The barley promoter sequence was obtained from the Morex genome assembly (Consortium-IBGS, 2012), whilst the rice and sorghum promoter sequences were obtained from Phytozome (Goodstein et al., 2011). DNA comparisons were performed on Geneious software (version 8.1.3, available from http://www.geneious.com). Putative cis-acting regulatory elements were identified by comparing sequences against the PLACE database (Higo et al., 1999).

# 5. *Sb*CSLF6 Expression in Transgenic Barley Plants Alters Grain (1,3;1,4)-β-Glucan Properties.

## 5.0 Introduction

As cereal grains provide such a large amount of our daily nutrient and energy requirements, efforts have been ongoing to improve their human health benefits. For this reason the cell walls of cereal species have attracted considerable attention in recent times. The network of cellulose microfibrils and matrix of non-cellulosic polysaccharides survive relatively intact through much of the digestive system because humans do not produce the digestive enzymes capable of their degradation. (1,3;1,4)-β-Glucans are one type of non-cellulosic polysaccharide and their consumption can help reduce the risk of developing colorectal cancer (Bingham, 1990; Larsson et al., 2005), and they can lower blood cholesterol levels (Gallaher et al., 1993), reduce bowel transit time, prevent constipation and help regulate blood glucose levels for diabetes management (Bornet et al., 1987).

(1,3;1,4)-β-Glucans are composed of unsubstituted, unbranched chains of (1,3)- and (1,4)-β-linked glucosyl residues. The single (1,3)-β-linkages are irregularly distributed (Staudte et al., 1983) and separate stretches of predominantly three (cellotriosyl) or four (cellotetraosyl) consecutive (1,4)-β-linkages. The polysaccharides physicochemical properties are governed by the relative proportions of the cellotriosyl and cellotetraosyl units, which is termed the DP3:DP4 ratio. In cereals the irregularly distributed (1,3)-β-linkages prevent extensive intermolecular alignment of chains and allows a gel-like matrix to form in the cell wall. This gel-like matrix is partially soluble and allows the polysaccharide to impact human health and numerous industrial applications (Collins et al., 2010).

(1,3;1,4)-β-Glucan biosynthesis has been shown to involve members of the *CslF* (Burton et al., 2006), *CslH* (Doblin et al., 2009) and *CslJ* (Little et al., 2015) gene families. Of all the family members in barley including ten *CslF* (Schreiber et al., 2014), one *CslH* (Doblin et al., 2009) and one *CslJ* (Little et al., 2015) genes, the production of the vast majority of (1,3;1,4)-β-glucan present has been attributed to the CSLF6 enzyme (Burton et al., 2008; Nemeth et al., 2010; Taketa et al., 2011; Vega-Sάnchez et al., 2012). When Burton et al. (2011) overexpressed *HvCslF6* in barley using a constitutive 35S promoter, leaf (1,3;1,4)-β-glucan levels increased three- to four-fold and caused severe plant growth defects. Use of the grain-specific *As*GLO promoter, however, alleviated the growth defects and led to a 50% increase in grain (1,3;1,4)-β-glucan levels. The polysaccharide DP3:DP4 ratio also decreased

from 2.3–2.8:1 to 2.1:1, presumably increasing the solubility of the (1,3;1,4)-β-glucan chains, which may also increase the associated human health benefits.

In Chapter 2 we showed that in the *N. benthamiana* heterologous expression system, a CSLF6 enzyme from sorghum (*Sb*) produced more (1,3;1,4)-β-glucan than *Hv*CSLF6 (**Figure 2-2**, p2828), and with a considerably lower DP3:DP4 ratio. Here, a transgenic approach was taken using *Sb*CSLF6 in an attempt to increase (1,3;1,4)-β-glucan levels in barley grains above those previously achieved using the orthologs barley *Hv*CSLF6 enzyme. In addition to this, the lower DP3:DP4 of the (1,3;1,4)-β-glucan produced by *Sb*CSLF6 was predicted to impact the total grain (1,3;1,4)-β-glucan fine structure.

## 5.1 Results

### 5.1.1 *Sb*CSLF6 Driven by the *As*GLO Promoter Alters Grain (1,3;1,4)-β-Glucan Properties.

Mature grain from nine $T_0$ and three $T_1$ transgenic barley lines expressing *Sb*CSLF6 were analysed for (1,3;1,4)-β-glucan content and structure. In the $T_1$ and $T_2$ grains, obtained from $T_0$ and $T_1$ lines respectively, (1,3;1,4)-β-glucan content (% w/w) increased by 24% and 38% respectively (**Figure 5-1**). This was however also associated with a 17% (6.4 mg) and 28% (14 mg) decrease in grain weight for the $T_1$ and $T_2$ grains, respectively. Hence on a per grain basis, both generations display equal amounts of (1,3;1,4)-β-glucan in the empty vector negative control and *Sb*CSLF6 expressing lines, at 1.7 mg and 2.2 mg per grain in the $T_1$ and $T_2$ grains respectively. This reduced grain weight was associated with an unusual phenotype, insofar as the grains retained their overall size yet exhibited a deep depression on the abaxial side (**Figure 5-2**).

Starch content was analysed to further understand the reduced grain weight associated with *Sb*CSLF6 expression. Compared with the empty vector lines, those expressing *Sb*CSLF6 displayed a 31% (6.7 mg) and 37% (9 mg) decrease in starch content per grain in the $T_1$ and $T_2$ grains respectively (**Figure 5-3**). By weight, the loss associated with the decreased starch content does not alone account for the overall decrease in grain weight, indicating that other factors are being influenced by *Sb*CSLF6 expression.

Even though (1,3;1,4)-β-glucan amounts per grain were unchanged with *Sb*CSLF6 expression, a considerable shift in polysaccharide DP3:DP4 ratio was evident (**Figure 5-1**). Grain from the six $T_0$ lines that displayed elevated (1,3;1,4)-β-glucan content per grain relative to the negative control also displayed DP3:DP4 ratios ranging from 1.2–2.2:1 (**Figure 5-4a**). This is compared with grain (1,3;1,4)-β-glucan DP3:DP4 ratios of 2.9–3.0:1 from the negative control lines and the three remaining $T_0$ lines with unaltered levels of (1,3;1,4)-β-glucan. Grain from the three $T_1$ lines also displayed reduced DP3:DP4 ratios ranging from 1.4–1.8:1 (**Figure 5-1d**).

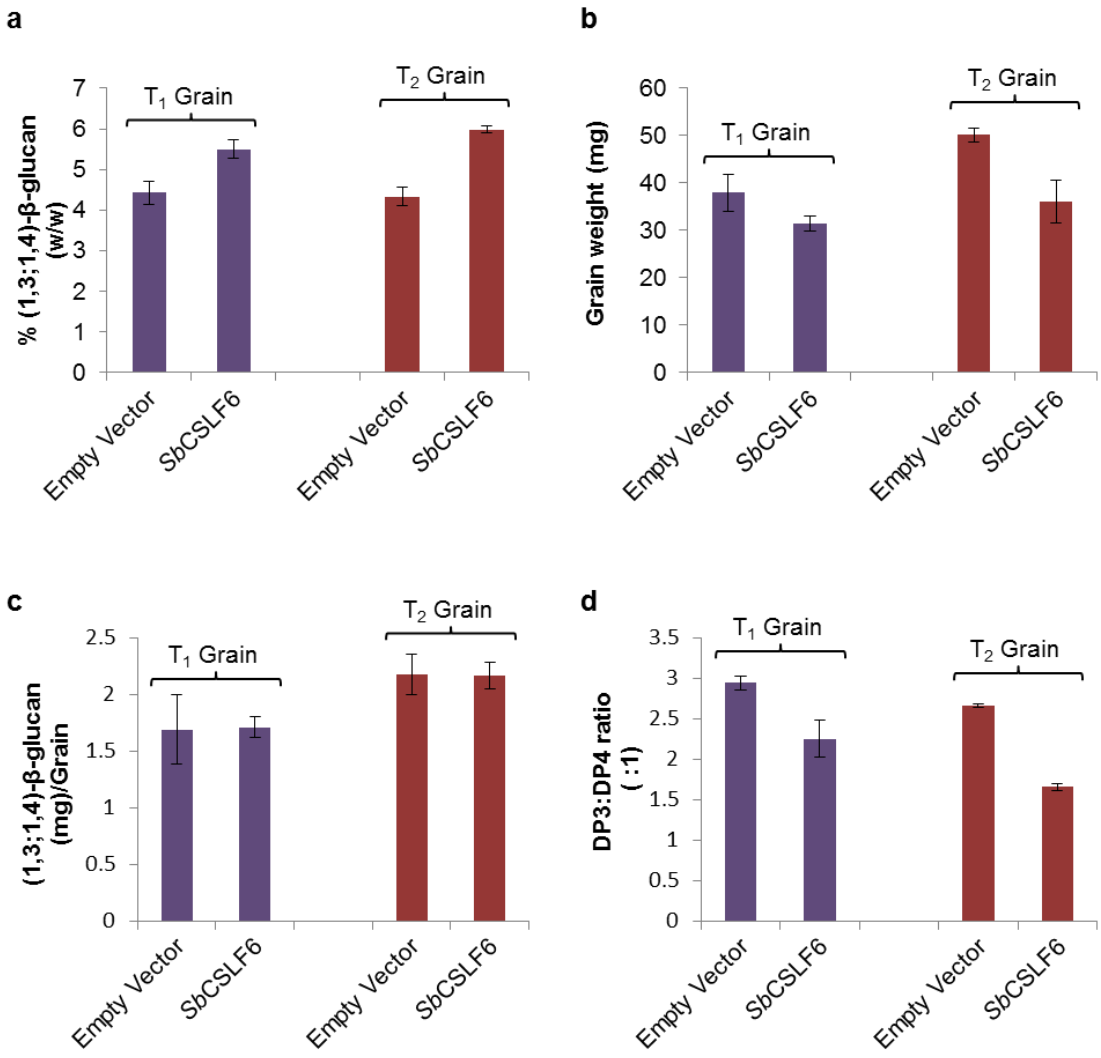


**Figure 5-1. The influence of *Sb*CSLF6 on grain (1,3;1,4)-β-glucan properties in $T_0$ and $T_1$ transgenic barley plants when expressed using the grain-specific (*As*GLO) promoter.**

(**a**) (1,3;1,4)-β-Glucan content (% w/w), (**b**) grain weight, (**c**) (1,3;1,4)-β-glucan content (mg) per grain and (**d**) polysaccharide DP3:DP4 ratios were each obtained from $T_1$ and $T_2$ transgenic barley grains.


**Figure 5-2. The influence of *Sb*CSLF6 on grain phenotype in $T_2$ transgenic barley plants.**

Photos are of mature $T_2$ barley grains driving *SbCslF6* transcription with the grain-specific (*As*GLO) promoter. The grain is generally shrivelled and arrows indicate where large depressions are located on the abaxial side of the grain.

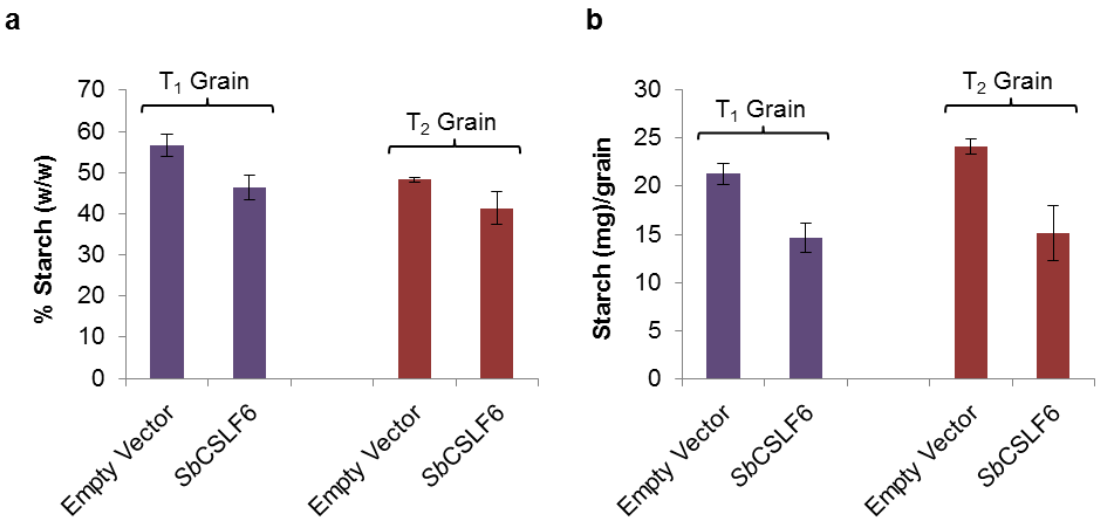


**Figure 5-3. The influence of *Sb*CSLF6 on starch levels in $T_1$ and $T_2$ transgenic barley grain when expressed using the grain-specific (*As*GLO) promoter.**

(**a**) Starch content (% w/w) and (**b**) starch content (mg) per grain were each obtained from $T_1$ and $T_2$ transgenic barley grains.

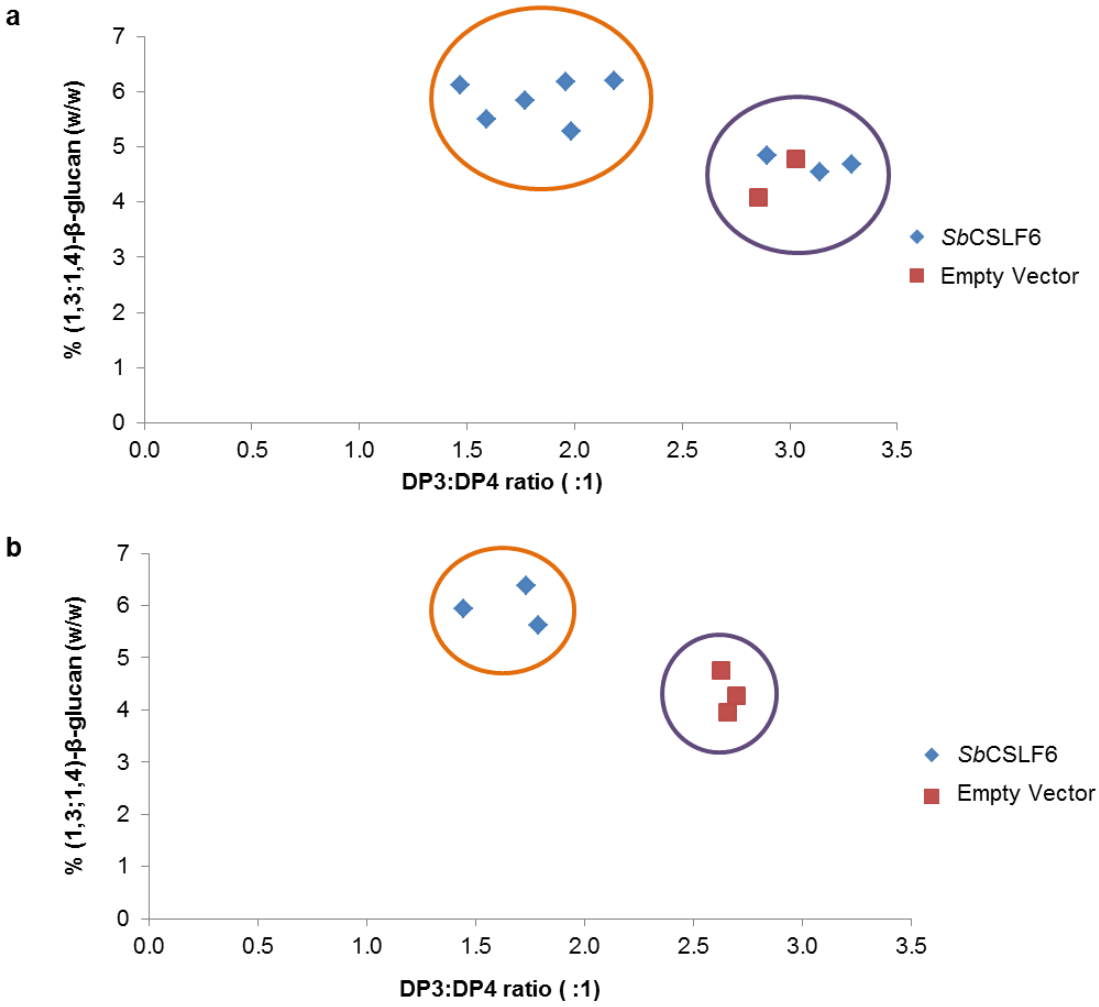


**Figure 5-4. The influence of *Sb*CSLF6 expression on (1,3;1,4)-β-glucan properties in transgenic barley grain.**

(1,3;1,4)-β-Glucan content (% w/w) and polysaccharide DP3:DP4 ratios were each obtained from $T_1$ (**a**) and $T_2$ (**b**) transgenic barley grain expressing constructs using the grain-specific (*As*GLO) promoter. Orange and purple circles highlight groups with distinctly different (1,3;1,4)-β-glucan properties.

## 5.2 Discussion

*Sb*CSLF6 consistently produced considerably more (1,3;1,4)-β-glucan than *Hv*CSLF6 in the *N. benthamiana* model system, and of a substantially lower DP3:DP4 ratio (Chapter 2, **Figure 2-2**, p28). Thus, this gene may be capable of significantly improving the human health attributes of cereals where more soluble (1,3;1,4)-β-glucan is desirable. In order to confirm whether *Sb*CSLF6 could be used to significantly lower the DP3:DP4 ratios in the grain, *Sb*CSLF6 was stably transformed into barley plants, using the grain-specific *As*GLO promoter to avoid deleterious effects on vegetative tissues.

When Burton et al. (2011) overexpressed *Hv*CSLF6 using the grain-specific *As*GLO promoter, (1,3;1,4)-β-glucan content increased by 66% yet overall grain weight did not change. A corresponding 15% decrease in starch content, which by weight is a greater loss than the weight gained from the increase in (1,3;1,4)-β-glucan, indicated that other elements contributing to overall grain weight were also affected. Here, $T_2$ grains expressing *Sb*CSLF6 displayed a 38% increase in (1,3;1,4)-β-glucan content compared with the empty vector controls. This was also associated with a decrease in grain weight of 28% (**Figure 5-1**), indicating that the amount of (1,3;1,4)-β-glucan per grain had not been altered significantly. Starch content in the $T_2$ grains also decreased by 37% compared with the empty vector controls (**Figure 5-3**). By weight this loss in starch is less than the overall decrease in grain weight, suggesting that factors such as free sugars, protein content or other wall polysaccharides have also been affected.

Compared to the empty vector lines, the $T_2$ grains expressing *Sb*CSLF6 displayed a decrease in DP3:DP4 ratio from 2.9–3.0:1 to 1.4–1.8:1, indicating that the properties of the (1,3;1,4)-β-glucan have been changed considerably. This decrease in ratio is much greater than that observed for *Hv*CSLF6 overexpression, where a ratio of 2.1:1 was generated compared with control levels of 2.3–2.8:1 (Burton et al., 2011). This is consistent with the results presented in chapter 2 where *Sb*CSLF6 expression in *Nicotiana benthamiana* leaves was associated with the synthesis of a (1,3;1,4)-β-glucan of a much lower DP3:DP4 ratio than *Hv*CSLF6, and therefore suggests that *Sb*CSLF6 is producing (1,3;1,4)-β-glucan in the barley grains. As the amount of (1,3;1,4)-β-glucan per grain has not been altered, a feedback regulatory mechanism may have detected the additional (1,3;1,4)-β-glucan synthesis and responded

by decreasing endogenous CSLF, CSLH or CSLJ expression, or has decreased the expression or activity of other factors contributing to biosynthesis. If this is the case, the response is completely different to that observed with the barley *HvCslF6* gene (Burton et al., 2011). Such regulatory changes may have, in fact, led to the decreased starch accumulation observed here (**Figure 5-3**) and by Burton et al. (2011). In any case, quantitative reverse transcription PCR (Q-PCR) of endogenous and transgenic *CslF* and *CslH* genes across a developing grain series should be performed to confirm transgene expression and to observe any changes to endogenous gene expression that may influence (1,3;1,4)-β-glucan production. Total protein measurements should also be performed to better understand the observed decrease in grain weight (**Figure 5-1**).

Further investigation is required into the observed depression on the abaxial side of the grain (**Figure 5-2**) associated with *Sb*CSLF6 expression, a phenotype also observed in some cases with the overexpression of *Hv*CSLF6 (Burton et al., 2011). Light microscopy with protein binding stains such as Serva Blue, glucose polymer binding stains such as Calcofluor White and (1,3;1,4)-β-glucan specific antibody (Meikle et al., 1994) staining techniques should be used to analyse grain morphology using both transverse and longitudinal sections. These techniques could reveal which tissue types have been affected and influence the abaxial depression phenotype, while observing starch granule size, cell wall thicknesses and the distribution of (1,3;1,4)-β-glucan.

By expressing *Sb*CSLF6 in barley, we have been able to dramatically alter the (1,3;1,4)-β-glucan properties of the grain, presumably increasing the polysaccharide's solubility (Collins et al., 2010), which may enhance the human health benefits associated with its consumption. However the abaxial depression phenotype displayed by the lines associated with reduced grain weight would render such a barley variety non-profitable for commercial applications. Future research should focus on understanding how (1,3;1,4)-β-glucan synthesis in cereals is regulated such that future attempts to manipulate its total amount or fine structure will limit negative effects such as reduced starch and grain weight.

## 5.3 Methods

### 5.3.1 Stable Barley Transformation and Plant Growth

All plants were grown under standard greenhouse conditions in the Plant Accelerator® (University of Adelaide) according to Burton et al. (2004). Stable barley transformation and confirmation of transgenic status of individual lines was performed according to Burton et al. (2011). The WI4330 barley variety was used, which has a pedigree including Maritime, Commander and Flagship (University of Adelaide).

### 5.3.2 (1,3;1,4)-β-Glucan Analysis

Analysis of (1,3;1,4)-β-glucan content was performed according to Burton et al. (2011) using 15mg of tissue and commercially available reagents (Megazyme International Ireland Ltd, Bray, Ireland), with the protocol based on McCleary and Codd (1991). Samples were also analysed by high performance liquid chromatography (HPLC) to determine the DP3:DP4 ratio, performed according to chapter 2, section 2.4.9, p50.

### 5.3.3 Starch Content Determination

Starch content was determined on 20 mg of flour using a scaled back version of the Megazyme Total Starch Assay (McCleary et al., 1994).

# 6. Summary and Future Directions.

# 6.0 Thesis Summary and Key Findings

The overarching goal of this research was to advance our understanding of (1,3;1,4)-β-glucan biosynthesis in cereals by focusing primarily on CSLF6 function and regulation. The future target is to precisely control (1,3;1,4)-β-glucan content and fine structure to enhance the human health benefits and improve the industrial utility of cereal tissues, and to control the deposition and rate of (1,3;1,4)-β-glucan synthesis to minimise negative plant growth defects.

**Two amino acid polymorphisms between *Hv*CSLF6 and *Sb*CSLF6 contribute to much of the difference in (1,3;1,4)-β-glucan production and polysaccharide fine structure**

It has previously been shown that CSLF6 enzymes from different species contain polymorphisms which lead to the production of different amounts of (1,3;1,4)-β-glucan and with different DP3:DP4 ratios (Dimitroff, 2011). A chimeric approach was therefore undertaken to identify regions or specific residues that were influencing how much (1,3;1,4)-β-glucan was being produced, and the frequency at which (1,3)-β-linkages were incorporated by either CSLF6 or by an interacting protein (Chapter 2). Compared to the wild-type synthases, when the $NH_2$-terminal region was exchanged between *Hv*CSLF6 and *Sb*CSLF6, both enzymes displayed the same increase in (1,3;1,4)-β-glucan production. When the cytoplasmic region termed C1 was exchanged between *Hv*CSLF6 and *Sb*CSLF6, different effects on (1,3;1,4)-β-glucan production and DP3:DP4 ratio were observed by the enzymes, and when the catalytic region (CR) was exchanged, reciprocal effects were observed (**Figure 2-4g**, p3131). Compared with their wild-type counterparts, *Hv*:*Sb*CR produced more (1,3;1,4)-β-glucan with a decreased DP3:DP4 ratio and *Sb*:*Hv*CR produced less (1,3;1,4)-β-glucan with an increased DP3:DP4 ratio, suggesting that the six polymorphisms within the CR may be leading to the observed difference in function between *Hv*CSLF6 and *Sb*CSLF6.

The *Sb*:Y680F mutant synthesised 72% less (1,3;1,4)-β-glucan than *Sb*CSLF6 (**Figure 2-5**, p35), indicating that this residue immediately upstream of the conserved QxxRW motif may be interacting with and influencing the function of the putative CSLF6 gating loop (**Figure 2-6**, p38) The *Sb*:G638D mutant however produced the same amount of (1,3;1,4)-β-glucan

as *Sb*CSLF6, yet the DP3:DP4 ratio increased from 1.01±0.02:1 to 1.62±0.06:1. This substitution may have altered the flexibility of the loop containing the TED motif and has provided evidence to suggest that the CSLF6 protein is able to catalyse the formation of both the (1,3)- and (1,4)-β-glycosidic linkages. The reciprocal *Hv*:D629G mutant, however, only displayed a partial opposite effect on DP3:DP4 ratio, highlighting how a number of amino acid substitutions within the catalytic region may influence the position and flexibility of specific residues surrounding the active site. Our current theory is that the conformation of the active site determines the stability of a (1,3)-linkage or a (1,4)-linkage and any amino acid change that improves the stability of a (1,3)-linkage conformation in the active site will result in a higher proportion of (1,3)-linkages being incorporated into the (1,3;1,4)-β-glucan chain, resulting in a decreased DP3:DP4 ratio.

**CSLF6 is active in complexes mediated by its $NH_2$-terminal and class specific regions.**

Using chimeric, internally deleted, truncated and mutated constructs, a co-expression approach in *N. benthamiana* leaves was used to investigate CSLF6 regulation and complex formation (Chapter 3). The requirement for the CSLF6 protein to form a functional complex was supported through the use of a dominant negative mutation. A P463T mutated *Hv*CSLF6 enzyme, created based on previous *At*CESA mutations (Zhong et al., 2003; Daras et al., 2009) had the predicted dominant negative effect on (1,3;1,4)-β-glucan biosynthesis (**Figure 3-7**, p71). Presumably this mutant protein imposed its dominant negative effect by interacting with and inhibiting the activity of the functional wild-type CSLF6 proteins (**Figure 3-4**, p64 and **Figure 3-11b**, p84). The $NH_2$-terminal region was shown to be essential for CSLF6 function and appeared to be involved in complex formation and enzyme activation (**Figure 3-2**, p59). Expression of an internally truncated construct (*Sb*:ΔCSR) showed that the class specific region (CSR) was not essential for enzyme function in the *N. benthamiana* system, yet did appear to be involved in CSLF6 complex formation (**Figure 3-7**, p71). Overall, complex formation appears to be a requirement for enzyme activity, but the exact mechanisms of complex formation and composition remain unclear.

**Activation of the CSLF6 protein may involve a putative $NH_2$-terminal PilZ motif**

In order to narrow down the section of the $NH_2$-terminal region involved in CSLF6 regulation, the region was divided into three sections and fourteen chimeric constructs were developed (Chapter 3) (**Figure 3-9**, p77). The greatest effect of the exchanges between *Hv*CSLF6 and *Sb*CSLF6 was driven by section C which lies immediately upstream of the first predicted amphipathic helix; this caused on average a 70% increase in (1,3;1,4)-β-glucan production. This section contains the 'DxSxxG' and 'RxxxR' motifs, which are in the opposite order but identical in sequence to those in the PilZ domain that are involved in c-di-GMP mediated activation of the bacterial cellulose synthase (BCSA) (Morgan et al., 2014). Sequence differences between *Sb*CSLF6 and *Hv*CSLF6 across section C may alter the availability of the region for $NH_2$-terminal-mediated CSLF6 complex formation or alter the strength of activator binding, both of which could result in increased (1,3;1,4)-β-glucan production.

Three *Sb*CSLF6 constructs with mutated PilZ motifs displayed reduced (1,3;1,4)-β-glucan production compared to *Sb*CSLF6, suggesting that the motifs are influencing biosynthesis (**Figure 3-10**, p81). When the first Arg of the 'RxxxR' motif was mutated in BCSA, the enzyme became constitutively activated (Morgan et al., 2014). The same effect was not observed in *Sb*CSLF6; however, mutating the second Arg of the 'RxxxR' motif did lead to a change in the (1,3;1,4)-β-glucan DP3:DP4 ratio. The current theory is that the PilZ motif in the CSLF6 $NH_2$-terminus may be regulating CSLF6 activity by a mechanism similar to BCSA (Morgan et al., 2014), by linking cofactor binding and enzyme activation. If proven with further experiments this will be the first evidence of a secondary messenger regulating the activity of plant cell wall synthetic machinery.

**Grain (1,3;1,4)-β-Glucan Properties are Altered in Barley Plants Expressing SbCSLF6**

The expression of *Sb*CSLF6 in barley grain (Chapter 5) supported results obtained in earlier work by Dimitroff (2011) and confirmed that differences in (1,3;1,4)-β-glucan synthesis identified in the *N. benthamiana* system could be transferred to cereal grains. Here *Sb*CSLF6 expression altered the properties of the (1,3;1,4)-β-glucan in barley grain by reducing the DP3:DP4 ratio from 2.9–3.0:1 to 1.4–1.8:1 (**Figure 5-1**, p113 and **Figure 5-4**, p114). This decrease is greater than that exhibited by *Hv*CSLF6 overexpression (Burton et al., 2011), supporting the *N. benthamiana* result where *Sb*CSLF6 consistently produced a

lower DP3:DP4 ratio than *Hv*CSLF6 (**Figure 2-2**, p27 and **Figure 2-3**, p28). However *Sb*CSLF6 expression did not result in more (1,3;1,4)-β-glucan per grain than *Hv*CSLF6 overexpression, as observed in *N. benthamiana* (Dimitroff, 2011), highlighting the need to understand the cellular regulation of (1,3;1,4)-β-glucan production so that more targeted alterations to grain properties can be made.

**A Putative Negative Regulatory Element Interacts with Part of the *HvCslF6* Promoter**

In order to better manipulate (1,3;1,4)-β-glucan properties in cereal grains, other factors contributing to its synthesis must be discovered and characterised. The barley *CslF6* promoter was therefore analysed to try and identify regulatory elements that may also influence the transcription of other factors related to (1,3;1,4)-β-glucan biosynthesis (Chapter 4). In an initial experiment, luciferase activity, driven by a deletion series of the putative *HvCslF6* promoter, was quantified after construct infiltration into barley first leaf base tissue (**Figure 4-2**, p9696 and **Figure 4-5**, p101). A putative repressive element was identified which appeared to influence transcription, binding between 1750bp and 2500bp upstream of the *HvCslF6* ORF. The region was run against the PLACE database, identifying 68 regulatory elements which may be responsible for the observed repression in luciferase activity (**Supplementary Table 9-2,** p146). Further experimentation is required to delimit more precisely the section of DNA where the putative negative regulatory element binds, allowing more confident predictions to be made.

## 6.1 Future Directions

### Investigating the Influence of Polymorphisms Within the Catalytic Region on CSLF6 Function

With two *Sb*CSLF6 mutant constructs showing such profound effects on (1,3;1,4)-β-glucan production and DP3:DP4 ratio (**Figure 2-5**, p35) (Chapter 2) the potential of manipulating the CSLF6 enzyme to produce even greater quantities of (1,3;1,4)-β-glucan and with different polysaccharide structures is supported. Random mutagenesis performed on residues surrounding the QxxRW and TED motifs, or chimeric constructs containing the catalytic region from other CSLF, CSLH or CSLJ family members may yield even more potent enzymatic variants. These constructs could all be assayed using the same procedures as outlined here using *N. benthamiana*, and then be transferred into transgenic barley lines that may exhibit altered grain properties with potentially enhanced human health or industrial applications.

### CSLF6 Protein-Protein Interaction Studies

Although the *N. benthamiana* system has been useful to look at changes in (1,3;1,4)-β-glucan production and quality, the conclusions drawn in Chapter 3 remain quite speculative in the absence of protein-protein interaction studies. Prior to publication, selected constructs must be tested using a suitable analysis to confirm that multi-protein complex formation does occur. This could include yeast-2-hybrid binding assays, bimolecular fluorescence complementation or gel shift assays in order to validate the results obtained from the *N. benthamiana* system.

### Understanding the Function of the CSLF6 PilZ Motif

With three mutant PilZ motif constructs each showing reduced (1,3;1,4)-β-glucan production compared to wild type *Sb*CSLF6 (**Figure 3-10**, p81), it appears that the motifs contained therein are contributing to CSLF6 activity. An additional mutant construct with all of the conserved residues knocked out should be developed to determine if these motifs are required for activity in *N. benthamiana*. Truncation constructs consisting of only the $NH_2$-terminal region could also be developed containing each separate PilZ motif mutation.

Most importantly the $NH_2$-terminal constructs could be expressed in bacteria or yeast, purified and analysed for their capacity to form homodimers, bind to the full length wild type CSLF6 protein and bind to putative secondary messengers such as c-di-GMP, c-GMP and c-AMP. The $NH_2$-terminal region should also be *de novo* modelled to help explain how the PilZ motif is influencing CSLF6 activity and to understand how exchanging the *Hv*CSLF6 and *Sb*CSLF6 $NH_2$-terminal regions led to increased (1,3;1,4)-β-glucan production (**Figure 3-2**, p59). Mutant or truncated constructs could then be developed to overcome the requirement of activator binding to allow constitutive (1,3;1,4)-β-glucan synthesis.

## 6.2 Summary

The work presented here has advanced our understanding of the mechanism governing (1,3;1,4)-β-glucan biosynthesis by CSLF6, and the regulation of CSLF6 at the protein level. The *N. benthamiana* model system has proven to be a useful tool to analyse the function of the CSLF6 enzyme in a system devoid of interfering factors, however there are limitations in a non-cereal system. The following points comprise the key findings contained in this thesis.

### 6.2.1 Key Findings

- The CSLF6 $NH_2$-terminal region influences (1,3;1,4)-β-glucan production without influencing the DP3:DP4 ratio. (Chapter 2)
- The putative CSLF6 gating loop influences (1,3;1,4)-β-glucan production in *N. benthamiana*. (Chapter 2)
- Amino acid substitutions of CSLF6 impact the DP3:DP4 ratio, putatively by altering the stability of the (1,3)-β-glycosidic linkage at the active site. (Chapter 2)
- The CSLF6 class specific region and 'CxCxxxCxC' motif are not required for enzyme function in *N. benthamiana*. (Chapter 3)
- *Sb*CSLF6 expression in barley alters grain (1,3;1,4)-β-glucan properties by reducing the DP3:DP4 ratio. (Chapter 5)

### 6.2.2 More Work is Required to Substantiate the Following

- Point mutations in the CSLF6 PilZ motif alter (1,3;1,4)-β-glucan production and DP3:DP4 ratio via potential interaction with the gating loop. (Chapter 3)
- Amino acid polymorphisms surrounding the PilZ motif in CSLF6 are responsible for the regulatory influence of the $NH_2$-terminal region. (Chapter 3)
- CSLF6 is active in complexes mediated by its $NH_2$-terminal region and class specific region. (Chapter 3)
- A *Hv*CSLF6 enzyme containing a P463T mutation is catalytically inactive yet is capable of interacting with and inhibiting the activity of wild-type CSLF6 when expressed in *N. benthamiana*. (Chapter 3)

# 7. Appendices (Chapter 2).

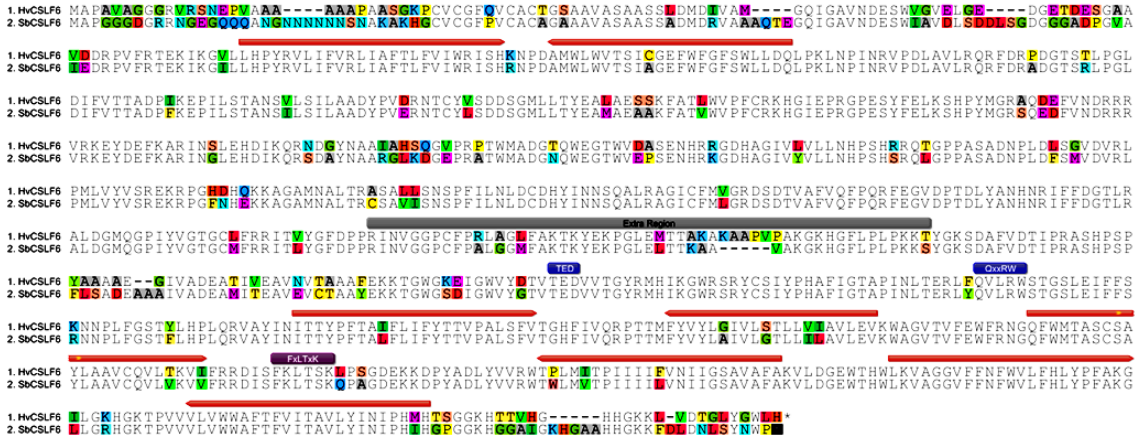


**Supplementary Figure 7-1. Amino acid alignment of *Hv*CSLF6 and *Sb*CSLF6.**

Alignment of *Hv*CSLF6 and *Sb*CSLF6 amino acids with coloured residues highlighting sequence differences, the predicted amphipathic helices (brown bars), the extra region (grey bar) and the FxLTxK (purple bar), TED and QxxRW (blue bars) motifs.

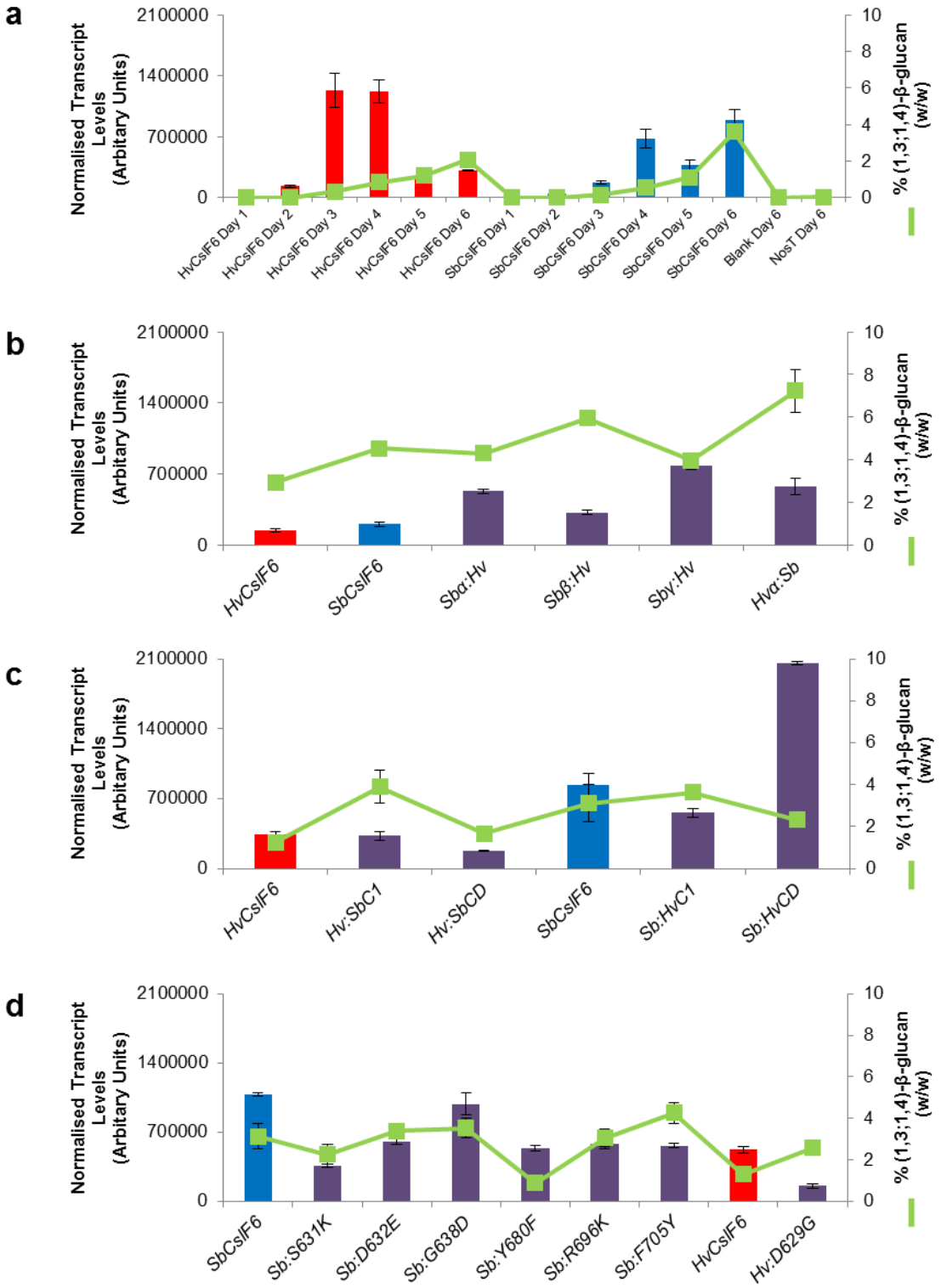
a
Normalised Transcript Levels (Arbitary Units)
% (1,3;1,4)-β-glucan (w/w)
2100000
1400000
700000
0
10
8
6
4
2
0
HvCslF6 Day 1
HvCslF6 Day 2
HvCslF6 Day 3
HvCslF6 Day 4
HvCslF6 Day 5
HvCslF6 Day 6
SbCslF6 Day 1
SbCslF6 Day 2
SbCslF6 Day 3
SbCslF6 Day 4
SbCslF6 Day 5
SbCslF6 Day 6
Blank Day 6
NosT Day 6
b
Normalised Transcript Levels (Arbitary Units)
% (1,3;1,4)-β-glucan (w/w)
HvCslF6
SbCslF6
Sbα:Hv
Sbβ:Hv
Sbγ:Hv
Hvα:Sb
c
Normalised Transcript Levels (Arbitary Units)
% (1,3;1,4)-β-glucan (w/w)
HvCslF6
Hv:SbC1
Hv:SbCD
SbCslF6
Sb:HvC1
Sb:HvCD
d
Normalised Transcript Levels (Arbitary Units)
% (1,3;1,4)-β-glucan (w/w)
SbCslF6
Sb:S631K
Sb:D632E
Sb:G638D
Sb:Y680F
Sb:R696K
Sb:F705Y
HvCslF6
Hv:D629G

**Supplementary Figure 7-2. mRNA abundances of *CslF6* constructs and respective (1,3;1,4)-β-glucan amounts produced when expressed in *N. benthamiana* leaves.**

(**a**) mRNA and (1,3;1,4)-β-glucan levels were measured for *HvCslF6* and *SbCslF6* across a six day time course in *N. benthamiana* leaves. Un-infiltrated (blank) and negative control (NosT) levels are shown at six days post infiltration. (**b**, **c** and **d**) mRNA and (1,3;1,4)-β-glucan levels were measured for chimeric and mutated *CslF6* constructs six days post infiltration.

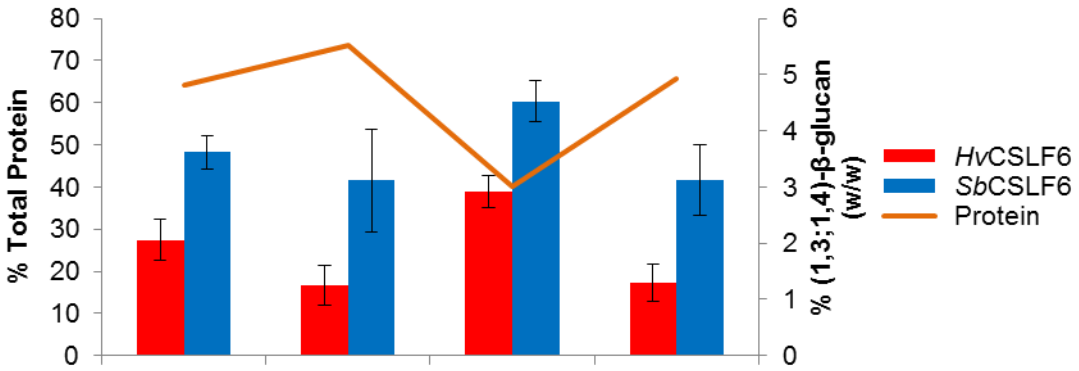


**Supplementary Figure 7-3. Differences in total protein levels and (1,3;1,4)-β-glucan amounts produced by CSLF6 orthologs from four separate experiments.**

Levels of (1,3;1,4)-β-glucan (% w/w) produced by *Hv*CSLF6 and *Sb*CSLF6 when expressed in *N. benthamiana* leaves in four separate experiments are shown. Total protein levels from the same leaf tissues are also shown. Error bars represent the standard error.

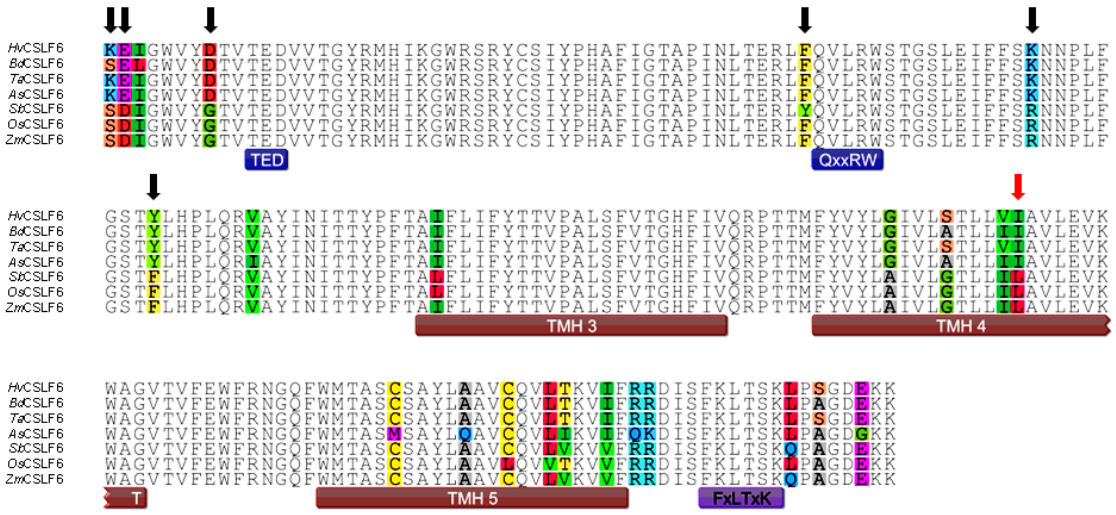


**Supplementary Figure 7-4. Amino acid alignment of CSLF6 orthologs.**

A partial alignment of CSLF6 orthologs from *Hv* (*Hordeum vulgare*), *Bd* (*Brachypodium distachyon*), *Ta* (*Triticum aestivum*), *As* (*Avena sativa*), *Sb* (*Sorghum bicolor*), *Os* (*Oryza sativa*) and *Zm* (*Zea mays*) with coloured residues highlighting sequence discrepancies. Shown are the predicted trans-membrane helices (brown bars), the FxLTxK motif (purple bar) and the TED and QxxRW motifs (blue bars). Black arrows highlight residues where point mutation constructs have been developed (**Figure 2-5**, p38), and the red arrow highlights the polymorphism identified by Jobling (2015) which influences DP3:DP4 ratio.

**Supplementary Table 7-1. Primers used for *CslF6* cDNA cloning and targeted recombination.**

| Construct | Fragment | Primer Direction | Primer Sequence (5' to 3') |
|---|---|---|---|
| ***SbCslF6*** | Full length cDNA | F | CGAGAGAGAAGAGCCACCACCGTC |
| | | R | TGGATGGACGGAAACGTACTCTTC |
| ***OsCslF6*** | Full length cDNA | F | CGTAAAACGACGGCCAGTC |
| | | R | CCAGGAAACAGCTATGACC |
| ***Sbα:Hv*** | Insert (*Sbα*) | F | TCGCCCTTATGGCGCCGGGCGGCGGAGACGGC |
| | | R | TAGGGGTGGAGGAGGATGCCCTTGATCTTCTC |
| | Remaining Vector | F | TCCTCCTCCACCCCTACCGGGTGCTGATTTTC |
| | | R | GGCGCCATAAGGGCGAATTCGGAGCCTGCTTT |
| ***Sbβ:Hv*** | Insert (*Sbδ*) | F | TCGCCCTTATGGCGCCGGGCGGCGGAGACGGC |
| | | R | ACCCGCCGAGGATCAACGTCGGCGGTCCCTGC |
| | Remaining Vector | F | AGAAGTCGTACGGCAAGTCGGACGCCTTCGTG |
| | | R | GGCGCCATAAGGGCGAATTCGGAGCCTGCTTT |
| ***Sbγ:Hv*** | Insert (*Sbε*) | F | TCGCCCTTATGGCGCCGGGCGGCGGAGACGGC |
| | | R | GTGGTGATGTTGATGTACGCCACGCGCTGCAG |
| | Remaining Vector | F | ACATCAACATCACCACTTACCCCTTCACCGCC |
| | | R | GGCGCCATAAGGGCGAATTCGGAGCCTGCTTT |
| ***Hvα:Sb*** | Insert (*Hvα*) | F | TCGCCCTTATGGCGCCAGCGGTGGCCGGAGGG |
| | | R | TAGGGGTGGAGGAGGACACCCTTGATCTTCTC |
| | Remaining Vector | F | TCCTCCTCCACCCCTACAGGGTGCTCATCTTC |
| | | R | GGCGCCATAAGGGCGAATTCGGAGCCTGCTTT |

**Supplementary Table 7-2. Primers used for *CslF6* targeted recombination.**

| Construct | Fragment | Primer Direction | Primer 5' to 3' |
|---|---|---|---|
| ***Hv:SbC1*** | Insert | F | TGGATCAGCTCCCCAAGCTGAACCCGATCAAC |
| | | R | TTGATCCTCGGCGGGTCGAAGCCGTAGAGCGT |
| | Remaining Vector | F | ACCCGCCGAGGATCAACGTCGGCGGTCCCTGC |
| | | R | TTGGGGAGCTGATCCAGCAGCCACGAGAAACC |
| ***Sb:HvC1*** | Insert | F | TGGACCAGCTGCCCAAGCTGAACCCCATCAAC |
| | | R | TTGATCCTCGGCGGGTCGAAGCCGTAGACGGT |
| | Remaining Vector | F | ACCCGCCGAGGATCAACGTCGGCGGGCC |
| | | R | TTGGGCAGCTGGTCCAGCAGCCAGGAGAAGCC |
| ***Hv:SbCR*** | Insert | F | AAGACCGGCTGGGGCAGCGACATCGGCT |
| | | R | GTGGTGATGTTGATGTACGCCACGCGCTGCAG |
| | Remaining Vector | F | ACATCAACATCACCACTTACCCCTTCACCGCC |
| | | R | GCCCCAGCCGGTCTTCTTCTCGAACGCG |
| ***Sb:HvCR*** | Insert | F | AAGACCGGCTGGGGCAAAGAGATCGGCTGGGT |
| | | R | GTGGTGATGTTGATGTAGGCGACGCGCTGCAG |
| | Remaining Vector | F | ACATCAACATCACCACCTACCCGTTCACGGCG |
| | | R | GCCCCAGCCGGTCTTCTTCTCGTACGC |

**Supplementary Table 7-3. Primers used to build *CslF6* point mutation constructs.**

| Construct | Fragment | Primer Direction | Primer 5' to 3' |
|---|---|---|---|
| ***Sb*:S631K** | Insert | F | TCGCCCTTATGGCGCCGGGCGGCGGAGACGGC |
| | | R | GATGTCTTTGCCCCAGCCGGTC |
| | Remaining Vector | F | TGGGGCAAAGACATCGGCTGGGTGTAC |
| | | R | GGCGCCATAAGGGCGAATTCGGAGCCTGCTTT |
| ***Sb*:D632E** | Insert | F | TCGCCCTTATGGCGCCGGGCGGCGGAGACGGC |
| | | R | GCCGATCTCGCTGCCCCAGCCG |
| | Remaining Vector | F | GGCAGCGAGATCGGCTGGGTGTACGG |
| | | R | GGCGCCATAAGGGCGAATTCGGAGCCTGCTTT |
| ***Sb*:G638D** | Insert | F | TCGCCCTTATGGCGCCGGGCGGCGGAGACGGC |
| | | R | GACGGTGTCGTACACCCAGCCGATGTC |
| | Remaining Vector | F | GTGTACGACACCGTCACCGAGGACG |
| | | R | GGCGCCATAAGGGCGAATTCGGAGCCTGCTTT |
| ***Sb*:Y680F** | Insert | F | TCGCCCTTATGGCGCCGGGCGGCGGAGACGGC |
| | | R | CACCTGGAACAGCCGCTCCGTCAG |
| | Remaining Vector | F | CGGCTGTTCCAGGTGCTCCGCTGG |
| | | R | GGCGCCATAAGGGCGAATTCGGAGCCTGCTTT |
| ***Sb*:R696K** | Insert | F | TCGCCCTTATGGCGCCGGGCGGCGGAGACGGC |
| | | R | GTTGTTCTTGGAGAAGAAGATCTCCAGCG |
| | Remaining Vector | F | TTCTCCAAGAACAACCCGCTGTTCG |
| | | R | GGCGCCATAAGGGCGAATTCGGAGCCTGCTTT |
| ***Sb*:F705Y** | Insert | F | TCGCCCTTATGGCGCCGGGCGGCGGAGACGGC |
| | | R | GTGCAGGTACGTGCTGCCGAACAG |
| | Remaining Vector | F | AGCACGTACCTGCACCCGCTGCA |
| | | R | GGCGCCATAAGGGCGAATTCGGAGCCTGCTTT |
| ***Hv*:D629G** | Insert | F | TCGCCCTTATGGCGCCAGCGGTGGCCGGAGGG |
| | | R | GACGGTGCCGTACACCCAGCCGAT |
| | Remaining Vector | F | GTGTACGGCACCGTCACGGAGGA |
| | | R | GGCGCCATAAGGGCGAATTCGGAGCCTGCTTT |

**Supplementary Table 7-4. Q-PCR primers and conditions**

| Gene | Fragment | 5' to 3' |
|---|---|---|
| **Elongation Factor Alpha** | Primer (F) | GATTGGTGGTATTGGAACTGTC |
| | Primer (R) | AGCTTCGTGGTGCATCTC |
| | PCR Fragment 77°C Acquisition | GATTGGTGGTATTGGAACTGTCCCTGTTGGGCGTGTTGAAACCG GTGTCCTCAAGCCTGGTATGGTTGTGACTTTTGGTCCTACTGGT TTGACCACTGAAGTTAAGTCTGTCGAGATGCACCACGAAGCT |
| **Ubiquitin** | Primer (F) | GCCGACTACAACATCCAGAAGG |
| | Primer (R) | TGCAACACAGCGAGCTTAACC |
| | PCR Fragment 77°C Acquisition | GCCGACTACAACATCCAGAAGGAGTCCACTCTCCACCTTGTGCT CCGTCTCCGTGGTGGTGCTAAGAAGAGTAAGAAGAAGACTTACA CTCAAGCCTAAGAAGATTAAGCACAAGAAGAAGAAGGTTAAGCT CGCTGTGTTGCA |
| **Actin** | Primer (F) | CCTTCCAGCAGATGTGGATT |
| | Primer (R) | CAATCAACTCCTTGCCCACT |
| | PCR Fragment 75°C Acquisition | CCTTCCAGCAGATGTGGATTGCTAAGGCAGAGTATGACGAATCT GGTCCGTCTATTGTCCACAGAAAGTGCTTCTGATTTTCCCAGAGT GACAATGTTGGTGAAAGGAAAATACTTACTTCCTACTGGATCAGA AATGCAGTTGCATTTATATTCCAGCTTTATTTTCTGTATTTTTGTT GTCATGTTGGATTGAAGATATTGAGTGGGCAAGGAGTTGATTG |
| **Cyclophilin** | Primer (F) | AAACGGTACCGGAGGTGAATC |
| | Primer (R) | CTTAGCGGTGCAGATGAAGAA |
| | PCR Fragment 81°C Acquisition | AAACGGTACCGGAGGTGAATCAATCTACGGCGCCAAATTCGCTG ACGAGAACTTCAAAAGGAAGCACACCGGTCCTGGAATCCTCTCC ATGGCTAATGCTGGACCTGGAACCAACGGTTCTCAGTTCTTCAT CTGCACCGCTAAG |
| ***CslF6*** | Primer (F) | CAGCACATACCTCCACCCGCTG |
| | Primer (R) | CCAGAACTGGCCGTTCCTGAACCACTCGAA |
| | PCR Fragment 84°C Acquisition | (*HvCslF6*)AGCACATACCTCCACCCGCTGCAGCGCGTCGCCTACA TCAACATCACCACTTACCCCTTCACCGCCATCTTCCTCATCTTCT ACACCACCGTGCCGGCGCTATCCTTCGTCACCGGCCACTTCATC GTGCAGCGCCCGACCACCATGTTCTACGTCTACCTGGGCATCG TGCTATCCACGCTGCTCGTCATCGCCGTGCTGGAGGTCAAGTG GGCCGGGGTCACAGTCTTCGAGTGGTTCAGGAACGGCCAGTTC TGG (*SbCslF6*)CAGCACGTTCCTGCACCCGCTGCAGCGCGTGGCGTA CATCAACATCACCACCTACCCGTTCACGGCGCTGTTCCTCATCT TCTACACCACCGTGCCGGCGCTGTCGTTCGTGACGGGGCACTT CATCGTGCAGCGGCCGACCACCATGTTCTACGTGTACCTGGCC ATCGTGCTGGGGACGCTGCTCATCCTGGCCGTCCTGGAGGTGA AATGGGCGGGCGTCACCGTCTTCGAGTGGTTCAGGAACGGGCA GTTCTGG |

# 8. Appendices (Chapter 3).

**Supplementary Table 8-1. The activity of unmodified, internally deleted and chimeric CSL constructs after transient expression in *N. benthamiana* leaves.**

| Construct | (1,3;1,4)-β-glucan % (w/w) | DP3:DP4 peaks on HPLC |
|---|---|---|
| *Hv*CSLF6 | 1.9 ± 0.15 | ✓ |
| *Hv*:ΔExR | 0 | × |
| *Hv*:ΔCSR | 0 | × |
| *Hv*:SbCSR | 2.6 ± 0.50 | ✓ |
| *Hv*CSLF3 | 0 | × |
| *Hv*CSLF3:F6ExR | 0 | × |
| *Hv*CSLF3:F6CSR | 0 | × |
| *Hv*CSLF4 | 0 | × |
| *Hv*CSLF4:F6ExR | 0 | × |
| *Hv*CSLF4:F6CSR | 0 | × |
| *Hv*CSLF7 | <0.05 | ✓ |
| *Hv*CSLF7:F6ExR | 0 | × |
| *Hv*CSLF7:F6CSR | 0 | × |
| *Hv*CSLF9 | <0.05 | ✓ |
| *Hv*CSLF9:F6CSR | 0 | × |
| *Hv*CSLF10 | 0 | × |
| *Hv*CSLF10:F6ExR | 0 | × |
| *Hv*CSLF10:F6CSR | 0 | × |
| *Hv*CSLJ | <0.05 | ✓ |
| *Hv*CSLJ:F6ExR | 0 | × |
| *Hv*CSLJ:F6CSR | 0 | × |
| *Hv*CSLH | <0.05 | ✓ |
| *Hv*CSLH:F6ExR | 0 | × |
| *Hv*CSLH:F6CSR | 0 | × |
| *Sb*CSLF6 | 2.5 ± 0.22 | ✓ |
| *Sb*:ΔExR | 0 | × |
| *Sb*:ΔCSR | 2.5 ± 0.45 | ✓ |
| *Sb*:HvCSR | 2.1 ± 0.07 | ✓ |

**Supplementary Table 8-2. Constructs with sections of the $NH_2$-terminal region interchanged between *HvCslF6* and *SbCslF6*, and their respective activities in *N. benthamiana*.** Red lettering highlights the sections, A, B or C, that have been interchanged between HvCslF6 and SbCslF.

| Construct Name | Backbone Enzyme | N-terminal Region Composition | (1,3;1,4)-β-glucan (% w/w) | DP3: DP4 ratio |
|---|---|---|---|---|
| *HvCslF6* | *HvCslF6* | *HvA HvB HvC* | 1.4 ± 0.15 | 1.62:1 |
| *Hv:SbA* | *HvCslF6* | ***SbA*** *HvB HvC* | 1.3 ± 0.34 | 1.70:1 |
| *Hv:SbAB* | *HvCslF6* | ***SbA SbB*** *HvC* | 0.5 ± 0.02 | 1.57:1 |
| *Hv:SbABC* | *HvCslF6* | ***SbA SbB SbC*** | 2.3 ± 0.45 | 1.62:1 |
| *Hv:SbC* | *HvCslF6* | *HvA HvB* ***SbC*** | 3.3 ± 0.61 | 1.72:1 |
| *Hv:SbBC* | *HvCslF6* | *HvA* ***SbB SbC*** | 2.2 ± 0.62 | 1.69:1 |
| *Hv:SbAC* | *HvCslF6* | ***SbA*** *HvB* ***SbC*** | 3.0 ± 0.54 | 1.72:1 |
| *Hv:SbB* | *HvCslF6* | *HvA* ***SbB*** *HvC* | 0.4 ± 0.03 | 1.69:1 |
| | | | | |
| *SbCslF6* | *SbCslF6* | *SbA SbB SbC* | 3.4 ± 0.38 | 1.03:1 |
| *Sb:HvA* | *SbCslF6* | ***HvA*** *SbB SbC* | 4.8 ± 1.01 | 1.00:1 |
| *Sb:HvAB* | *SbCslF6* | ***HvA HvB*** *SbC* | 1.8 ± 0.40 | 0.98:1 |
| *Sb:HvABC* | *SbCslF6* | ***HvA HvB HvC*** | 5.2 ± 0.18 | 0.97:1 |
| *Sb:HvC* | *SbCslF6* | *SbA SbB* ***HvC*** | 3.6 ± 0.42 | 1.04:1 |
| *Sb:HvBC* | *SbCslF6* | *SbA* ***HvB HvC*** | 4.1 ± 0.32 | 0.94:1 |
| *Sb:HvAC* | *SbCslF6* | ***HvA*** *SbB* ***HvC*** | 6.5 ± 0.33 | 1.02:1 |
| *Sb:HvB* | *SbCslF6* | *SbA* ***HvB*** *SbC* | 2.8 ± 0.47 | 1.00:1 |
| *Sb:*(C-S) | *SbCslF6* | *SbA SbB*(C-S) *SbC* | 3.5 ± 0.30 | 1.04:1 |

**Supplementary Table 8-3. Primers used to generate truncated, mutated and chimeric *CslF6* constructs.**

| PCR fragment | Orientation | Sequence 5′ to 3′ |
|---|---|---|
| *Hv-TR* Insert | Forward | CGCCCTTATGCTCCACCCCTACCG |
| | Reverse | GATTTTGAGACACGGGCC |
| *Hv-TR* Remaining Vector | Forward | CCGTGTCTCAAAATCTCTGATG |
| | Reverse | TGGAGCATAAGGGCGAATTCGGAGC |
| N-terminal Fragment | Forward | TCGCCCTTATGGCGCC |
| | Reverse | TCACTTGATCTTCTCGGTGCGGAA |
| *Hv:*P474T N-terminal | Forward | CAGTTCACACAGCGCTTCGAGGGCGT |
| | Reverse | GATTTTGAGACACGGGCC |
| *Hv:*P474T C-terminal | Forward | CCGTGTCTCAAAATCTCTGATG |
| | Reverse | GCGCTGTGTGAACTGGACGAAGGCAACCGT |
| N-terminal Insert | Forward | TCGCCCTTATGGCGCC |
| | Reverse | TTGATCTTCTCGGTGCGGAA |
| N-terminal Remaining Vector | Forward | TTCCGCACCGAGAAGATCAA |
| | Reverse | GGCGCCATAAGGGCGA |
| Mutated N-terminal Insert | Forward | TCGCCCTTATGGCGCCGGGCGGCGGAGACGGC |
| | Reverse | TAGGGGTGGAGGAGGATGCCCTTGATCTTCTC |
| Mutated Remaining Vector | Forward | TCCTCCTCCACCCCTACAGGGTGCTCATCTTC |
| | Reverse | GGCGCCATAAGGGCGAATTCGGAGCCTGCTTT |

**Supplementary Table 8-4. Primers used to generate internally deleted and chimeric *CslF6* constructs.**

| PCR fragment | Orientation | Sequence 5′ to 3′ |
|---|---|---|
| *Hv:ΔExR* | Forward | CTTCGACGACGCCTTCGTGGACAC |
| | Reverse | AAGGCGTCGTCGAAGCCGTAGACGG |
| *Hv:ΔCSR* | Forward | CTTCGACAAAGAGATCGGCTGGGTGTA |
| | Reverse | ATCTCTTTGTCGAAGCCGTAGACGGT |
| *Hv:SbCSR* Insert | Forward | CCGCCGAGGATCAACGTC |
| | Reverse | GCCCCAGCCGGTCTTCTTC |
| *Hv:SbCSR* Remaining Vector | Forward | AAGACCGGCTGGGGCAAAGAGATCGGCTGGGT |
| | Reverse | TTGATCCTCGGCGGGTCGAAGCCGTAGACGGT |
| *Sb:ΔExR* | Forward | CTTCGACGACGCGTTCGTCGACAC |
| | Reverse | AACGCGTCGTCGAAGCCGTAGAGCGT |
| *Sb:ΔCSR* | Forward | CTTCGACAGCGACATCGGCTGGGT |
| | Reverse | ATGTCGCTGTCGAAGCCGTAGAGCG |
| *Sb:HvCSR* Insert | Forward | CCGCCGAGGATCAACGTC |
| | Reverse | GCCCCAGCCGGTCTTCTTC |
| *Sb:HvCSR* Remaining Vector | Forward | AAGACCGGCTGGGGCAGCGACATCGGCT |
| | Reverse | TTGATCCTCGGCGGGTCGAAGCCGTAGAGCGT |

**Supplementary Table 8-5. Primers used to generate chimeric constructs.**

| PCR fragment | Orientation | Sequence 5′ to 3′ |
|---|---|---|
| *HvCslF6 ExR Insert* | Forward | CCGCCGAGGATCAACGTC |
| | Reverse | CGACTTGCCGTACGTCTTCTT |
| *HvCslF3:F6ExR* | Forward | ACGTACGGCAAGTCGATACCCTTCCTAGATTCCGTA |
| | Reverse | GTTGATCCTCGGCGGGTCAATGCCATAAAGTGCTATG |
| *HvCslF3:F6CSR* | Forward | AAGACCGGCTGGGGCAAGGGTGTTGGGTACATATATGA |
| | Reverse | GTTGATCCTCGGCGGGTCAATGCCATAAAGTGCTATG |
| *HvCslF4:F6ExR* | Forward | ACGTACGGCAAGTCGACGTCTTTCATCAATTCCATGC |
| | Reverse | GTTGATCCTCGGCGGCTCCATGCCATAGAGCGT |
| *HvCslF4:F6CSR* | Forward | AAGACCGGCTGGGGCAGAGACGTTGGGTGGGTG |
| | Reverse | GTTGATCCTCGGCGGCTCCATGCCATAGAGCGT |
| *HvCslF7:F6ExR* | Forward | ACGTACGGCAAGTCGACGCCGTTCCTTGGCTC |
| | Reverse | GTTGATCCTCGGCGGGTCGATGCTGTATAGCGC |
| *HvCslF7:F6CSR* | Forward | AAGACCGGCTGGGGCAGGGAAATCGGCTGGATATAC |
| | Reverse | GTTGATCCTCGGCGGGTCGATGCTGTATAGCGC |
| *HvCslF9:F6CSR* | Forward | AAGACCGGCTGGGGCAACGACGTTGGGTGGGTG |
| | Reverse | GTTGATCCTCGGCGGGTCGGCGCTGTAGAGAG |
| *HvCslF10:F6ExR* | Forward | ACGTACGGCAAGTCGTTACCCTTCCTCAACTCAGTA |
| | Reverse | GTTGATCCTCGGCGGATCAATTCCATAGAGTGCAAGG |
| *HvCslF10:F6CSR* | Forward | AAGACCGGCTGGGGCAGGGGCATTGGCTACATATAC |
| | Reverse | GTTGATCCTCGGCGGATCAATTCCATAGAGTGCAAGG |
| *HvCslJ:F6ExR* | Forward | ACGTACGGCAAGTCGAATGGTCACATAGCGTCGCT |
| | Reverse | GTTGATCCTCGGCGGCCGGGCGCCGTAGAGG |
| *HvCslJ:F6CSR* | Forward | AAGACCGGCTGGGGCGAGGAGGTCGGCTTCTTGTA |
| | Reverse | GTTGATCCTCGGCGGCCGGGCGCCGTAGAGG |
| *HvCslH:F6ExR* | Forward | ACGTACGGCAAGTCGAAGGTGTTGATCGAATCATCTAGG |
| | Reverse | GTTGATCCTCGGCGGCGGCATGCCGTAAATGACTT |
| *HvCslH:F6CSR* | Forward | AAGACCGGCTGGGGCAAGGAGATTGGTTGGGTCTAT |
| | Reverse | GTTGATCCTCGGCGGCGGCATGCCGTAAATGACTT |

# 9. Appendices (Chapter 4).

**Supplementary Table 9-1. Cis-acting regulatory elements predicted to bind in regions conserved between barley, sorghum and rice *CslF6* promoters.**

| Name | Binding Sequence | PLACE Site Code |
|---|---|---|
| DOFCOREZM | AAAG | S000265 |
| NODCON2GM | CTCTT | S000462 |
| OSE2ROOTNOD | CTCTT | S000468 |
| CAATBOX1 | CAAT | S000028 |
| AACACOREOSGLUB1 | AACAAAC | S000353 |
| ANAERO1CONSENSU | AAACAAA | S000477 |
| AACACOREOSGLUB1 | AACAAAC | S000353 |
| CIACADIANLELHC | CAANNNNATC | S000252 |
| ARR1AT | NGATT | S000454 |
| DOFCOREZM | AAAG | S000265 |
| TAAAGSTKST1 | TAAAG | S000387 |
| POLASIG1 | AATAAA | S000080 |
| ARR1AT | NGATT | S000454 |
| GTGANTG10 | GTGA | S000378 |
| MYCATRD22 | CACATG | S000174 |
| MYCCONSENSUSAT | CANNTG | S000407 |
| EBOXBNNAPA | CANNTG | S000144 |
| MYCATERD1 | CATGTG | S000413 |
| ROOTMOTIFTAP | ATATT | S000098 |
| CACTFTPPCA1 | YACT | S000449 |
| BOXLCOREDCPAL | ACCWWCC | S000492 |
| MYBPLANT | MACCWAMC | S000167 |
| MYBPZM | CCWACC | S000179 |
| PALBOXLPC | YCYYACCWACC | S000138 |
| CBFHV | RYCGAC | S000497 |
| DRE2COREZMRAB17 | ACCGAC | S000402 |
| DRECRTCOREAT | RCCGAC | S000418 |
| LTREATLTI78 | ACCGACA | S000157 |
| LTRECOREATCOR15 | CCGAC | S000153 |
| ABRELATERD1 | ACGTG | S000414 |
| ACGTOSGLUB1 | GTACGTG | S000278 |
| ACGTATERD1 | ACGT | S000415 |
| CURECORECR | GTAC | S000493 |
| CACTFTPPCA1 | YACT | S000449 |
| NTBBF1ARROLB | ACTTTA | S000273 |
| DOFCOREZM | AAAG | S000265 |
| TAAAGSTKST1 | TAAAG | S000387 |

**Supplementary Table 9-2. Cis-acting regulatory elements predicted to bind between 1750bp and 2500bp upstream of the *HvCslF6* start codon.**

| Name | Binding Sequence | PLACE Site Code |
|---|---|---|
| ABRELATERD1 | ACGTG | S000414 |
| ACGTATERD1 | ACGT | S000415 |
| RHERPATEXPA7 | KCACGW | S000512 |
| GTGANTG10 | GTGA | S000378 |
| DOFCOREZM | AAAG | S000265 |
| PALBOXAPC | CCGTCC | S000137 |
| CACTFTPPCA1 | YACT | S000449 |
| CURECORECR | GTAC | S000493 |
| LTRE1HVBLT49 | CCGAAA | S000250 |
| GATABOX | GATA | S000039 |
| NODCON1GM | AAAGAT | S000461 |
| OSE1ROOTNODULE | AAAGAT | S000467 |
| TAAAGSTKST1 | TAAAG | S000387 |
| GT1CONSENSUS | GRWAAW | S000198 |
| GT1GMSCAM4 | GAAAAA | S000453 |
| TATABOX4 | TATATAA | S000111 |
| ERELEE4 | AWTTCAAA | S000037 |
| ARR1AT | NGATT | S000454 |
| POLLEN1LELAT52 | AGAAA | S000245 |
| HDZIP2ATATHB2 | TAATMATTA | S000373 |
| POLASIG3 | AATAAT | S000088 |
| CPBCSPOR | TATTAG | S000491 |
| ROOTMOTIFTAPOX1 | ATATT | S000098 |
| ELRECOREPCRP1 | TTGACC | S000142 |
| WBOXATNPR1 | TTGAC | S000390 |
| WBOXNTERF3 | TGACY | S000457 |
| WRKY71OS | TGAC | S000447 |
| CARGCW8GAT | CWWWWWWWWG | S000431 |
| TATABOX2 | TATAAAT | S000109 |
| SEF4MOTIFGM7S | RTTTTTR | S000103 |
| EECCRCAH1 | GANTTNC | S000494 |
| POLASIG1 | AATAAA | S000080 |
| TATABOX5 | TTATTT | S000203 |
| -300ELEMENT | TGHAAARK | S000122 |
| INRNTPSADB | YTCANTYY | S000395 |
| EBOXBNNAPA | CANNTG | S000144 |
| MYCCONSENSUSAT | CANNTG | S000407 |
| WBOXHVISO1 | TGACT | S000442 |

| Name | Binding Sequence | PLACE Site Code |
|---|---|---|
| RAV1BAT | CACCTG | S000315 |
| ASF1MOTIFCAMV | TGACG | S000024 |
| SURECOREATSULTR11 | GAGAC | S000499 |
| CGCGBOXAT | VCGCGB | S000501 |
| PRECONSCRHSP70A | SCGAYNRNNNNNNNNNNNNNNNHD | S000506 |
| HEXAMERATH4 | CCGTCG | S000146 |
| CGACGOSAMY3 | CGACG | S000205 |
| CBFHV | RYCGAC | S000497 |
| DRECRTCOREAT | RCCGAC | S000418 |
| LTRECOREATCOR15 | CCGAC | S000153 |
| MYBCOREATCYCB1 | AACGG | S000502 |
| E2FAT | TYTCCCGCC | S000417 |
| IBOXCORE | GATAA | S000199 |
| CATATGGMSAUR | CATATG | S000370 |
| CBFHV | RYCGAC | S000497 |
| RAV1AAT | CAACA | S000314 |
| MYBCORE | CNGTTR | S000176 |
| GT1CORE | GGTTAA | S000125 |
| SORLIP1AT | GCCAC | S000482 |
| SV40COREENHAN | GTGGWWHG | S000123 |
| PYRIMIDINEBOXOSRAMY1A | CCTTTT | S000259 |
| MYB1AT | WAACCA | S000408 |
| SEBFCONSSTPR10A | YTGTCWC | S000391 |
| BIHD1OS | TGTCA | S000498 |
| SEF3MOTIFGM | AACCCA | S000115 |
| CAATBOX1 | CAAT | S000028 |
| SORLIP1AT | GCCAC | S000482 |
| SV40COREENHAN | GTGGWWHG | S000123 |
| BIHD1OS | TGTCA | S000498 |
| SEF3MOTIFGM | AACCCA | S000115 |

**Supplementary Table 9-3. Primers used to generate promoter constructs.**

| PCR fragment | Orientation | Sequence 5′ to 3′ |
|---|---|---|
| HvPr | Reverse | GGCCGTCGTCCTCAATGCACG |
| HvPrA | Forward | TAACGCACACGATTAGTCCTTTGCGGTA |
| HvPrB | Forward | CACATGAGCGAGTTGAATCCAAAACCTC |
| HvPrC | Forward | CCTAGAACTACGTGAAAGACTTATACC |
| HvPrD | Forward | GTTTTTGCGGGACAGCTTACGAATTACT |
| HvPrE | Forward | GTAAATGCTTTGGGACTCGTTGATTG |
| HvPrF | Forward | CCTAACAACTGGCCTAATTTGCAAATTG |
| HvPrG | Forward | GGGACCAATGCATTCCTTCTCGTG |
| HvPrH | Forward | TCCTCCAAAATGCATCCCCCAACCA |
| HvPrI | Forward | GGGCAACAACCAAGCACAAGCTCA |
| HvPrJ | Forward | CCTGTACTAATAAGAATCGGAAATGCAAGCT |
| HvPrK | Forward | GAAGGAAGTGCTTGGCACCACCTAC |
| HvPrL | Forward | CCACGTACTTTACTCGTCATTTCTCGC |
| 35S | Forward | GGTCAACATGGTGGAGCACGACACA |
| | Reverse | GTCCTCTCCAAATGAAATG |
| NosT | Forward | GAATTTCCCCGATCGTTCAAAC |
| | Reverse | CAGGAAACAGCTATGAC |
| pGR-GW Insert | Forward | ATCGATAAGCTTGATACAGAGTTTTCCCGTGGTTTTC |
| | Reverse | CTGCAGGAATTCGATAATGAAACCAGAGTTAAAGGATC |

# 10. References Cited.

Almirall, M., Francesch, M., Perez-Vendrell, A.M., Brufau, J. and Esteve-Garcia, E. (1995) The differences in intestinal viscosity produced by barley and β-glucanase alter digesta enzyme activities and ileal nutrient digestibilities more in broiler chicks than in cocks. *The Journal of Nutrition* **125**, 947-955.

Bamforth, C.W. (2009) Current perspectives on the role of enzymes in brewing. *Journal of Cereal Science* **50**, 353-357.

Belobrajdic, D.P., Jobling, S.A., Morell, M.K., Taketa, S. and Bird, A.R. (2015) Wholegrain barley *β*-glucan fermentation does not improve glucose tolerance in rats fed a high-fat diet. *Nutrition Research* **35**, 162-168.

Bingham, S.A. (1990) Mechanisms and experimental and epidemiological evidence relating dietary fibre (non-starch polysaccharides) and starch to protection against large bowel cancer. *Proceedings of the Nutrition Society* **49**, 153-171.

Boerjan, W., Ralph, J. and Baucher, M. (2003) Lignin Biosynthesis. *Annual Review of Plant Biology* **54**, 519-546.

Bornet, F.R.J., Costagliola, D., Rizkalla, S.W., Blayo, A., Fontvieille, A.M., Haardt, M.J., Letanoux, M., Tchobroutsky, G. and Slama, G. (1987) Insulinemic and glycemic indexes of six starch-rich foods taken alone and in a mixed meal by type 2 diabetics. *The American Journal of Clinical Nutrition* **45**, 588-595.

Brennan, C.S., Cleary, L J (2005) The potential use of cereal (1→3,1→4)-β-D-glucans as functional food ingredients. *Journal of Cereal Science* **42**, 1-13.

Buckeridge, M.S., Vergara, C.E. and Carpita, N.C. (1999) The mechanism of synthesis of a mixed-linkage (1→3),(1→4)-β-d-glucan in maize. Evidence for multiple sites of glucosyl transfer in the synthase complex. *Plant Physiology* **120**, 1105-1116.

Burton, R.A., Collins, H.M., Kibble, N.A.J., Smith, J.A., Shirley, N.J., Jobling, S.A., Henderson, M., Singh, R.R., Pettolino, F., Wilson, S.M., Bird, A.R., Topping, D.L., Bacic, A. and Fincher, G.B. (2011) Over-expression of specific *HvCslF* cellulose synthase-like genes in transgenic barley increases the levels of cell wall (1,3;1,4)-β-D-glucans and alters their fine structure. *Plant Biotechnology Journal* **9**, 117-135.

Burton, R.A. and Fincher, G.B. (2009) (1,3;1,4)-β-D-glucans in cell walls of the poaceae, lower plants, and fungi: a tale of two linkages. *Molecular Plant* **2**, 873-882.

Burton, R.A. and Fincher, G.B. (2012) Current challenges in cell wall biology in the cereals and grasses. *Frontiers in Plant Science* **3**.

Burton, R.A., Gidley, M.J. and Fincher, G.B. (2010) Heterogeneity in the chemistry, structure and function of plant cell walls. *Nature Chemical Biology* **6**, 724-732.

Burton, R.A., Jobling, S.A., Harvey, A.J., Shirley, N.J., Mather, D.E., Bacic, A. and Fincher, G.B. (2008) The genetics and transcriptional profiles of the cellulose synthase-like *HvCslF* gene family in barley (*Hordeum vulgare* L.). *Plant Physiology* **146**, 1821-1833.

Burton, R.A., Shirley, N.J., King, B.J., Harvey, A.J. and Fincher, G.B. (2004) The *CesA* Gene Family of Barley. Quantitative Analysis of Transcripts Reveals Two Groups of Co-Expressed Genes. *Plant Physiology* **134**, 224-236.

Burton, R.A., Wilson, S.M., Hrmova, M., Harvey, A.J., Shirley, N.J., Medhurst, A., Stone, B.A., Newbigin, E.J., Bacic, A. and Fincher, G.B. (2006) Cellulose synthase-like *CslF* genes mediate the synthesis of cell wall (1,3;1,4)-β-D-glucans. *Science* **311**, 1940-1942.

Carpita, N., C, and McCann, M., C (2010) The maize mixed-linkage (1→3),(1→4)-β-D-glucan polysaccharide is synthesized at the golgi membrane. *Plant Physiology* **153**, 1362-1371.

Carpita, N.C. and McCann, M.C. (2008) Maize and sorghum: genetic resources for bioenergy grasses. *Trends in Plant Science* **13**, 415-420.

Chiu, W.-l., Niwa, Y., Zeng, W., Hirano, T., Kobayashi, H. and Sheen, J. (1996) Engineered GFP as a vital reporter in plants. *Current Biology* **6**, 325-330.

Close, T.J., Wanamaker, S.I., Caldo, R.A., Turner, S.M., Ashlock, D.A., Dickerson, J.A., Wing, R.A., Muehlbauer, G.J., Kleinhofs, A. and Wise, R.P. (2004) A New Resource for Cereal Genomics: 22K Barley GeneChip Comes of Age. *Plant Physiology* **134**, 960-968.

Collins, H.M., Burton, R.A., Topping, D.L., Liao, M.L., Bacic, A. and Fincher, G.B. (2010) Variability in fine structures of noncellulosic cell wall polysaccharides from cereal grains: potential importance in human health and nutrition. *Cereal Chemistry* **87**, 272–282

Consortium-IBGS (2012) A physical, genetic and functional sequence assembly of the barley genome. *Nature* **491**, 711-716.

Curtis, M., D, and Grossniklaus, U. (2003) A gateway cloning vector set for high-throughput functional analysis of genes in planta. *Plant Physiology* **133**, 462-469.

Daras, G., Rigas, S., Penning, B., Milioni, D., McCann, M.C., Carpita, N.C., Fasseas, C. and Hatzopoulos, P. (2009) The *thanatos* mutation in *Arabidopsis thaliana* cellulose synthase 3 (*AtCesA3*) has a dominant-negative effect on cellulose synthesis and plant growth. *New Phytologist* **184**, 114-126.

Dikeman, C.L. and Fahey, G.C. (2006) Viscosity as Related to Dietary Fiber: A Review. *Critical Reviews in Food Science and Nutrition* **46**, 649-663.

Dimitroff, G. (2011) Cell wall biosynthesis: An alternative model system for gene function analysis. In: *School of Agriculture, Food and Wine* p. 77. Adelaide: University of Adelaide.

Doblin, M.S., Kurek, I., Jacob-Wilk, D. and Delmer, D.P. (2002) Cellulose biosynthesis in plants: from genes to rosettes. *Plant and Cell Physiology* **43**, 1407-1420.

Doblin, M.S., Pettolino, F. and Bacic, A. (2010) Plant cell walls: the skeleton of the plant

world. *Functional Plant Biology* **37**, 357–381.

Doblin, M.S., Pettolino, F.A., Wilson, S.M., Campbell, R., Burton, R.A., Fincher, G.B., Newbigin, E. and Bacic, A. (2009) A barley *cellulose synthase*-like *CslH* gene mediates (1,3;1,4)-β-D-glucan synthesis in transgenic *Arabidopsis*. *Proceedings of the National Academy of Sciences* **106**, 5996-6001.

Ermawar, R.A., Collins, H.M., Byrt, C.S., Betts, N.S., Henderson, M., Shirley, N.J., Schwerdt, J., Lahnstein, J., Fincher, G.B. and Burton, R.A. (2015) Distribution, structure and biosynthetic gene families of (1,3;1,4)-β-glucan in Sorghum bicolor (L.) Moench. *Journal of Integrative Plant Biology*, n/a-n/a.

Fincher, G.B. (2009a) Exploring the evolution of (1,3;1,4)-β-D-glucans in plant cell walls: comparative genomics can help! *Current Opinion in Plant Biology* **12**, 140-147.

Fincher, G.B. (2009b) Revolutionary times in our understanding of cell wall biosynthesis and remodeling in the grasses. *Plant Physiology* **149**, 27-37.

Fincher, G.B. and Stone, B.A. (2004) Chemistry of non-starch polysaccharides from cereal grains. In: *Encyclopedia of Grain Science* (Wrigley, C., Corke, H. and Walker, C.E. eds) pp. 206-223. Elsevier Academic Press.

Gallaher, D.D., Hassel, C.A., Lee, K.J. and Gallaher, C.M. (1993) Viscosity and fermentability as attributes of dietary fiber responsible for the hypocholesterolemic effect in hamsters. *The Journal of Nutrition* **123**, 244-252.

Gibeaut, D.M. and Carpita, N.C. (1993) Synthesis of (1-->3), (1-->4)-beta-D-glucan in the Golgi apparatus of maize coleoptiles. *Proceedings of the National Academy of Sciences* **90**, 3850-3854.

Goodstein, D.M., Shu, S., Howson, R., Neupane, R., Hayes, R.D., Fazo, J., Mitros, T., Dirks, W., Hellsten, U., Putnam, N. and Rokhsar, D.S. (2011) Phytozome: a comparative platform for green plant genomics. *Nucleic Acids Research*.

Gretton, S. and Harris, M. (2008) Dual luciferase assay to assess the replication of the hepatitus C virus subgenomic replicon. *Application Note 172 BMG LABTECH*.

Han, F., Ullrich, S.E., Chirat, S., Menteur, S., Jestin, L., Sarrafi, A., Hayes, P.M., Jones, B.L., Blake, T.K., Wesenberg, D.M., Kleinhofs, A. and Kilian, A. (1995) Mapping of β-glucan content and β-glucanase activity loci in barley grain and malt. *Theoretical and Applied Genetics* **91**, 921-927.

Harris, P.J. and Fincher, G.B. (2009) Distribution, Fine Structure and Function of (1,3;1,4)-β-Glucans in the Grasses and Other Taxa. In: *Chemistry, Biochemistry, and Biology of (1,3)-β-Glucans and Related Polysaccharides* (Stone B A, Bacic T and B, F.G. eds), pp. 621-654. Philadelphia, USA: Elsevier Inc.

Hazen, S.P., Scott-Craig, J.S. and Walton, J.D. (2002) Cellulose Synthase-like Genes of Rice. *Plant Physiology* **128**, 336-340.

Hellens, R.P., Allan, A., Friel, E.N., Bolitho, K., Grafton, K., Templeton, M.D.,

Karunairetnam, S., Gleave, A.P. and Laing, W.A. (2005) Transient expression vectors for functional genomics, quantification of promoter activity and RNA silencing in plants. *Plant Methods* **1**.

Henry, R.J. and Stone, B.A. (1982) Solubilization of *β*-glucan synthases from the membranes of cultured ryegrass endosperm cells. *Biochemistry Journal* **203**, 629-636.

Heredia, A., Jiménez, A. and Guillén, R. (1995) Composition of plant cell walls. *Zeitschrift für Lebensmitteluntersuchung und Forschung A* **200**, 24-31.

Higo, K., Ugawa, Y., Iwamoto, M. and Korenaga, T. (1999) Plant cis-acting regulatory DNA elements (PLACE) database: 1999. *Nucleic Acids Research* **27**, 297-300.

Jacob, J.P. and Pescatore, A.J. (2012) Using barley in poultry diets—A review. *The Journal of Applied Poultry Research* **21**, 915-940.

Jefferson, R.A., Kavanagh, T.A. and Bevan, M.W. (1987) GUS fusions: beta-glucuronidase as a sensitive and versatile gene fusion marker in higher plants. *The EMBO Journal* **6**, 3901-3907.

Jobling, S.A. (2015) Membrane pore architecture of the CslF6 protein controls (1-3,1-4)-β-glucan structure. *Science Advances* **1**.

Kapila, J., De Rycke, R., Van Montagu, M. and Angenon, G. (1997) An *Agrobacterium*-mediated transient gene expression system for intact leaves. *Plant Science* **122**, 101-108.

Kim, S.-J., Zemelis, S., Keegstra, K. and Brandizzi, F. (2015) The cytoplasmic localization of the catalytic site of CSLF6 supports a channeling model for the biosynthesis of mixed-linkage glucan. *The Plant Journal* **81**, 537-547.

Kurek, I., Kawagoe, Y., Jacob-Wilk, D., Doblin, M. and Delmer, D. (2002) Dimerization of cotton fiber cellulose synthase catalytic subunits occurs via oxidation of the zinc-binding domains. *Proceedings of the National Academy of Sciences* **99**, 11109-11114.

Larsson, S., Giovannucci, E., Bergkvist, L. and Wolk, A. (2005) Whole grain consumption and risk of colorectal cancer: a population-based cohort of 60 000 women. *British Journal of Cancer* **92**, 1803-1807.

Laskowski, R., Rullmann, J.A., MacArthur, M., Kaptein, R. and Thornton, J. (1996) AQUA and PROCHECK-NMR: Programs for checking the quality of protein structures solved by NMR. *J Biomol NMR* **8**, 477-486.

Lazaridou, A. and Biliaderis, C.G. (2007) Molecular aspects of cereal β-glucan functionality: Physical properties, technological applications and physiological effects. *Journal of Cereal Science* **46**, 101-118.

Li, J.-F., Park, E., von Arnim, A.G. and Nebenführ, A. (2009) The FAST technique: a simplified *Agrobacterium*-based transformation method for transient gene

expression analysis in seedlings of Arabidopsis and other plant species. *Plant Methods* **5**, 6.

Little, A., Schwerdt, J.G. and Burton., R.A. (2015). Adelaide: ARC Centre of Excellence in Plant Cell Walls, University of Adelaide.

Martinez-Atienza, J., Van Ingelgem, C., Roef, L. and Maathuis, F.J.M. (2007) Plant Cyclic Nucleotide Signalling: Facts and Fiction. *Plant Signaling & Behavior* **2**, 540-543.

Matzke, A.J.M., Stöger, E.M., Schernthaner, J.P. and Matzke, M.A. (1990) Deletion analysis of a zein gene promoter in transgenic tobacco plants. *Plant Molecular Biology* **14**, 323-332.

McCleary, B.V. and Codd, R. (1991) Measurement of (1 → 3),(1 → 4)-β-D-glucan in barley and oats: A streamlined enzymic procedure. *Journal of the Science of Food and Agriculture* **55**, 303-312.

McCleary, B.V., Solah, V. and Gibson, T.S. (1994) Quantitative Measurement of Total Starch in Cereal Flours and Products. *Journal of Cereal Science* **20**, 51-58.

McLaren, J. (2005) Crop biotechnology provides an opportunity to develop a sustainable future. *Trends in Biotechnology* **23**, 339-342.

Meikle, P.J., Hoogenraad, N.J., Bönig, I., Clarke, A.E. and Stone, B.A. (1994) A (1→3,1→4)-β-glucan-specific monoclonal antibody and its use in the quantitation and immunocytochemical location of (1→3,1→4)-β-glucans. *The Plant Journal* **5**, 1-9.

Morgan, J.L.W., McNamara, J.T. and Zimmer, J. (2014) Mechanism of activation of bacterial cellulose synthase by cyclic di-GMP. *Nature Structural and Molecular Biology* **21**, 489-496.

Morgan, J.L.W., Strumillo, J. and Zimmer, J. (2013) Crystallographic snapshot of cellulose synthesis and membrane translocation. *Nature* **493**, 181-186.

Nemeth, C., Freeman, J., Jones, H.D., Sparks, C., Pellny, T.K., Wilkinson, M.D., Dunwell, J., Andersson, A.A.M., Åman, P., Guillon, F., Saulnier, L., Mitchell, R.A.C. and Shewry, P.R. (2010) Down-regulation of the *CSLF6* gene results in decreased (1,3;1,4)-β-D-glucan in endosperm of wheat. *Plant Physiology* **152**, 1209–1218.

Nishimura, A., Aichi, I. and Matsuoka, M. (2007) A protocol for *Agrobacterium*-mediated transformation in rice. *Nature Protocols* **1**, 2796-2802.

Pear, J.R., Kawagoe, Y., Schreckengost, W.E., Delmer, D.P. and M, S.D. (1996) Higher plants contain homologs of the bacterial *celA* genes encoding the catalytic subunit of cellulose synthase. *Plant Biology* **93**, 12637-12642.

Popper, Z.A. and Fry, S.C. (2003) Primary cell wall composition of bryophytes and charophytes. *Annals of Botany* **91**, 1-12.

Richmond, T.A. and Somerville, C.R. (2000) The Cellulose Synthase Superfamily. *Plant*

*Physiology* **124**, 495-498.

Riken (2011) Rice genome project. National Institute of Agrobiological Sciences.

Rozaklis, T., Ramsay, S.L., Whitfield, P.D., Ranieri, E., Hopwood, J.J. and Meikle, P.J. (2002) Determination of oligosaccharides in pompe disease by electrospray ionization tandem mass spectrometry. *Clinical Chemistry* **48**, 131-139.

Sainsbury, F., Thuenemann, E.C. and Lomonossoff, G.P. (2009) pEAQ: versatile expression vectors for easy and quick transient expression of heterologous proteins in plants. *Plant Biotechnology Journal* **7**, 682-693.

Šali, A. and Blundell, T.L. (1993) Comparative Protein Modelling by Satisfaction of Spatial Restraints. *Journal of Molecular Biology* **234**, 779-815.

Scheller, H.V. and Ulvskov, P. (2010) Hemicelluloses. In: *Annual Review of Plant Biology* pp. 263-289. Palo Alto: Annual Reviews.

Schreiber, M., Wright, F., MacKenzie, K., Hedley, P.E., Schwerdt, J.G., Little, A., Burton, R.A., Fincher, G.B., Marshall, D., Waugh, R. and Halpin, C. (2014) The Barley Genome Sequence Assembly Reveals Three Additional Members of the *CslF* (1,3;1,4)-β-Glucan Synthase Gene Family. *PLoS ONE* **9**, e90888.

Sethaphong, L., Haigler, C.H., Kubicki, J.D., Zimmer, J., Bonetta, D., DeBolt, S. and Yingling, Y.G. (2013) Tertiary model of a plant cellulose synthase. *Proceedings of the National Academy of Sciences* **110**, 7512-7517.

Sievers, F., Wilm, A., Dineen, D., Gibson, T.J., Karplus, K., Li, W., Lopez, R., McWilliam, H., Remmert, M., Söding, J., Thompson, J.D. and Higgins, D.G. (2011) Fast, scalable generation of high-quality protein multiple sequence alignments using Clustal Omega. *Molecular Systems Biology* **7**, 539-539.

Simmons, C.W., Van der Gheynst, J.S. and Upadhyaya, S.K. (2009) A model of *Agrobacterium tumefaciens* vacuum infiltration into harvested leaf tissue and subsequent in planta transgene transient expression. *Biotechnology and Bioengineering* **102**, 965-970.

Sippl, M. (1993) Recognition of errors in three-dimensional structures of proteins. *PROTEINS: Structure, Function and Genetics* **17**, 355-362.

Somerville, C., Bauer, S., Brininstool, G., Facette, M., Hamann, T., Milne, J., Osborne, E., Paredez, A., Persson, S., Raab, T., Vorwerk, S. and Youngs, H. (2004) Toward a Systems Approach to Understanding Plant Cell Walls. *Science* **306**, 2206-2211.

Staudte, R.G., Woodward, J.R., Fincher, G.B. and Stone, B.A. (1983) Water-soluble (1→3), (1→4)-β-D-glucans from barley (*Hordeum vulgare*) endosperm. III. Distribution of cellotriosyl and cellotetraosyl residues. *Carbohydrate Polymers* **3**, 299-312.

Taketa, S., Yuo, T., Tonooka, T., Tsumuraya, Y., Inagaki, Y., Haruyama, N., Larroque, O. and Jobling, S.A. (2011) Functional characterization of barley betaglucanless mutants demonstrates a unique role for CslF6 in (1,3;1,4)-β-D-glucan biosynthesis.

*Journal of Experimental Botany* **63**, 381-392.

Topping, D. (2007) Cereal complex carbohydrates and their contribution to human health. *Journal of Cereal Science* **46**, 220-229.

Topping, D.L. and Clifton, P.M. (2001) Short-Chain Fatty Acids and Human Colonic Function: Roles of Resistant Starch and Nonstarch Polysaccharides. *Physiological Reviews* **81**, 1031-1064.

Vega-Sάnchez, M.E., Verhertbruggen, Y., Christensen, U., Chen, X., Sharma, V., Varanasi, P., Jobling, S.A., Talbot, M., White, R.G., Joo, M., Singh, S., Auer, M., Scheller, H.V. and Ronald, P.C. (2012) Loss of *Cellulose Synthase-Like F6* function affects mixed-linkage glucan deposition, cell wall mechanical properties, and defense responses in vegetative tissues of rice. *Plant Physiology* **159**, 56-69.

Vickers, C.E., Xue, G. and Gresshoff, P.M. (2006) A novel *cis*-acting element, ESP, contributes to high-level endosperm-specific expression in an oat globulin promoter. *Plant Molecular Biology* **62**, 195-214.

Voinnet, O., Rivas, S., Mestre, P. and Baulcombe, D. (2003) An enhanced transient expression system in plants based on suppression of gene silencing by the p19 protein of tomato bushy stunt virus. *The Plant Journal* **33**, 949–956

Wilson, S., Burton, R., Doblin, M., Stone, B., Newbigin, E., Fincher, G. and Bacic, A. (2006) Temporal and spatial appearance of wall polysaccharides during cellularization of barley (*Hordeum vulgare*) endosperm. *Planta* **224**, 655-667.

Wilson, S.M., Burton, R.A., Collins, H.M., Doblin, M.S., Pettolino, F., Shirley, N., Fincher, G.B. and Bacic, A. (2012) Pattern of deposition of cell wall polysaccharides and transcript abundance of related cell wall synthesis genes during differentiation in barley (*Hordeum vulgare*) endosperm. *Plant Physiology* **159**, 655-670.

Wilson, S.M., Ho, Y.Y., Lampugnani, E.R., Van de Meene, A.M.L., Bain, M.P., Bacic, A. and Doblin, M.S. (2015) Determining the Subcellular Location of Synthesis and Assembly of the Cell Wall Polysaccharide (1,3; 1,4)-β-D-Glucan in Grasses. *Plant Cell* in press.

Woodward, J.R., Fincher, G.B. and Stone, B.A. (1983) Water-soluble (1→3), (1→4)-β-D-glucans from barley (*Hordeum vulgare*) endosperm. II. Fine structure. *Carbohydrate Polymers* **3**, 207-225.

Wydro, M., Kozubek, E. and Lehmann, P. (2006) Optimization of transient *Agrobacterium*-mediated gene expression system in leaves of *Nicotiana benthamiana*. *Acta Biochimica Polonica* **53**, 289–298.

Yang, J., Yan, R., Roy, A., Xu, D., Poisson, J. and Zhang, Y. (2015) The I-TASSER Suite: protein structure and function prediction. *Nature Methods* **12**, 7-8.

Zhong, R., Morrison, W.H., Freshour, G.D., Hahn, M.G. and Ye, Z.-H. (2003) Expression of a mutant form of cellulose synthase *AtCesA7* causes dominant negative effect on cellulose biosynthesis. *Plant Physiology* **132**, 786-795.